

Investigating the Post Mortem Applications of
Hard Parts from Two Common New Zealand
Squid Species: *Onykia ingens* and *Nototodarus
sloanii*

Tyler Jon Northern

A thesis submitted for the degree of
Master of Science (MSc) in Marine Science
University of Otago,
Dunedin, New Zealand

June 2016

Abstract

Hard parts of squid are used in a variety of post mortem analyses, such as diet studies, which shed light on various aspects of the squid's life. In this thesis, hard parts were reviewed. Beaks and statoliths were found to contain the most information about the squid's life history and are the most widely used squid hard parts.

Allometric equations were created to explore the correlation between beak and body growth in *Onykia ingens* and *Nototodarus sloanii*. The resulting regressions were analysed to find the best predictors of body size for use in diet analyses. Beak weights were analysed for the first time and were found to be good predictors of squid size in *O. ingens*; however, rostral lengths were shown to be the best squid size predictors in *N. sloanii*.

The structure and composition of statoliths from both *O. ingens* and *N. sloanii* were analysed using scanning electron microscopy (SEM), Raman spectroscopy and laser-ablation-inductively-coupled-plasma- mass-spectrometry (LA-ICP-MS). Statoliths of both species were shown to consist of calcium carbonate crystals in the aragonitic polymorph. Statoliths of both species contained all 10 of the trace elements that were analysed using LA-ICP-MS (Be, Mn, Mg, Cu, Zn, Sr, Y, Zr, Ba, U) and this was the first time that Be was recorded in squid statoliths. Trace elements were compared between zones within statoliths (inner and outer zones), between locations within *O. ingens* and between species. There were significant differences in some trace elements between zones, locations and species. As trace element incorporation is different depending on location of capture and species, trace elements in statoliths of these two species have the potential to be used as geographic markers.

The trace element composition of beaks of *O. ingens* was analysed using both LA-ICP-MS and solution-based-ICP-MS and 26 trace elements were recorded. This is the first time that trace elements have been reported in squid beaks. Trace element incorporation mechanisms for these squid beaks is unknown; however, recording the presence of trace elements is the first step in gathering this information. Further directions for this research, including its possible use in fisheries forensics, are discussed.

Acknowledgements

This thesis would not have been possible without the support of a large number of people. Thank you to my principal supervisor Prof. Abby Smith, your support over my thesis year when I was a bit too stressed out to write made all the difference. I would also like to thank my two other supervisors: Dr Jean McKinnon, and Dr Kathrin Bolstad, your expertise in all things squid allowed this thesis to happen.

I would like to thank the ALCES lab at AUT: Heather Braid, Aaron Evans and Jesse Kelly (PhD candidates) for all of your hard work, advice and help with dissecting tiny statoliths out of large squid! I would like to thank the National Institute of Water and Atmospheric Research (NIWA) and the crew of the *R.V. Tangaroa* for the collection and donation of the squid samples used in this thesis.

Thank you to all of the staff and students in the marine science department at the University of Otago and the New Zealand Marine Studies Center who gave me advice, helped set things up or just listened to me while I rambled about the troubles of trace element analysis. In particular, thank you to Dr Doug Mackie, Linda Groenewegen and Reuben Pooley for help with microscopes and everything else.

Thank you to Dr Geoff Smith and Prof. Keith Gordon for your donation of time on the Raman Spectrometer and help with interpreting my results. A huge thanks to Bryce Peebles (PhD candidate) for all of your help with my Raman output! I would also like to thank the trace element team in the chemistry department at the University of Otago for help and guidance with my trace element analyses. In particular, I would like to thank Dr Malcolm Reid, Dr Karl Bailey and David Barr for all of your help with the technical side of doing the analyses. I would also like to thank Dr Michael Palin and Rebecca McMullin for helping me to analyse and interpret my trace element data. Thank you to Liz Girvan for your help with SEM.

I would like to thank my parents for their continued support (both moral and financial) over all of my schooling, I couldn't have done it without you. Last, but not least, I would like to thank my partner Ali Rogers for her proof-reading prowess and her ability to make me keep writing even when all I wanted to do was throw my computer out of the window!

Apologies to anyone to anyone that I may have missed, I really appreciated your help.

Table of Contents

Abstract.....	i
Acknowledgements.....	ii
Table of Contents.....	iii
Chapter One: General Introduction.....	1
1 General introduction.....	2
1.1 The anatomy and importance of squid.....	2
1.2 <i>Onykia ingens</i>	3
1.3 <i>Nototodarus sloanii</i>	5
1.4 Squid as prey.....	6
1.5 Hard parts: what they can tell us about the animal?.....	7
1.6 Aim of this thesis.....	9
Chapter Two: Allometric Relationships Between Beak Size and Squid Size in <i>Onykia ingens</i> and <i>Nototodarus sloanii</i>	11
2.1 Introduction.....	13
2.1.1 The hard parts of a squid.....	13
2.1.2 Hard parts in diet analyses.....	19
2.1.3 Aims.....	21
2.2 Methods.....	22
2.2.1 Specimen collection.....	22
2.2.2 Morphometric measurements.....	24
2.2.3 Data analysis.....	24
2.3 Results.....	26
2.3.1 Measurements.....	26
2.3.2 Size-to-weight relationship.....	31
2.3.3 Mantle length vs. beak measurements.....	32
2.3.4 Squid weight vs. beak measurements.....	34
2.3.5 Best predictors of squid biomass.....	34
2.3.6 Eye lens growth in <i>Onykia ingens</i>	37
2.4 Discussion.....	39
2.4.1 Sex and size.....	39
2.4.2 Best predictors of squid biomass.....	40
2.4.3 Eye lens growth in <i>Onykia ingens</i>	41
2.4.4 Findings compared to other studies.....	41
2.4.5 Conclusions.....	45
Chapter Three: Structure and Composition of Statoliths of <i>Onykia ingens</i> and <i>Nototodarus sloanii</i> ..	47
3.1 Introduction.....	49

3.1.1 Structure and composition	49
3.1.2 Hard parts used to understand squid life history	50
3.1.3 Aims of this chapter	51
3.2. Review of methods	52
3.2.1 Common structural analysis methods	52
3.2.2 Common composition analysis methods.....	53
3.2.3 Methods used in this study.....	55
3.3 Methods.....	57
3.3.1 Squid collection and statolith extraction	57
3.3.2 Statolith preparation.....	57
3.3.3 Scanning electron microscopy (SEM).....	58
3.3.4 Raman Spectroscopy.....	58
3.3.5 LA-ICP-MS.....	59
3.4 Results.....	64
3.4.1 SEM	64
3.4.2 Raman spectra	66
3.4.3 LA-ICP-MS.....	70
3.5 Discussion.....	78
3.5.1 Raman shifts and structure	78
3.5.2 Trace elements: what might they mean?	79
3.5.3 Overall statolith chemistry.....	81
3.5.4 Conclusions	86
Chapter Four: Trace Element Composition of Beaks of <i>Onykia ingens</i>	87
4.1 Introduction	89
4.1.1 Aims of this chapter	91
4.2 Methods.....	92
4.2.1 Squid collection.....	92
4.2.2 Beak collection	92
4.2.3 ICP-MS preparation.....	94
4.2.4 Laser ablation preparation.....	94
4.2.5 Solution-based ICP-MS.....	95
4.2.6 LA-ICP-MS spot ablation	95
4.2.7 Data analyses	96
4.3 Results.....	97
4.3.1 Solution based ICP-MS	97
4.3.2 LA-ICP-MS.....	97
4.4 Discussion.....	104
4.4.1 Conclusion.....	106

Chapter Five: General Conclusions	109
Final conclusion.....	114
References	115

Chapter One: General Introduction

1 General introduction

1.1 The anatomy and importance of squid

Squid (order: Teuthoidea) (Fig. 1) are marine invertebrates belonging to the phylum Mollusca. At the posterior end, squid possess a muscular mantle, which contains the majority of the squid's organs (digestive organs, hearts (x3), reproductive organs, gills, and ink sac). On the outside of the mantle, there are fins to aid in swimming and a funnel anterior to the mantle which allows fast swimming using jet propulsion. Anterior to the funnel is the head which houses the eyes, brain, beak, radula and oesophagus. Anterior to the head are eight arms and (typically) two tentacles. Along each of the limbs are suckers ringed on the inside with hard toothed structures called sucker rings. These sucker rings are present in squid and not octopus and their presence is the most reliable way to tell the two taxa apart.

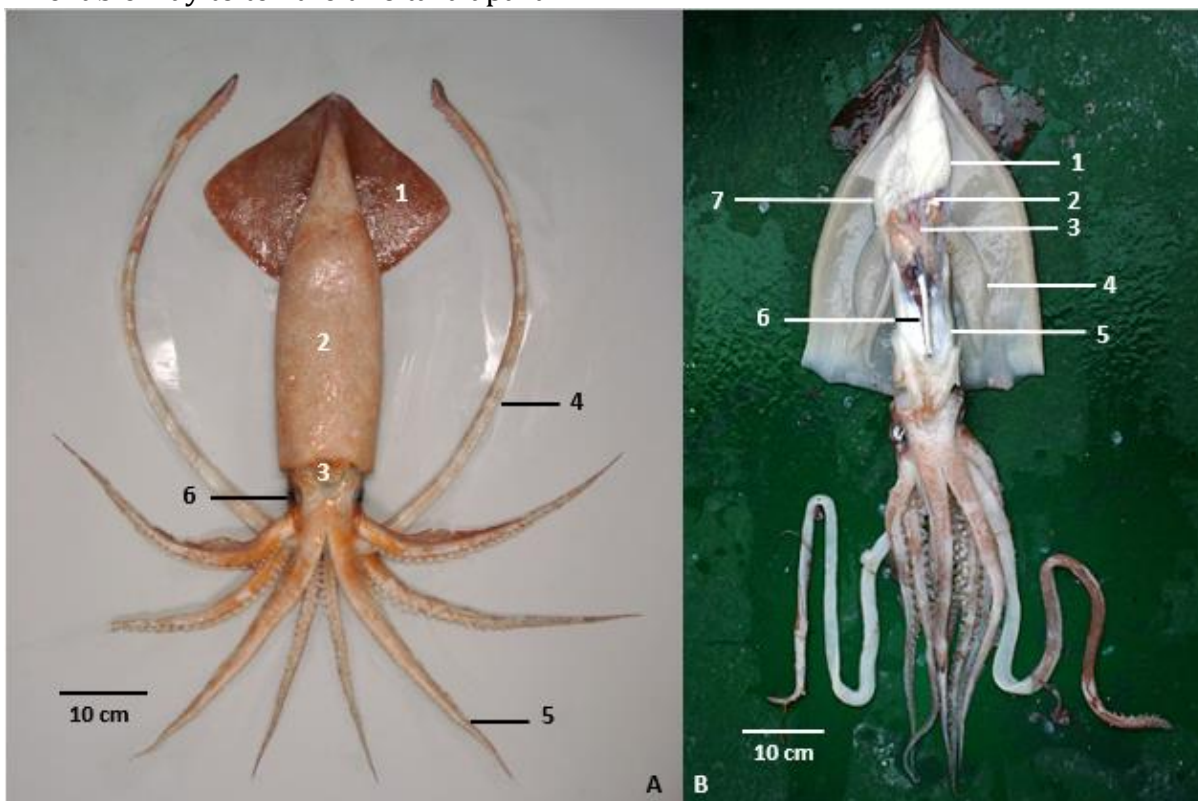


Figure 1: A: ventral view of *Onykia ingens* with scale bar. External features indicated: 1: fins (x2), 2: mantle, 3: funnel, 4: tentacles (x2), 5: arms (x8), 6: eyes. Photo credit: Darren Stevens NIWA. B: ventral view inside a mature male *O. ingens* with scale bar. Internal features indicated: 1: gonad, 2: stomach/caecum, 3: heart (x3), 4: gills (x2), 5: digestive gland/liver, 6: ink sac, 7: Needham's sac. Photo credit: Vladimir Laptikhovskiy.

Squid are a significant food source for a diverse range of marine animals, including giant petrels (*Macronectes* spp.) (Hunter & Brooke 1992), sperm whales

(*Physeter macrocephalus*) (Clarke & Roper 1998) and swordfish (*Xiphias gladius*) (Hernández-García 1995). Animals from many different marine habitats rely on squid for nutrition at some point in their life cycle and many cetaceans feed almost exclusively on squid (Gaskin & Cawthorn 1967, Clarke 1996). Squid exhibit a “live fast, die young” semelparous life-history strategy meaning that most species only live for around one year and die shortly after reproduction. Many species of squid also exhibit different forms of non-asymptotic growth (Jackson et al. 2000a, O’Dor 2000). This growth strategy means that their biomass is turned over very quickly, making them a major resource to other organisms as a source of organic carbon.

It has been suggested that squid could take over the role of top predator in some food webs around the world as we remove large fish from ecosystems through commercial fishing (Rodhouse & White 1995). This possibility means that a good understanding of population dynamics and how squid fit into food webs now is crucial in predicting, understanding and managing future changes to the marine ecosystems.

Squid are a commercial group that are economically important to humans. Of the 290 species of squid around the globe, 30-40 have commercial importance, with the global squid catch being around 4 million tonnes per year in recent years (Arkhipkin et al. 2015). Worldwide, squid fisheries have the possibility to keep growing as there are some species currently being underexploited (Roper et al. 2010). A search of ‘teleost’ in a science journal database (Google Scholar) brings up 172,000 results, ‘cetacean’ brings up 45,800 and ‘teuthoidea’ only brings up 2,070. Squid are a valuable resource both commercially and ecologically, yet they are understudied when compared to marine mammals and fish.

1.2 *Onykia ingens*

Onykia ingens (E A Smith, 1881) (formerly *Moroteuthis ingens*) (Fig. 1) is a deep-sea squid belonging to the family Onychoteuthidae, found in waters around New Zealand. It has a circumpolar distribution between the subtropical and Antarctic polar fronts (Nesis 1987, Jackson 1995, Jackson et al. 1998). It is not a commercial species as it has high concentrations of ammonia in its mantle which allows it to be neutrally, or possibly positively, buoyant as ammonia is less dense than water (Lu & Williams 1994). There has been suggestion of using chemical processes to extract the ammonia from the mantle of these types of squid, making them palatable and worth fishing commercially

(Pierce & Portela 2014). *Onykia ingens* is an important predator of mesopelagic fish and other squid (Jackson et al. 1998, Phillips et al. 2003).

Onykia ingens are caught between ~500 meters and ~1500 meters deep and are thought to undergo an ontogenetic migration to deep waters with maturity (Jackson 1993, Jackson et al. 2000b). The hypothesis of ontogenetic migration in *O. ingens* has been supported for females; however males don't seem to show a clear pattern in depth distribution (Jackson 1997). These squid are also thought to have an epipelagic lifestyle as paralarvae and juveniles, then switch to a predominantly demersal habitat after maturity (Jackson 1993). The mantle of *O. ingens* is streamlined (Fig. 1), but not as streamlined as other squid that spend their lives in the pelagic environment such as *Nototodarus sloanii* (southern arrow squid) (Fig. 2).

Onykia ingens shows remarkable sexual dimorphism where the female grows much larger than the male. Males grow to around 380mm mantle length and attain a weight of ~1400g while females can grow to over 520mm in mantle length and weigh around 6000g (Jackson et al. 2000b). Based on statolith:mantle length growth ratios, on average, female squid grow almost twice as fast as males with females growing 2.11mm/day and males growing 1.13mm/day (Jackson 1997). In addition to being larger and faster growing, female *O. ingens* have a longer life span than males with upper age estimates lying around 393 days for females and 358 days for males (Jackson 1997). The difference in life spans between the sexes is possibly due to the fact that males die shortly after copulation with the females. After spawning the females then migrate to deeper water and deposit their eggs (Jackson 2001).

Reproduction in the Chatham Islands population of *O. ingens* occurs in winter (Jackson 2001) with egg hatching peaking between June and August (Jackson 1997). Reproduction is terminal in *O. ingens* with muscle degeneration occurring with maturity in females and possibly occurring in males (Jackson 2001). This muscular degeneration in spent females means that the mantle is no longer firm and its consistency has been likened to that of a jellyfish rather than a squid (Jackson 2001).

There are two main areas in New Zealand waters in which *O. ingens* are regularly caught and found in predator stomachs: the Chatham Rise (Jackson 1995) and from the south end of the South Island to the Antarctic Polar Front (Jackson et al. 2000b). It is not

clear whether these are two separate populations or whether there is mixing occurring between them.

1.3 *Nototodarus sloanii*

Nototodarus sloanii (Gray, 1849), also known as the southern arrow squid or Wheketere in Māori (Fig. 2) is a pelagic squid belonging to the family Ommastrephidae (subfamily Todarodinae). *Nototodarus sloanii* is found in waters around the South Island and the southeast coast of the North Island, as well as south to the Auckland Islands and west to the Chatham Islands (Jackson et al. 2000b). This species is mainly found in shallower waters than *O. ingens*; they are often caught in waters shallower than 600 meters (Jackson et al. 2000b). *Nototodarus sloanii* has a very streamlined shape (Fig. 2) which aids fast movement through the water allowing it to be an active predator of mesopelagic fishes (Dunn 2009).

Nototodarus sloanii in New Zealand waters has been estimated to have a growth rate between 0.66mm/day and 1.5mm/day (Tung 1978, Mattlin et al. 1985). These squid can attain around 406mm in mantle length (Uozumi & Ohara 1993, Jackson & McKinnon 1996, Uozumi 1998) and can weigh over 1300g (Jackson & McKinnon 1996). *Nototodarus sloanii* upper age estimates lie around 374 days (Uozumi & Ohara 1993, Uozumi 1998). There seems to be no significant difference in growth between sexes when the squid are smaller than 25-30cm; however females grow faster past this size class (Uozumi & Ohara 1993).

Nototodarus sp. are the target of the only commercial cephalopod fisheries in New Zealand waters (Dunn 2009). They are much more palatable than *O. ingens* as they don't have high levels of ammonia in their mantle. This fishery consists of two very closely related species of ommastrephid: *N. sloanii* and *N. gouldi*. *Nototodarus sloanii* lives in and to the south of the subtropical convergence and *N. gouldi* occurs to the north of the convergence; both of these species are managed as separate stocks of one fishery (MPI 2013). There are also two separate stocks of *N. sloanii*, a mainland stock and a stock in the Sub-Antarctic Islands called the SQU 6T (Southern Islands fishery). The SQU 6T stock is managed separately as there is little finfish bycatch and a larger amount of Hooker's sea lion (*Phocarctos hookeri*) bycatch (MPI 2013).

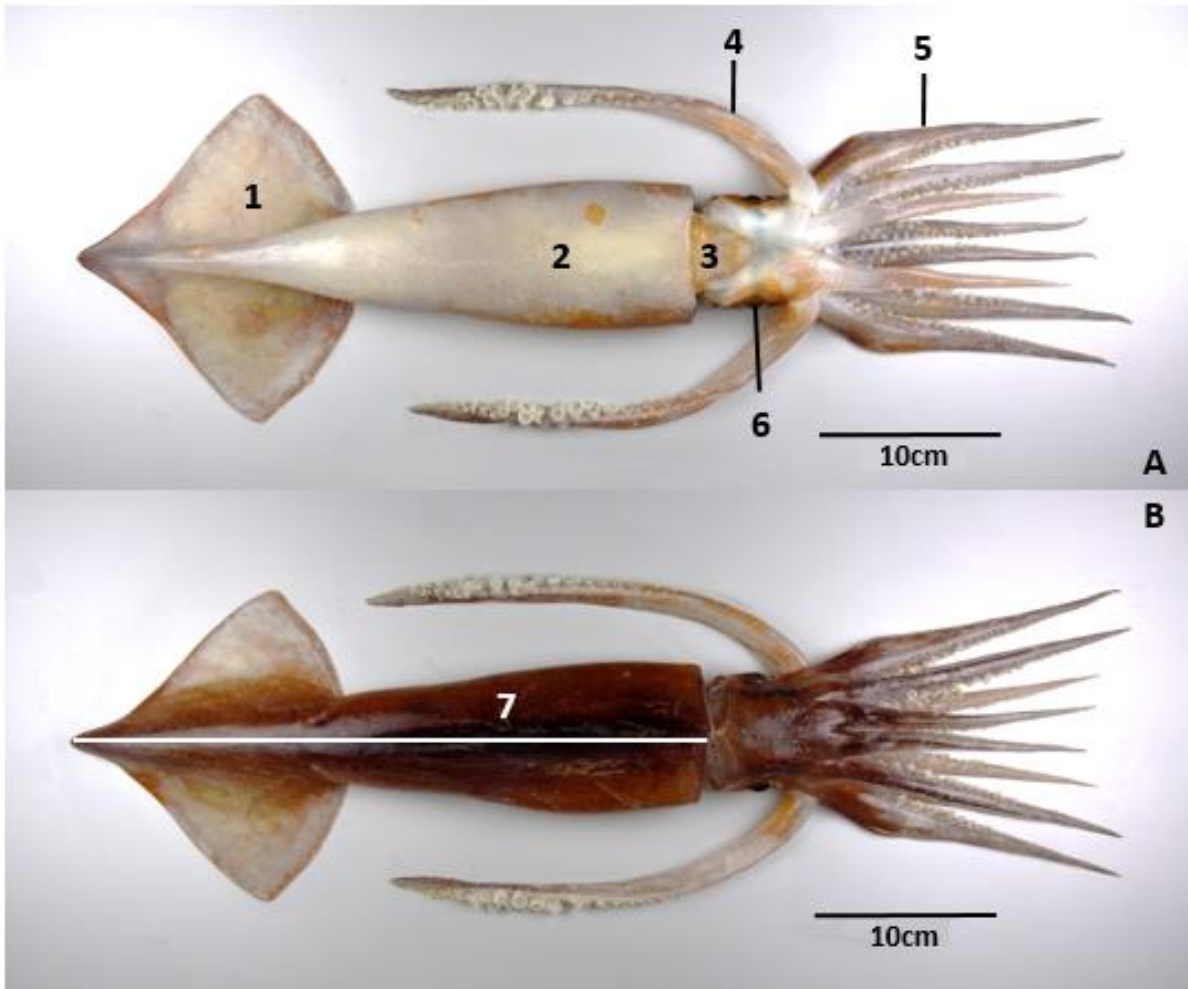


Figure 2: *Nototodarus sloanii* with scale bar and external features labeled. A: ventral view, labels: 1: fins (x2), 2: mantle, 3: funnel, 4: tentacles (x2), 5: arms (x8), 6: eyes (x2). B: dorsal view, labeled: 7: mantle length. Photo credit: Darren Stevens NIWA.

1.4 Squid as prey

Squid are important in the diets of many large vertebrates in New Zealand waters that are both ecologically and economically important. *N. sloanii* is important in the diets of the commercial fish including hake (*Merluccius australis*), hoki (*Macruronus novaezelandiae*), ling (*Genypterus blacodes*), red gurnard (*Chelidonichthys kumu*) and southern blue whiting (*Micromesistius australis*) (Stevens et al. 2012). *Nototodarus sloanii* is also important in the diet of large marine mammals such as New Zealand fur seals (*Arctocephalus forsteri*) (Fea et al. 1999, Boren 2008) and common dolphins (*Delphinus* sp.) (Meynier et al. 2008). *Onykia ingens* is important in the diet of large, ecologically important, marine mammals such as sperm whales (*Physeter macrocephalus*) (Gaskin & Cawthorn 1967, Clarke & Roper 1998) and large sea birds including king penguins (*Aptenodyes patagonicus*) (Cherel et al. 2002). *Onykia ingens*

also makes up a portion of the diet of many commercial fish species such as hoki, southern blue whiting, and small-scaled notothenoid (*Notothenia microlepidota*) (Clark 1985).

To successfully conserve and manage commercially and ecologically important predators, there needs to be an understanding of where the species fits in the food web. We can infer diets of predators (and therefore infer their place in the food web) primarily by analysing their stomach contents and scat (Clarke & Roper 1998, Cherel et al. 2002, Boren 2008). Diet analysis that use these methods rely primarily on hard parts of prey that either resist digestion completely or dissolve slowly in stomachs. Squid beaks are very resistant to digestion and their morphology is species-specific which allows identification of squid as prey (Bolstad 2006).

1.5 Hard parts: what they can tell us about the animal?

Squid live in a complex three dimensional environment and are active predators; to aid them in this life-style they have specialised organs that often require hard parts to function. Squid have a hard beak and radula to break up their food; two eye lenses to focus light onto their retinas for vision; a gladius (sometimes referred to as a pen) which is thought to be the remnant shell of the mollusc; two statoliths for acceleration reception (Budelmann 1988); and sucker rings/hooks on their arms and tentacles that are used to hold on to prey and occasionally used in mating. All of these hard parts can be used to tell us particular things about the squid's life history, but beaks and statoliths are among the most often studied. Statoliths are often used to age squid and estimate their growth rates (Rodhouse & Hatfield 1990, Natsukari & Komine 1992, Arkhipkin & Shcherbich 2012) . Beaks often stay in a predator's stomach long after ingestion meaning that they can be used in diet analyses (Gaskin & Cawthorn 1967, Clark 1985, Stevens et al. 2012)

The beak of a squid is a structure made of chitin that sits inside the arm crown (Fig. 3) and macerates food before it is swallowed. Food must be broken into small pieces before the squid swallows it as the oesophagus of the squid passes straight through the middle of the brain (Budelmann 1990). Beaks can also be used to age squid; however, as they are actively used to cut flesh and bone, the tip of the beak erodes over time which masks the age lines, making estimates less accurate (Liu et al. 2015a).

Beaks are resistant to digestion and therefore are often found in the stomach contents of predators (Gaskin & Cawthorn 1967, Clark 1985, Hunter & Brooke 1992, Cherel et al. 2002). Squid species can be identified by their unique beaks (Gaskin & Cawthorn 1967, Clarke 1996, Bolstad 2006) and a relationship between beak size and squid size can be constructed, allowing a prey biomass estimate to be calculated (Jackson & McKinnon 1996, Jackson et al. 1997, Bolstad 2006). There have been recent efforts by researchers using stable isotopes of beaks from predators' stomachs to better understand the trophic position and foraging areas of cephalopods in their original food web (Cherel & Hobson 2005, Cherel et al. 2009). Trace-element analysis of beaks has been suggested as the next step in these post-mortem beak analyses to further identify the habitats and populations of the squid (Cherel et al. 2009).

Statoliths are paired calcium carbonate structures located in the cephalic region of the squid inside the cartilaginous skull (Fig. 4a). They sit inside paired organs called statocysts and are attached at one end while floating in a liquid that is roughly the same density as the water outside the animal. The statocysts are responsible for the reception of acceleration and gravitational information by the squid (Stephens & Young 1978).

Statoliths grow in layers that are thought to be deposited daily (Rodhouse & Hatfield 1990) which allows aging of the squid by sectioning the statolith (Fig. 4c). However, validation of daily ring deposition is difficult in squid, especially large, deep sea species like *O. ingens*, as it is not easy to keep squid alive in captivity and other age validation methods, such as tagging, encounter problems due to short life cycles and high mortality rates (Jackson 1997). Trace element analysis has been used in squid statoliths in the past for their potential use as environmental recorders. The incorporation of individual elements into statoliths have been correlated to environmental factors, such as a link between strontium incorporation and sea temperature (Arkhipkin et al. 2004).

Statoliths have two distinct 'zones', an inner opaque zone and an outer translucent one. It has been hypothesized that these zones are due to a structural difference in the crystals that compose the statolith. This structural difference has been suggested to reflect a change in life style from an epipelagic lifestyle to a demersal one in *O. ingens* (Jackson 1993).

1.6 Aim of this thesis

The hard parts of two common New Zealand squids, *Onykia ingens* and *Nototodarus sloanii*, were examined in order to better describe and understand their life histories, distributions, and contribution to the food web. *Onykia ingens* and *N. sloanii* exhibit two of many different life-history growth strategies that are utilised by squid. These different life strategies reflect only two of the niches that different species of squid occupy over the world. The life history strategies of squid, while variable in some aspects, are also surprisingly universal in others, such as a short, one to two year life span. The variability in life history strategies while having a fast generational turn-over means that squid, as a global group, are an efficient nutrient vector in oceanic ecosystems and have the potential to withstand large changes in their ecosystem. These life-history traits give squid the ability to quickly fill gaps in trophic webs that appear due to over-fishing (Baum & Worm 2009). This ability has the possibly to reduce, negate or amplify the effects of over-fishing; however, it is difficult to predict this without knowing more about squid and where they fit in to food webs around the world. More information is needed on the growth rate and population sizes of both commercial and non-commercial squid so that the effects of fishing can be understood.

Analyses were made using morphometrics, Raman Spectroscopy, ICP-MS, LA-ICP-MS and SEM. These aims will be addressed in three chapters; the first will address the morphometric relationships between hard parts and squid size; the second will focus on the structure and composition of statoliths; and the last will investigate the trace element composition of beaks.

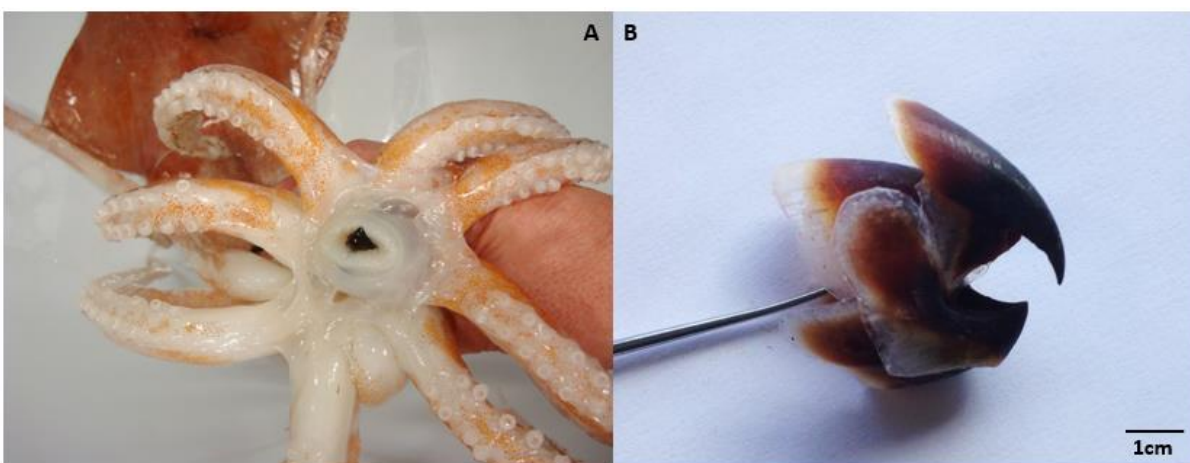


Figure 3: *Onykia ingens* beak. A: open arm crown showing beak, photo credit: Darren Stevens NIWA, B: beak removed from squid.

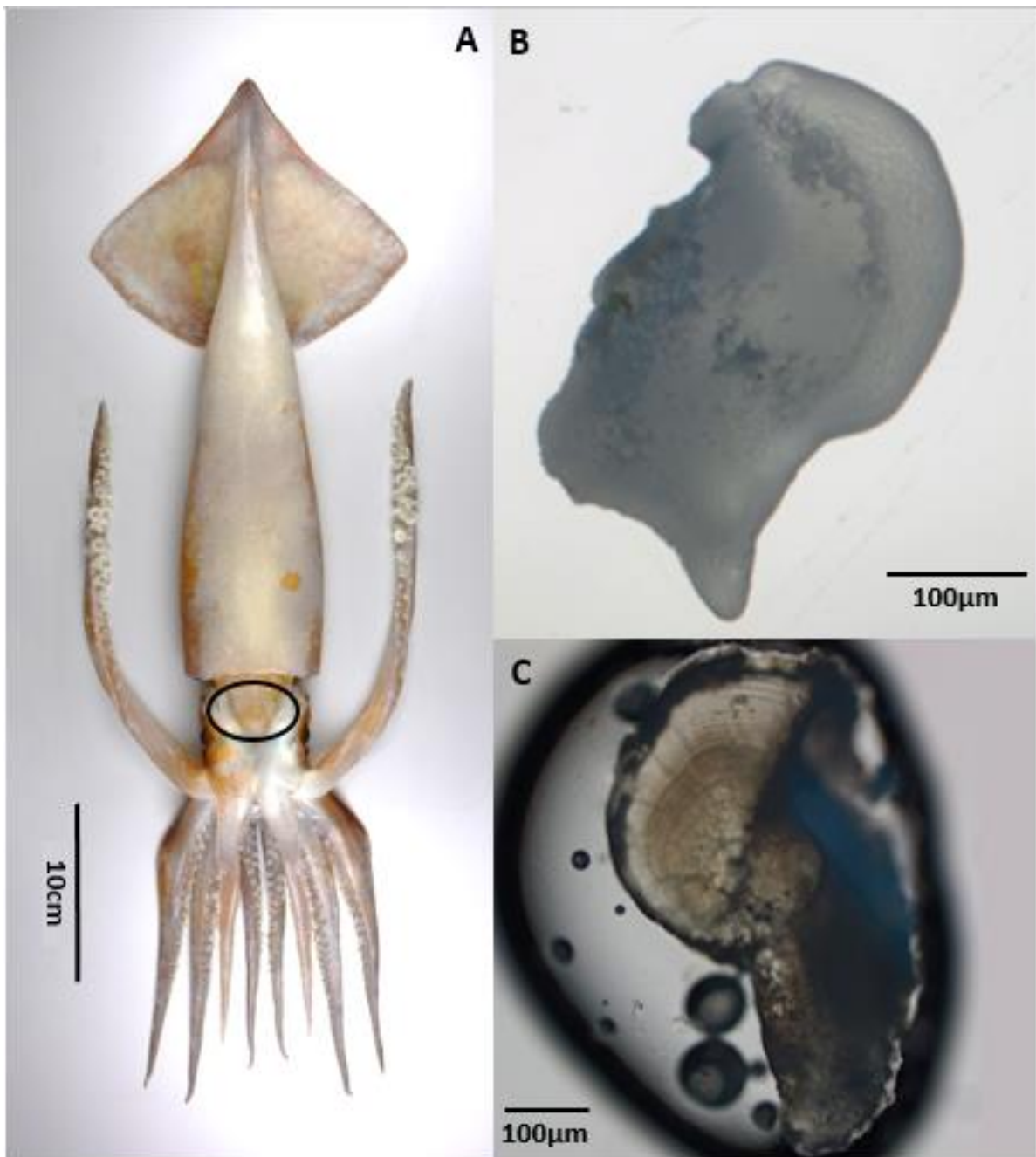


Figure 4: A: *Nototodarus sloanii* with statolith area circled, photo credit: Darren Stevens NIWA, B: whole statolith, C: Statolith sectioned to show growth lines.

Chapter Two: Allometric Relationships
Between Beak Size and Squid Size in *Onykia*
ingens and *Nototodarus sloanii*

Table of Contents

2.1 Introduction	13
2.1.1 The hard parts of a squid.....	13
2.1.1.1 Gladius	13
2.1.1.2 Eye lenses	14
2.1.1.3 Beak	16
2.1.1.4 Statoliths.....	17
2.1.1.5 Sucker rings	18
2.1.2 Hard parts in diet analyses	19
2.1.3 Aims	21
2.2 Methods	22
2.2.1 Specimen collection.....	22
2.2.2 Morphometric measurements.....	24
2.2.3 Data analysis.....	24
2.3 Results	26
2.3.1 Measurements	26
2.3.2 Size to weight relationship	31
2.3.3 Mantle length vs. beak measurements	32
2.3.4 Squid weight vs. beak measurements	34
2.3.5 Best predictors of squid biomass	34
2.3.6 Eye lens growth in <i>Onykia ingens</i>	37
2.4 Discussion.....	39
2.4.1 Sex and size	39
2.4.2 Best predictors of squid biomass	40
2.4.3 Eye lens growth in <i>Onykia ingens</i>	41
2.4.4 Findings compared to other studies	41
2.4.5 Conclusions	45

2.1 Introduction

2.1.1 The hard parts of a squid

Hard parts of animals are more resistant to post-mortem decomposition and digestion than soft parts. Hard remains can be used to gain information about the life of a deceased animal such as: species, age, cause of mortality, perhaps even provenance. The information gained from hard parts can also be used to study parameters of a population such as age structure (Arkhipkin & Shcherbich 2012), growth (Natsukari & Komine 1992) and trophic ecology (Cherel & Hobson 2005).

Squid tissues are generally soft, but there are exceptions to this. Squid have specialised organs distributed through the body, many of which are mineralised or sclerotised (Fig. 2.1). Squid have a chitinous gladius (or 'pen') (Fig. 2.1D) running dorsally along the length of the mantle which provides some overall body strengthening along with sites for muscle attachment (Yang et al. 2014). Squid eye lenses, each split into two halves, or 'hemispheres' (Fig. 2.1F), focus light onto their retinas for vision. Squid eat using a hard chitinous beak (Fig 2.1B) and radula encapsulated within a buccal mass. Calcium carbonate statoliths (Fig. 2.1C) lie inside small paired cavities called statocysts, in the cephalic region for acceleration reception (Budelmann 1988). Finally, sclerotised sucker rings/hooks (Fig. 2.1E) on their arms and tentacles assist squid with holding on to prey and may serve additional sexual functions in some groups. These hard parts are thought to have developed alongside analogous structures (e.g., jaw, eye lenses, spine) in teleost fish due to convergent evolution and competition pressures (Packard 1972). In this introduction, I will provide a review of the known composition, morphology and function of the hard parts of squid and make suggestions for further investigations.

2.1.1.1 Gladius

The gladius is an internal remnant of the molluscan shell (Arkhipkin & Perez 1998). The structure of the gladius consists of a central axis (the rachis), thin lateral expansions (the vane) and a terminal conus (Fig. 2.2) (Arkhipkin & Perez 1998). The internal structure of the gladius is analogous to the shell in other molluscs, in that it has a medium layer (ostracum), an inner layer (hypostracum) and an outer layer (periostracum). The gladius is made up of a chitin-protein complex with the chitin

having a β -crystalline structure (Hunt & Nixon 1981). The gladius of a squid gives sites for muscle attachment and allows the coordinated contraction of the mantle (Yang et al. 2014). The gladius also may provide some overall strengthening to the mantle of the squid keeping it in a streamlined shape (Yang et al. 2014).

Squid gladii follow a variety of forms and species that inhabit similar niches have similarly shaped gladii; therefore, the overall shape of the gladius can give information on the lifestyle of the squid (Arkhipkin & Perez 1998). In most species, the gladius runs the entire length of the squid's mantle which means that the gladius length can be used as a proxy for mantle length. The gladius is secreted in layers that have been validated to have a daily periodicity in some species and can be used to age squid and deduce their growth rate (Arkhipkin & Perez 1998, Perez & O'Dor 2000, McKinnon 2006, Perez et al. 2006). Gladius deposition rates were used in *Loligo plei* to decipher differing growth rates over the life history of the animals (Perez et al. 2006). This study showed that individuals of *L. plei* employed both linear and exponential growth strategies at different stages of their lives. The growth lines from the squid's juvenile period, however, may be masked as the squid grows older meaning that aging from the gladius can result in underestimations of age (Perez et al. 2006).

2.1.1.2 Eye lenses

Squid rely heavily on eyesight to catch their prey, with optic lobes containing 50 – 80% of the brain's neurons (Saibil 1990). The cephalopod eye and the teleost eye are surprisingly similar in terms of form and function (Packard 1972). The squid eye has a spherical lens that is split into two hemispheres (Fig. 2.1F) which work together to focus light onto the retina (Sivak et al. 1994). The muscles of the eye move the lens back and forth much like a camera lens (Packard 1972). The lens of a squid eye, with its spherical shape and camera-like focus, allows the squid to have good vision as it has a short focal length which in turn allows for a theoretically infinite depth of field (Packard 1972).

Eye lens size has the potential to show how the structure grows and develops as the squid grows. This can be done by plotting lens size against animal size or analysing the refractive index of lenses of animals of different ages (Sivak et al. 1994). The eye lens of a squid can be analysed post mortem to discern the focal length of the lens along with other aspects of the eye and therefore infer vision capabilities (Sivak 1982, Nilsson

et al. 2012). It was found that the eyes of *Sepioteuthis lessoniana* had reached their optical 'peak' when the squid were 7 to 9 weeks old (Sivak et al. 1994). The eye can be compared to vertebrate counterparts (teleost fish eyes) to explore convergent evolution (Packard 1972). Stable isotopes, such as carbon and nitrogen, in lens tissue have also been used to infer the geographic natal origin of squid (Onthank & Lee 2013).

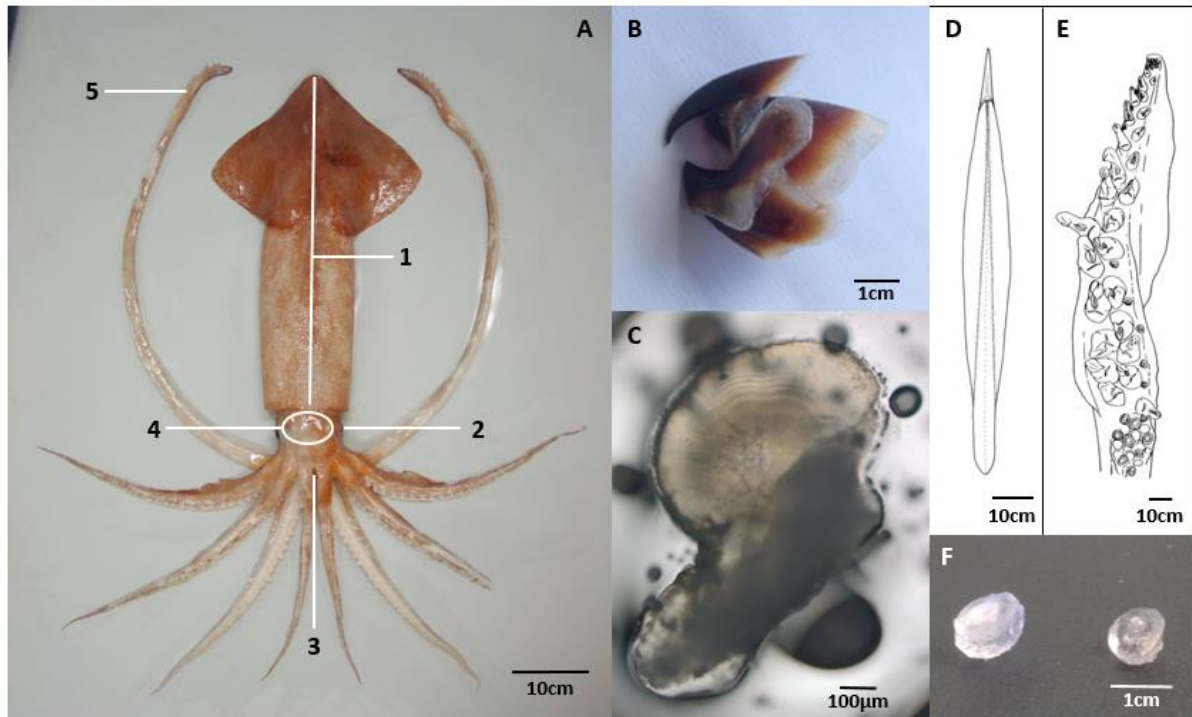


Figure 2.1: The location of hard parts in *Onykia ingens* and their morphology. A: mature *O. ingens* with locations of hard parts labelled, 1: gladius; 2: eye lens; 3: beak; 4: statoliths; 5: sucker rings and hooks, photo credit: Darren Stevens, NIWA. B: upper and lower beak. C: cross-section of a statolith. D: drawing of a gladius from *O. ingens* (Bolstad, 2010, p. 154, Fig. 47). E: tentacle club with sucker rings and hooks (Tsuchiya & Okutani, 1991, p. 145, Fig. 35). F: one eye lens split into its two hemispheres.

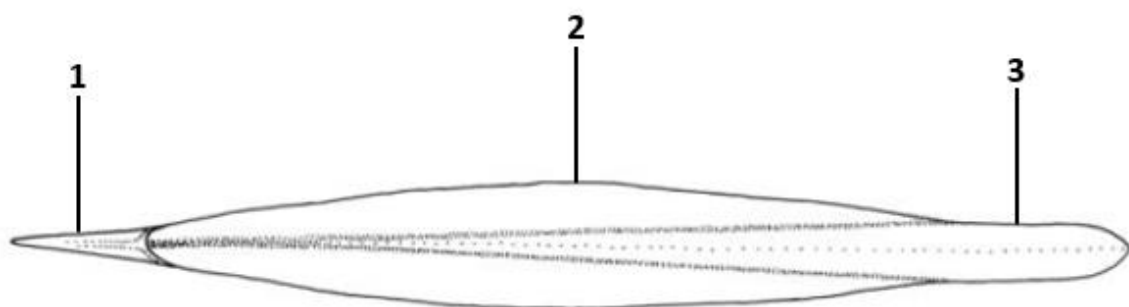


Figure 2.2: Labeled gladius of *O. ingens*, 1: terminal conus; 2: vane; 3: rachis. Drawing from Bolstad, 2010, p. 154, Fig. 47.

2.1.1.3 Beak

The beak is located in the middle of the arm crown within a bulb of muscle called the buccal mass. The beak consists of an upper and a lower half (Fig. 2.1B). The lower beak has two wings which allow for muscle attachment and both halves of the beak have a tip with sharp cutting edges. The beak is made of a chitin-protein complex similar to that of the gladius; however, the chitin in the beak has an α -crystalline structure rather than a β -structure. The beak has a stiffness gradient from soft and flexible at the wings, to help with muscle attachment, to hard and stiff at the tip and cutting edge. This gradient is controlled by the ratio of protein to chitin and the water content of the beak material (Miserez et al. 2008).

The buccal mass holds the beak in place by the wings of the beak, using muscular contractions to open and close the beak (Miserez et al. 2008). The sharp rostral edges of the beak allow the squid to slice prey while the radula manipulates and rasps it. The food then passes through the oesophagus which runs through the middle of the squid's donut-shaped brain (Budelmann 1990). This layout means that any pieces of food ingested must be smaller than the hole in the middle of the brain.

The beak can be used to infer the size, age and even the sex of the individual in some species (Jackson 1995, Bolstad 2006, Xavier et al. 2007, Liu et al. 2015a). The relationship between rostral length of the beak (Fig. 2.3B) and body weight or mantle length of the squid gives an equation which can then be used to back-calculate the original size (Gaskin & Cawthorn 1967, Jackson 1995, Bolstad 2006). These allometric equations are useful when designing management tools for important predators of squid as they give a realistic estimation of overall biomass consumed (Clark 1985).

Counting growth rings in beaks is not commonly used to age squid; however, it can be done as growth rings seem to be laid down with a daily periodicity in at least some species (Liu et al. 2015a). Beaks are not often used for aging because the tip of the beak wears as the squid eats prey over its life, destroying its juvenile growth marks (Liu et al. 2015a). Beaks can also give information on how the taxa consume prey (Voight 2014) and how the beaks work when the animal is living (Miserez et al. 2008). Stable isotopes from beaks can be analysed to study the trophic ecology of the species which is helpful in deep-sea species whose ecology is not well known (Cherel & Hobson 2005, Ruiz-Cooley et al. 2006).

2.1.1.4 Statoliths

The statocysts are paired fluid-filled chambers located within the cartilaginous cephalon (“skull”) of the squid. Each statocyst contains a hard statolith. Statolith shape is apparently species-specific but they are always very small (less than ~2mm) and have the same basic components (Clarke 1978). There are four main parts to a statolith: the lateral dome, dorsal dome, rostrum and the wing (Clarke 1978) (Fig. 2.3A). The statolith is attached to the statocyst at one point and the rest is suspended in the fluid of the statocyst which has the same density as the external environment (Dilly 1976). The statoliths are made predominantly of CaCO₃ in the aragonite polymorph embedded in a protein matrix (Radtke 1983, Arkhipkin & Perez 1998).

The statocysts work as acceleration receptors for both gravity and movement (Budelmann 1990). These statocysts allow the squid to orient itself within the water column and therefore aid in finding and catching prey. The statolith has a higher density than the surrounding fluid meaning that when the squid accelerates, the statolith lags behind and touches sensory epithelia in the statocyst. This information is then processed and interpreted as movement and orientation (Budelmann 1990).

Statoliths increase in size as a squid ages by the addition of layers to the outside of the statolith. Statoliths can be sectioned through their medial axis to expose these growth layers, or rings (Fig. 2.4), which have been validated as daily increments in a growing number of species (Hurley et al. 1985, Nakamura & Sakurai 1991, Jackson & Forsythe 2002, Aguiar et al. 2012). These rings can be used to both calculate squid age and infer squid growth as they age (Jackson & Choat 1992, Jackson 1994). The validation of growth rings at a daily level means that statolith aging is potentially an accurate and high-resolution method of aging squid; growth increments do not tend to get lost or masked as they do in other structures, such as beaks (Arkhipkin & Shcherbich 2012). Statoliths are the most commonly used hard part when aging squid (Morris & Aldrich 1984, Lipinski 1986, Arkhipkin & Shcherbich 2012). However, it is difficult to keep squid alive in captivity, particularly large, deep-sea species such as *Onychia ingens*, which means that validating growth- ring periodicity in these types of squid is not as straightforward, nor as prominent in the literature as those that are easier to keep in culture.

The stable isotope history of statoliths has the potential to be used to infer the ecological history of the animal and it has been used to infer the habitat of giant squid (Landman et al. 2004). The trace element history of statoliths can also be analysed. The ratios of different trace elements to calcium have been suggested to correlate to different environmental conditions (Zumholz et al. 2007b).

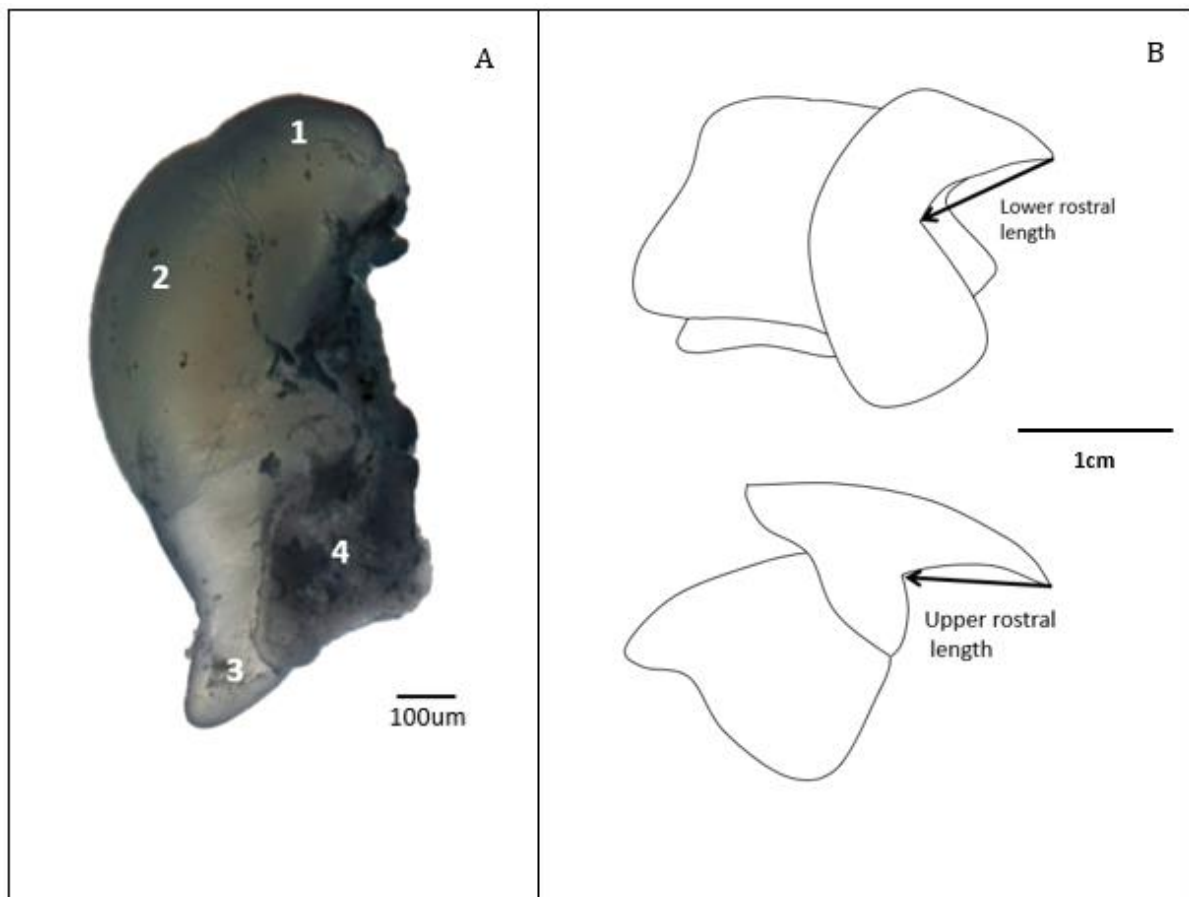


Figure 2.3: Beak and statolith. A: labeled statolith from *Nototodarus sloanii*. 1: dorsal dome; 2: lateral dome; 3: rostrum; 4: wing. B: standard upper and lower rostral length measurements from a beak.

2.1.1.5 Sucker rings

One of the main morphological features that divides squid and octopus is the presence of hard, often toothed, structures along the inside edge of the suckers on the arms of squid where octopus have muscular disks. These sucker rings are sclerotised, non-chitinous structures appearing to be almost entirely proteinaceous with high concentrations of glycine, tyrosine and histidine (Miserez et al. 2009).

Sucker rings are often used to hold struggling prey; the sucker muscles can contract to dig the sucker ring teeth (which are present in most species) into prey and hold on, possibly giving more gripping power than suction alone as used in octopus (Miserez et al. 2009). In some families (such as Onychoteuthidae, the family of *O. ingens*), some paralarval sucker rings transform into hooks with ontogeny (Fig. 2.1E). In some groups of squid, the hooks primary function may be sexual, as suggested for *Lepidoteuthis grimaldii* where the only the males have large 'sabre-like' hooks (Jackson & O'Shea 2003).

In *Onykia ingens*, a small number of sucker rings are present on the tentacle clubs through maturity, but the majority of suckers develop into hooks during early ontogeny (Fig. 2.1E); the arms possess smooth-ringed suckers throughout the life span (Bolstad 2010). *Nototodarus sloanii*, on the other hand, has no hooks, and possess toothed sucker rings down each arm (excluding both arms IV in males as they are hectocotylized) and on each tentacle club (Fig. 2.5) (Roper et al. 2010).

2.1.2 Hard parts in diet analyses

Some of the hard parts of squid play a role in diet analyses when a predator has eaten squid. Often hard parts can be recovered from the remains or stomach contents of a predator (Gaskin & Cawthorn 1967, Hunter & Brooke 1992, Cherel et al. 2002). The information extracted from the analysis of these hard parts can be used to help manage or conserve both the predator and the squid.

The hard parts of squid have varying degrees of resistance to dissolution, especially when the squid has been ingested by a predator or the animal has died by natural causes. The gladius, sucker rings and the eye lenses dissolve rapidly in a predator's stomach after ingestion as the gladius and sucker rings are thin and the eye lens is soft. The statoliths of squid dissolve rapidly when exposed to acidic conditions as they are small and made of fairly soluble CaCO_3 (Arkhipkin & Perez 1998). Beaks resist dissolution for the longest period of time after being ingested by a predator and, thus, are often found in the predator's stomach (Gaskin & Cawthorn 1967, VanHeezik & Seddon 1989). Beaks are resistant to dissolution, and can be useful for species identification and age/size determination. Beaks are therefore the preferred hard part for use in diet analysis studies of those animals that eat whole squid such as seals,

seabirds, and turtles (Clark 1985, Hunter & Brooke 1992, Jackson 1995, Clarke & Roper 1998, Cherel et al. 2002).

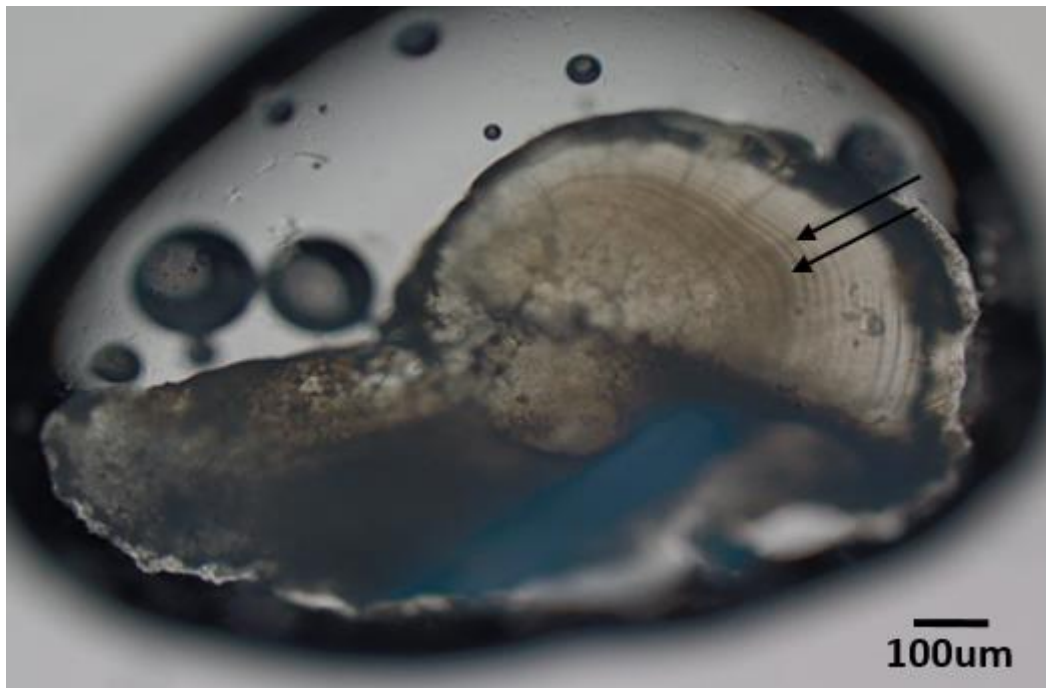


Figure 2.4: Sectioned statolith from *O. ingens*; arrows indicate prominent growth lines.

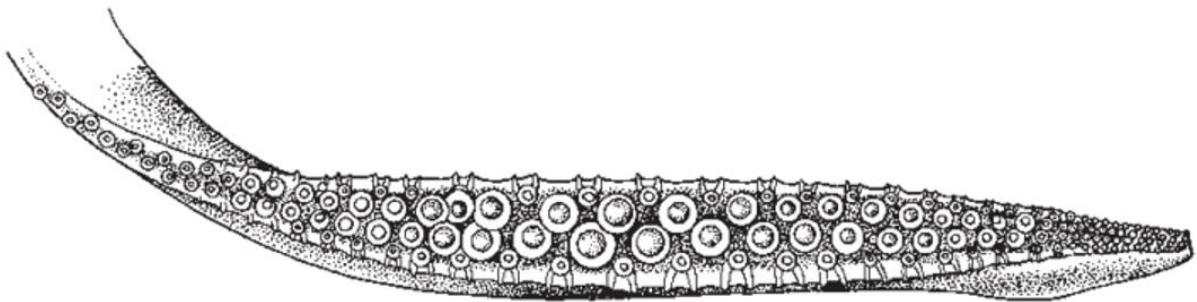


Figure 2.5: Tentacle club of *N. sloanii* with sucker rings shown, drawing from Roper et al. 2010 p. 337, Fig. 319.

2.1.3 Aims

The use of beak measurements (rostral lengths (Fig. 3B)) to predict squid biomass (mantle length or squid weight (Fig. 2.1A)) is well established in the literature (Gaskin & Cawthorn 1967, Hernández-García 1995, Fea et al. 1999, Boren 2008). Past studies have analysed the allometric relationship between rostral length and squid size in both *O. ingens* (Jackson 1995, Bolstad 2006) and *N. sloanii* (Clarke 1986, Jackson & McKinnon 1996) in New Zealand waters. It has been suggested that beak weight may also be a good predictor of squid biomass, and its relationship with squid size may give more information on how the structure grows (Jackson 1995).

In this chapter I aim to validate and extend the relationships between rostral length and squid size in *O. ingens* and *N. sloanii* via the addition of new data. In particular, I will compare the relationships between rostral length and squid size over the life history of both *O. ingens* and *N. sloanii*. This chapter also aims to give a preliminary analysis of the use of beak weight as a predictor of original squid biomass in both *O. ingens* and *N. sloanii* and to examine the relationship between eye lens size and squid size in *O. ingens*. This analysis will give a preliminary insight into the growth of eye lenses over time. Characterisation of statoliths will be covered in later chapters. Gladii and sucker rings are not being investigated further as they are not so useful in dietary analysis due to rapid dissolution.

2.2 Methods

2.2.1 Specimen collection

Onykia ingens were collected on two summer trawl surveys; the first (TAN1117) was carried out between the 24th of November and the 23 of December 2011 in the Sub-Antarctic by scientists from NIWA aboard the *RV Tangaroa*. All squid used from TAN1117 were collected at one station on the 2nd of December at 49°35.23'S 175°26.11'E at a depth of 600m to 800m at a temperature of 8°C (Fig. 2.6) (Bagley et al. 2013). The second survey (TAN1401) was carried out from the 1st of January to the 28th of January 2014 on the Chatham Rise by scientists from NIWA and AUT University on the *RV Tangaroa*. Squid used were collected from 11 different stations over the Chatham Rise, from depths ranging from 460m to 1222m with a temperature range of 5°C to 8°C (Fig. 2.6) (Stevens et al. 2015). These samples were tagged with the locality where they were collected, then frozen on board and sent to AUT. In 2014 the specimens were defrosted and dissected. For each specimen, body length (ML) and weight (W) were measured. Hard parts (beaks, eye lenses and statoliths) were collected for analysis. The sex of each specimen was determined during dissection where possible. The subsamples collected were then taken back to Portobello Marine Laboratory and stored at -20°C until measurements could be made.

Nototodarus sloanii individuals were caught between the Chaslands and Waikawa off of the South Island of New Zealand in approximately 50m of water in April 2015 as part of the commercial arrow squid fisheries. Temperature data for these squid were not taken. These squid were taken into the University of Otago for use in teaching at the New Zealand Marine Studies Centre in Portobello, New Zealand. Sex, mantle length and body weight measurements were taken from each specimen by high-school students before dissection and the hard parts (beaks and statoliths) were removed by myself post-dissection. Each specimen and associated samples were then labelled and frozen at -20°C until measurements could be made.

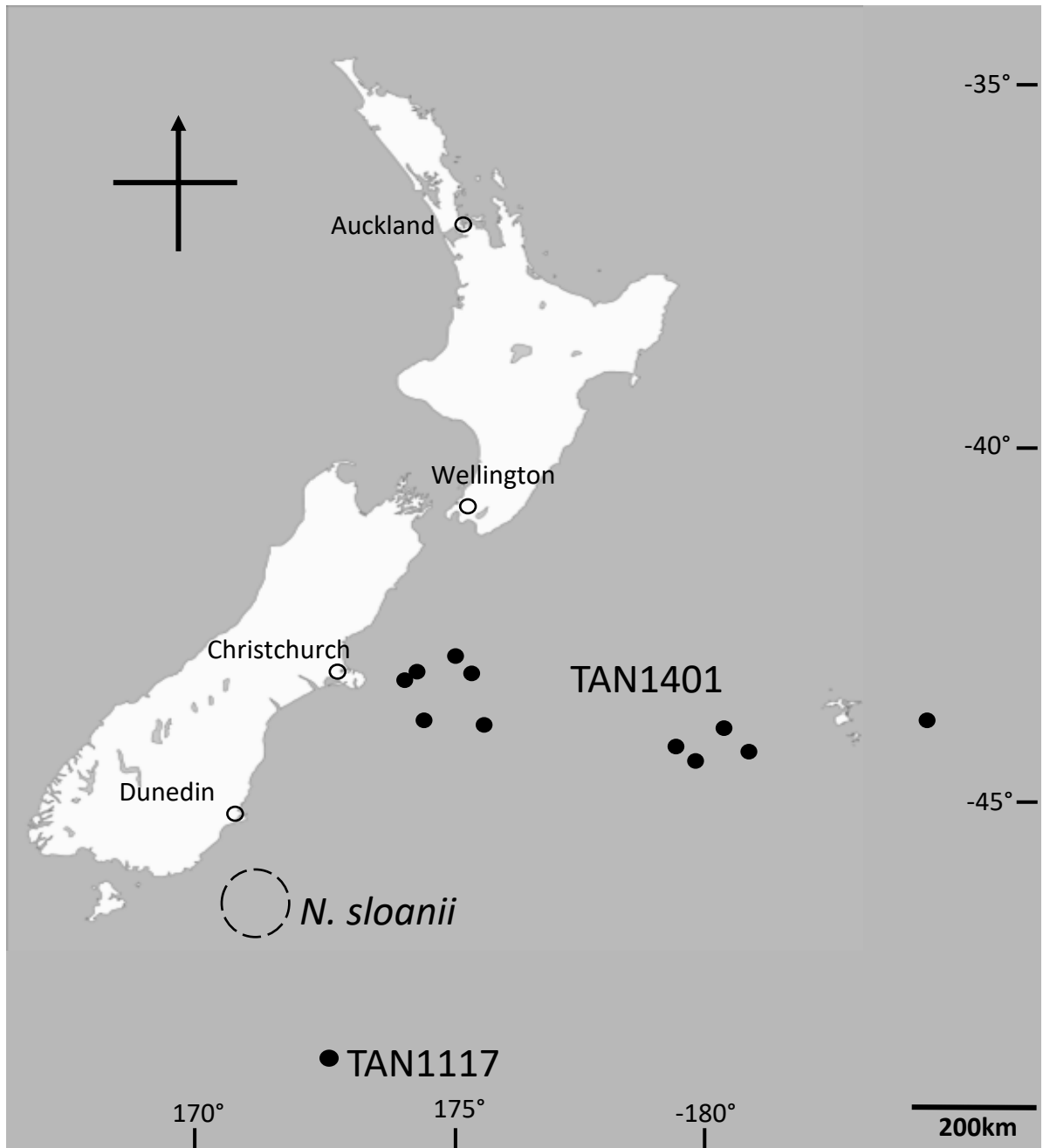


Figure 2.6: Locations where squid were caught; black dots, *O. ingens* (TAN1401 and TAN1117); *N. sloanii* dotted circle.

2.2.2 Morphometric measurements

Beaks were dissected from *O. ingens* and frozen in April and June 2014, then thawed at room temperature in October 2014 for measurement. Beaks from *N. sloanii* were dissected and measured in July 2015. Lower rostral length (LRL) (Fig. 2.3B) and upper rostral length (URL) (Fig. 2.3B) of each squid were measured using digital callipers with a PC interface. LRL was measured from the outside of the beak. During mating, there is erosion of a cartilaginous zone on the lower beak at the end of the cutting edge (Bolstad 2006). When males with this zone were measured, the middle of the curve within the zone was taken to be the end of the rostrum. Calliper measurements were taken three times and the mean of the measurements was calculated and used as the final measurement. The weight of the upper and lower beaks were measured to ± 0.1 mg (Fig 2.8) and the overall beak weight was calculated.

Eye lenses were dissected from *O. ingens* and frozen in April and June 2014, then thawed at room temperature in October for measurement, the lens from the left eye was used where possible. Eye lens diameter (Fig. 2.7B) and weight of one whole eye lens (both hemispheres) were measured from each squid (Fig. 2.7C). Lens diameter was measured using a digital calliper with a PC interface (Fig. 2.7A). Calliper measurements were taken three times and the mean was calculated and used as the final measurement. Weight was measured to ± 0.1 mg.

2.2.3 Data analysis

Data were analysed by carrying out regressions and comparing trend lines and r^2 values between paired measurements. Relationships between beak and biomass were separated by sex for *O. ingens* as they exhibit a large degree of sexual dimorphism (Jackson 1995), but relationships where sex was pooled were also observed.

Data were not log-transformed so that growth curves were able to be visualised. P values were found for each regression. Regression analyses were done in Microsoft Excel (2010) and p values were analysed using R (v.3.2.0).

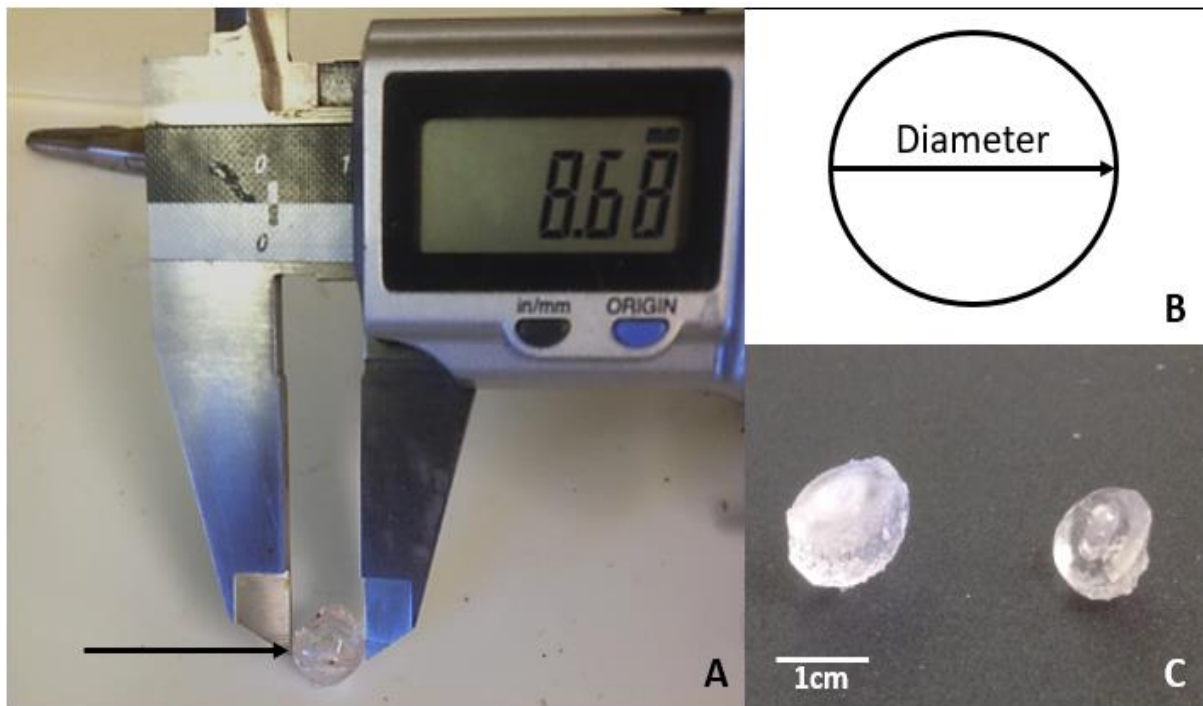


Figure 2.7: Measurements of an eye lens from *O. ingens*. A: an eye lens being measured using digital callipers, arrow indicating position of lens. B: the measurement of eye lens diameter. C: an eye lens split into its two hemispheres.



Figure 2.8: An upper and lower beak being weighed on an analytical balance.

2.3 Results

2.3.1 Measurements

Female *Onykia ingens*, which can grow larger than males, ranged from 10cm to 51cm in mantle length (mean=23.3cm, standard deviation=10.6cm, n=26). Males, on the other hand, ranged from 11cm to 37cm; however, males have a larger mean size than females with a smaller range (mean=26.8cm, standard deviation=8.8cm, n=15) (Table 2.1) (Fig. 2.9A). Similarly, female body weight ranged from 47g to 4500g (mean=732.9g, standard deviation=1091.4g, n=25) and male body weight occupied a much smaller range from 61g to 1375g (mean=719.5g, standard deviation=431.9g, n=15) (Table 2.1) (Fig. 2.9B).

The beaks of female *O. ingens* had an upper rostral length that ranged from 3.3mm to 10.4mm (mean=6.2mm, standard deviation=2.1mm, n=26) and a lower rostral length that ranged from 3.2mm to 11.0mm (mean=6.3mm, standard deviation=2.1mm, n=26) (Table 2.1) (Fig. 2.9C). Males had similar rostral lengths, with their upper rostral lengths ranging from 3.3mm to 9.6mm (mean=6.93mm, standard deviation=2.0mm, n=15) and their lower rostral lengths ranging from 3.3mm to 11.9mm (mean=8.0, standard deviation=2.9, n=15) (Table 2.1) (Fig. 2.9C).

Female *Nototodarus sloanii* in this sample had a mantle length that ranged from 12cm to 33cm (mean=25.1cm, standard deviation=5.5cm, n=26). Similarly, males had a mantle length ranging from 14cm to 32cm (mean=22.8cm, standard deviation=4.7cm, n=25) (Table 2.1) (Fig. 2.9A). Female body weight varied from 41g to 964g (mean=474.3g, standard deviation=269.2g, n=26) while male body weight ranged from 70g to 890g (mean=339.4g, standard deviation=224.6g, n=25) (Table 2.1) (Fig. 2.9B).

The upper rostral lengths of the beaks of the female *N. sloanii* ranged from 2.4mm to 7.5mm (mean=5.4mm, standard deviation=1.5mm, n=22). The lower rostral lengths of the beaks from the females ranged from 1.4mm to 7.2mm (mean=5.0mm, standard deviation=1.6mm, n=22) (Table 2.1) (Fig. 2.9C). Beaks from male *N. sloanii* had a similar range of rostral lengths, with upper rostral lengths ranging from 2.6mm to 7.0mm (mean=5.0mm, standard deviation=1.3mm, n=25) and lower rostral lengths ranging from 2.1mm to 6.9mm (mean=4.7mm, standard deviation=1.4mm, n=25) (Table 2.1) (Fig. 2.9C).

The eye lenses of female *O. ingens* had a diameter ranging from 4.02mm to 11.58mm (mean=7.56mm, standard deviation=2.22mm, n=29) and a weight ranging from 0.04g to 1.09g (mean=0.38g, standard deviation=0.29g, n=26) (Table 2.2) (Fig. 2.10A). Males had similar eye lens sizes, with diameters ranging from 3.41mm to 8.11mm (mean=8.11mm, standard deviation=2.15, n=14) and weights ranging from 0.02g to 0.86g (mean=0.40g, standard deviation=0.25g, n=13) (Table 2.2) (Fig. 2.10B).

The upper beak weight of male *O. ingens* ranged from 0.04g to 0.47g (mean=0.25g, standard deviation=0.16g, n=11) while the lower beak weight ranged from 0.03g to 0.63g (mean=0.30g, standard deviation=0.22g, n=11); the combination of these two parts of the beaks gave an overall beak weight range of 0.07g to 1.10g (mean=0.55g, standard deviation=0.38g, n=11) (Table 2.3) (Fig. 2.11). Female *O. ingens* had a similar minimum and mean for the beak weights; however they had a higher maximum weight. Female upper beaks ranged from 0.03g to 0.94g (mean=0.25g, standard deviation=0.22g, n=24), with lower beak weight ranging from 0.02g to 0.81g (mean=0.23g, standard deviation=0.22, n=25) and the overall beak weight ranging from 0.05g to 1.72g (mean=0.47g, standard deviation=0.44g, n=24) (Table 2.3) (Fig. 2.11)

The upper beak weight of male *N. sloanii* ranged from 0.03g to 0.40g (mean=0.21g, standard deviation=0.13g, n=13) while the lower beak weight ranged from 0.02g to 0.24g (mean=0.14g, standard deviation=0.07g, n=13); the overall beak weight ranged from 0.05g to 0.64g (mean=0.35g, standard deviation=0.20g, n=13) (Table 2.3) (Fig. 2.11). Females had similar mean and maximum values for the beak weights; however they had a higher minimum weight. Female upper beaks ranged from 0.17g to 0.41g (mean=0.28g, standard deviation=0.07g, n=11), with lower beak weight ranging from 0.13g to 0.28g (mean=0.19g, standard deviation=0.04, n=11) and the overall beak weight ranging from 0.30g to 0.69g (mean=0.47g, standard deviation=0.11g, n=11) (Table 2.3) (Fig. 2.11).

Table 2.1: Summary of mantle length, weight, lower rostral length and upper rostral length data for both species measured.

	Mantle length (cm)			Weight (g)			Lower rostral length (mm)			Upper rostral length (mm)											
	Min	Mean	Max	Min	Mean	Max	Min	Mean	Max	Min	Mean	Max									
<i>Onychia ingens</i>	Male	11.3	26.8	37.4	8.80	15	61.2	720	1375	461.9	15	3.33	7.97	11.88	2.87	15	3.33	6.93	9.55	1.98	15
	Female	9.7	23.3	51.0	10.6	26	47.0	733	4500	1091.4	26	3.24	6.34	11.04	2.14	26	3.25	6.21	10.39	2.11	26
<i>Nototodarus sloanii</i>	Male	14.0	22.8	32.0	4.70	25	70.2	339	890	224.6	25	2.10	4.74	6.89	1.39	25	2.60	4.99	7.04	1.33	25
	Female	12.3	25.1	33.0	5.51	26	41.6	474	964	269.2	26	1.40	5.04	7.22	1.63	22	2.40	5.40	7.52	1.48	22

Table 2.2: The eye lens diameter and weight range, mean, standard deviation and sample size for both sexes of *O. ingens*.

	Eye lens diameter (mm)				Eye lens weight (g)				
	Min	Mean	Max	Stdev	Min	Mean	Max	Stdev	
Male	3.41	8.11	11.4	2.15	14	0.02	0.40	0.86	0.25
Female	4.02	7.56	11.6	2.22	29	0.04	0.38	1.09	0.29

Table 2.3: The upper, lower and overall beak weight range, mean, standard deviation and sample size for both species measured

	Upper beak weight (g)				Lower beak weight (g)				Overall beak weight (g)							
	Min	Mean	Max	Stdev	Min	Mean	Max	Stdev	Min	Mean	Max	Stdev				
<i>Onychia ingens</i>	Male	0.04	0.25	0.47	0.16	11	0.03	0.30	0.63	0.22	11	0.07	0.55	1.10	0.38	11
	Female	0.03	0.25	0.94	0.22	24	0.02	0.23	0.81	0.22	25	0.05	0.47	1.72	0.44	24
<i>Nototodarus sloanii</i>	Male	0.03	0.21	0.40	0.13	13	0.02	0.14	0.24	0.07	13	0.05	0.35	0.64	0.20	13
	Female	0.17	0.28	0.41	0.07	11	0.13	0.19	0.28	0.04	11	0.30	0.47	0.69	0.11	11

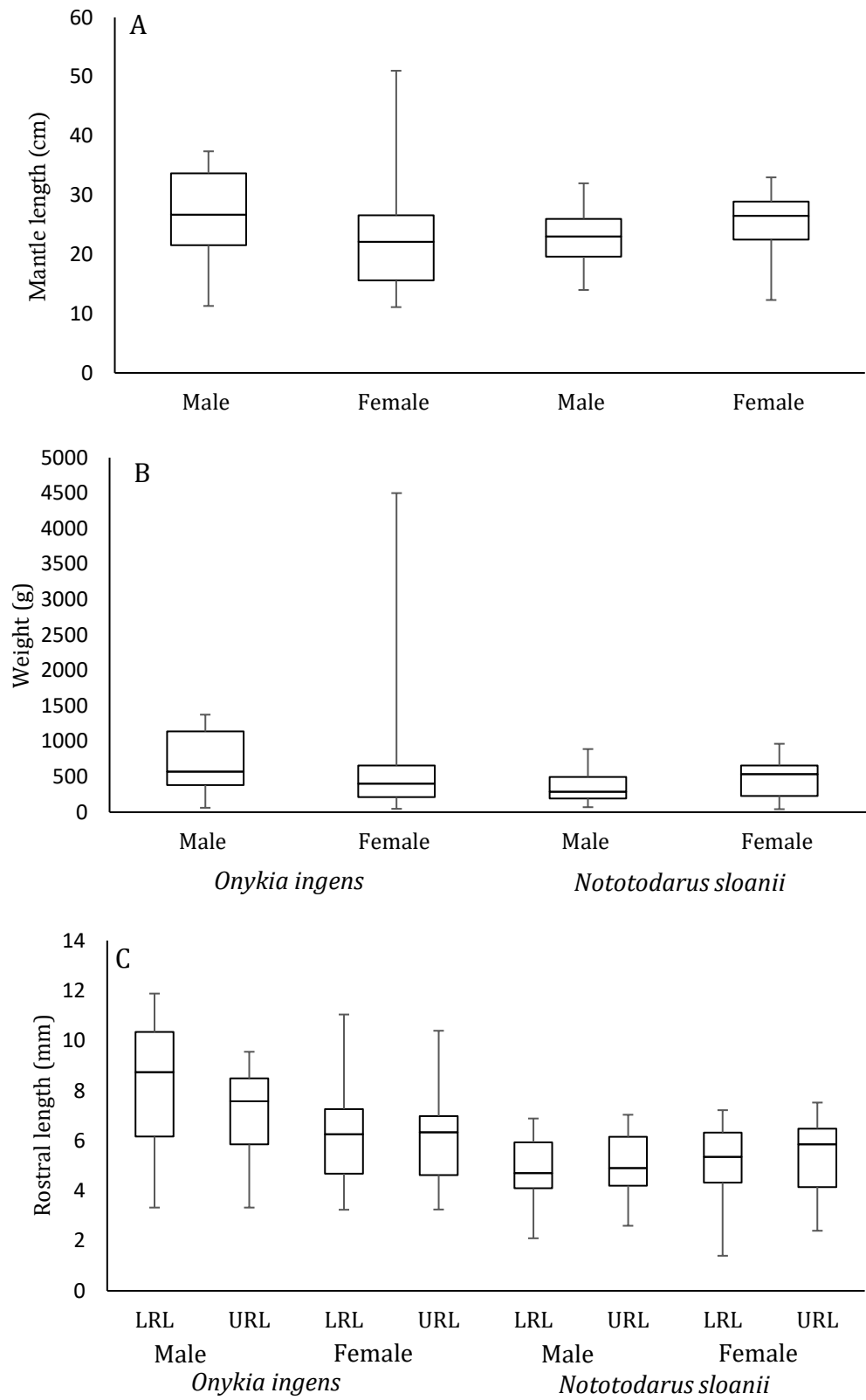


Figure 2.9: Box and whisker plots showing the median, upper and lower quartiles and range of the mantle lengths (A), weight (B) and rostral lengths (C) of males and females of *O. ingens* and *N. sloanii*. Sample sizes are the same as in Table 2.1.

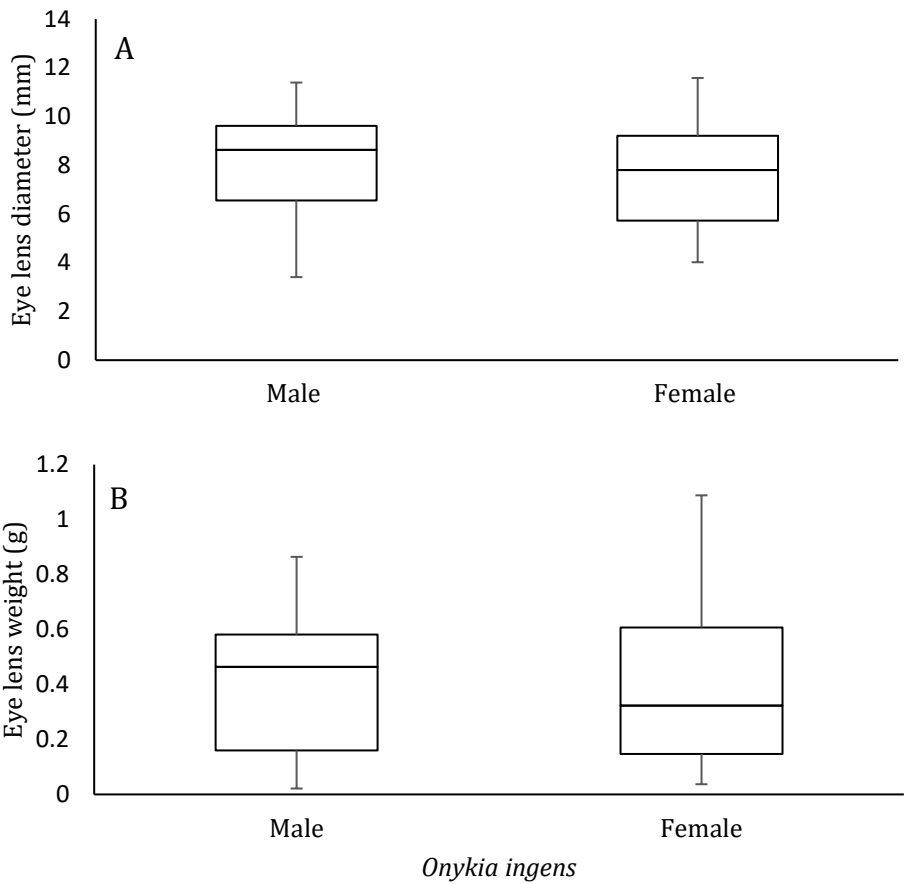


Figure 2.10: Box and whisker plots of the range, median and upper and lower quartiles of the diameter (A) and weight (B) of the eye lenses of male and female *O. ingens*. Sample sizes in Table 2.2.

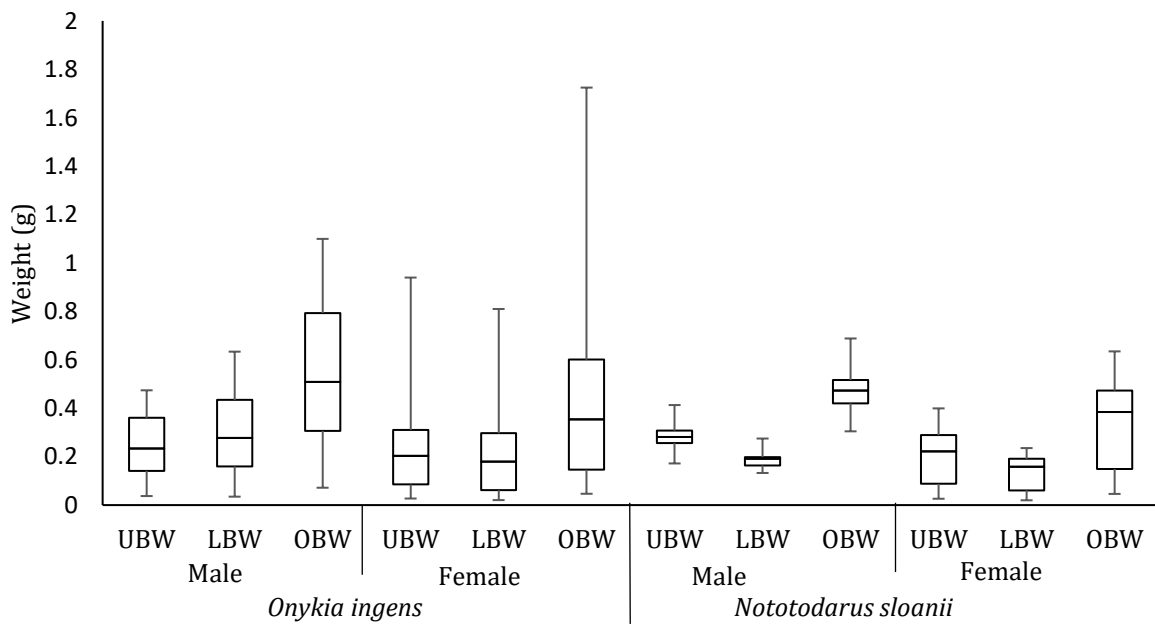


Figure 2.11: Box and whisker plots of the range, median and upper and lower quartiles of the weight of the upper (UBW), lower (LBW), and overall (OBW) beak weights of male and female *O. ingens* and *N. sloanii*. Sample sizes in Table 2.3.

2.3.2 Size-to-weight relationship

The overall relationship between body weight and mantle length was different between sexes in *O. ingens* (Fig. 2.12). When males and females are separated the relationship between body weight and mantle length for females is exponential (Fig. 2.12). This relationship for males is linear; however, it follows the same starting trend as the female relationship (Fig. 2.12). *Onykia ingens* data are separated by sex in all following relationships due to the sexual dimorphism exhibited.

The overall relationship between body weight and mantle length for *N. sloanii* is the same for both sexes (Fig. 2.13). Both sexes follow an exponential growth curve (Fig. 2.13)

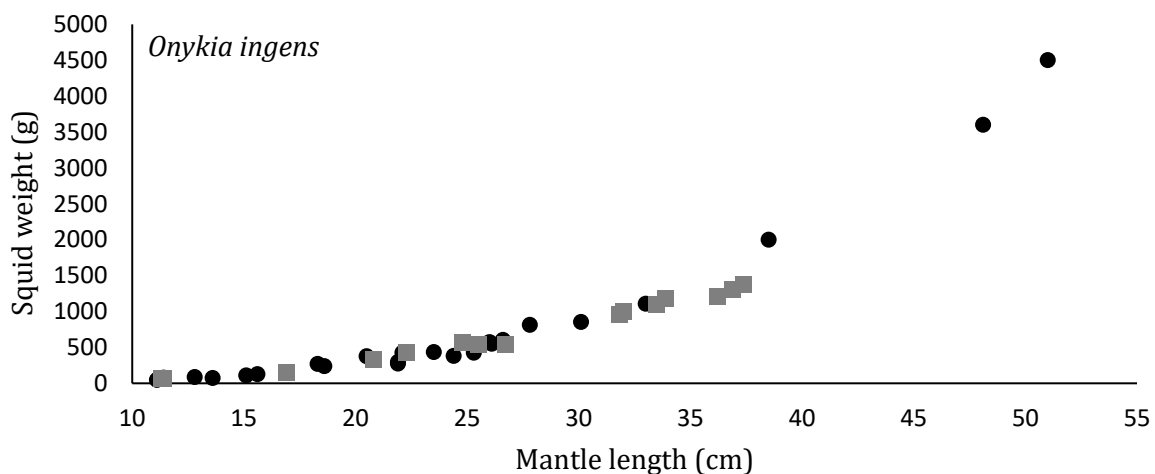


Figure 2.12: Mantle length and weight measurements of *O. ingens* males (grey squares, n=15) and females (black circles, n=25).

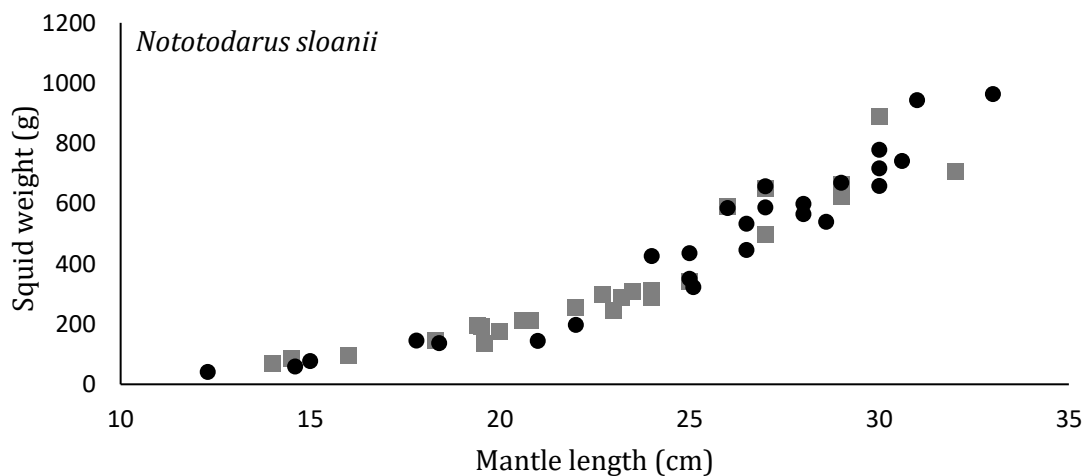


Figure 2.13: Mantle length versus weight in *N. sloanii*, males (grey squares, n=25) and females (black dots, n=26).

2.3.3 Mantle length vs. beak measurements

The relationship between beak measurements (rostral length and beak weight) and mantle length is linear for *O. ingens*. For females, upper beak weight was the best predictor of mantle length ($ML=40.3(UBW) + 12.638, r^2=0.94, p<0.001$) (Fig. 2.14A). For males the best relationship was lower beak weight versus mantle length ($ML=38.186(LBW) + 12.343, r^2 = 0.94, p<0.001$) (Fig 2.14B).

The relationship between beak measurements (rostral length and beak weight) and mantle length is also linear for *N. sloanii*. Lower rostral length was the best predictor of mantle length ($ML= 3.2702(LRL) +7.5137, r^2 = 0.92, p<0.001$) (Fig. 2.14C). Regressions were not split by sex due to the very similar growth curves exhibited by both sexes.

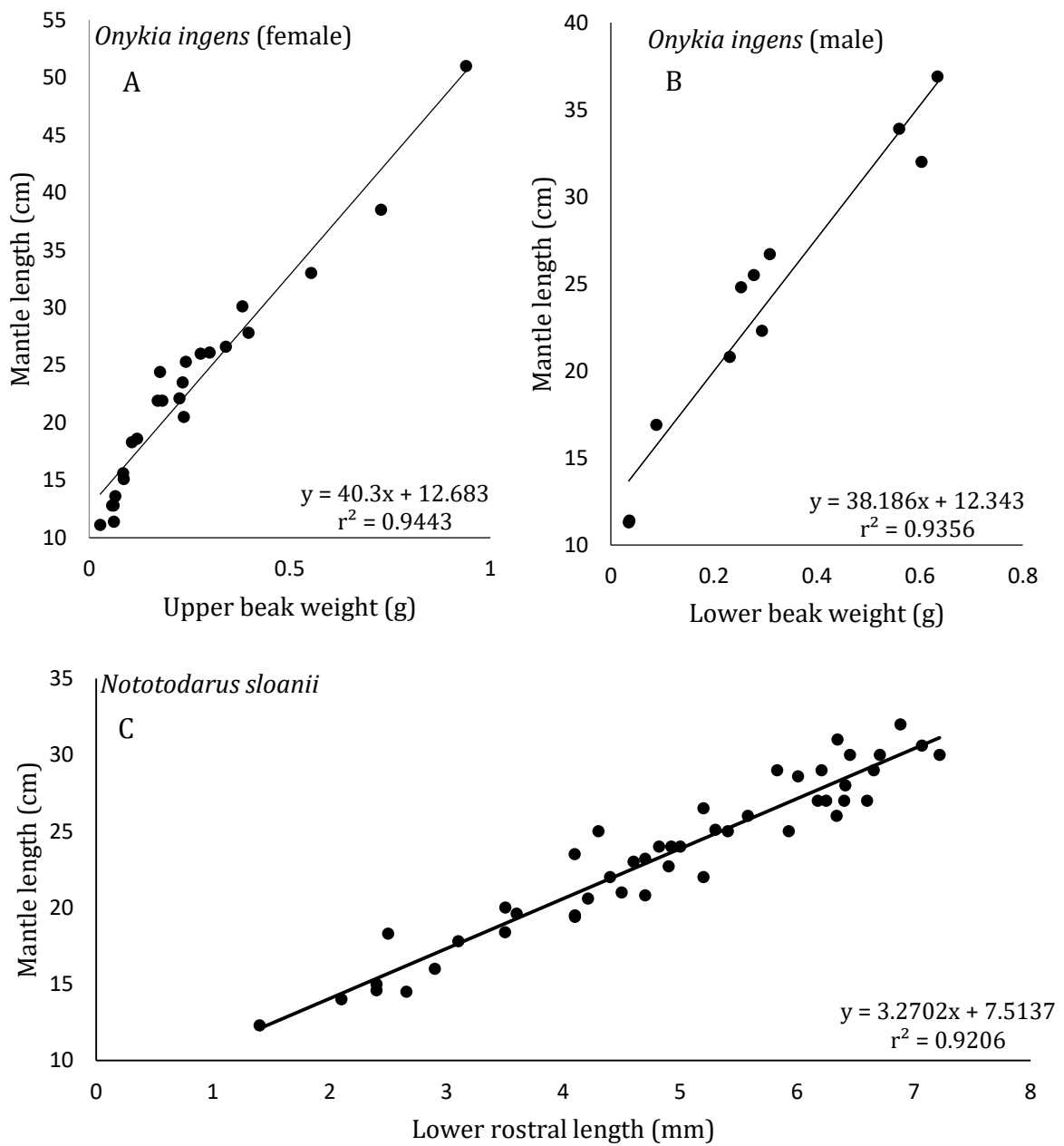


Figure 2.14: The best predictors of mantle length for both species of squid with line equations and r^2 values on graphs. A: female *O. ingens* (n=24); B: male *O. ingens* (n=11); C: *N. sloanii* (not separated by sex) (n=47).

2.3.4 Squid weight vs. beak measurements

In *O. ingens*, the relationship between beak measurements (rostral length and beak weights) and squid weight is linear for males and exponential for females. The best predictor of squid weight for females was lower rostral length ($W=10.521e^{0.5481(LRL)}$, $r^2 = 0.94$, $p<0.001$) (Fig. 2.15A). The best predictor of squid weight for males was lower beak weight ($W=1954.4(LBW) - 29.395$, $r^2 = 0.96$, $p<0.001$) (Fig. 2.15B).

For *N. sloanii*, all body-weight-to-rostral-length relationships are exponential and all body weight to beak weight relationships are linear. Lower rostral length was the best predictor of weight ($W=25.198e^{0.5049(LRL)}$, $r^2= 0.92$, $p<0.001$) (Fig. 2.15C). Regressions were not split by sex due to the very similar growth curves exhibited by both sexes.

2.3.5 Best predictors of squid biomass

For male *O. ingens*, all measures of beak size are good predictors of squid biomass, with lower beak weight being the best predictor for both mantle length and squid weight (Table 2.4). Lower rostral length is the best predictor of squid weight and upper beak weight is the best predictor of mantle length in female *O. ingens* (Table 2.4). Relationships between beak measurements and squid weight for *N. sloanii* are relatively strong, with lower rostral length being the best predictor. Lower rostral length is also the best predictor for mantle length, with upper rostral length being the second best and beak weights being relatively poor predictors (Table 2.4).

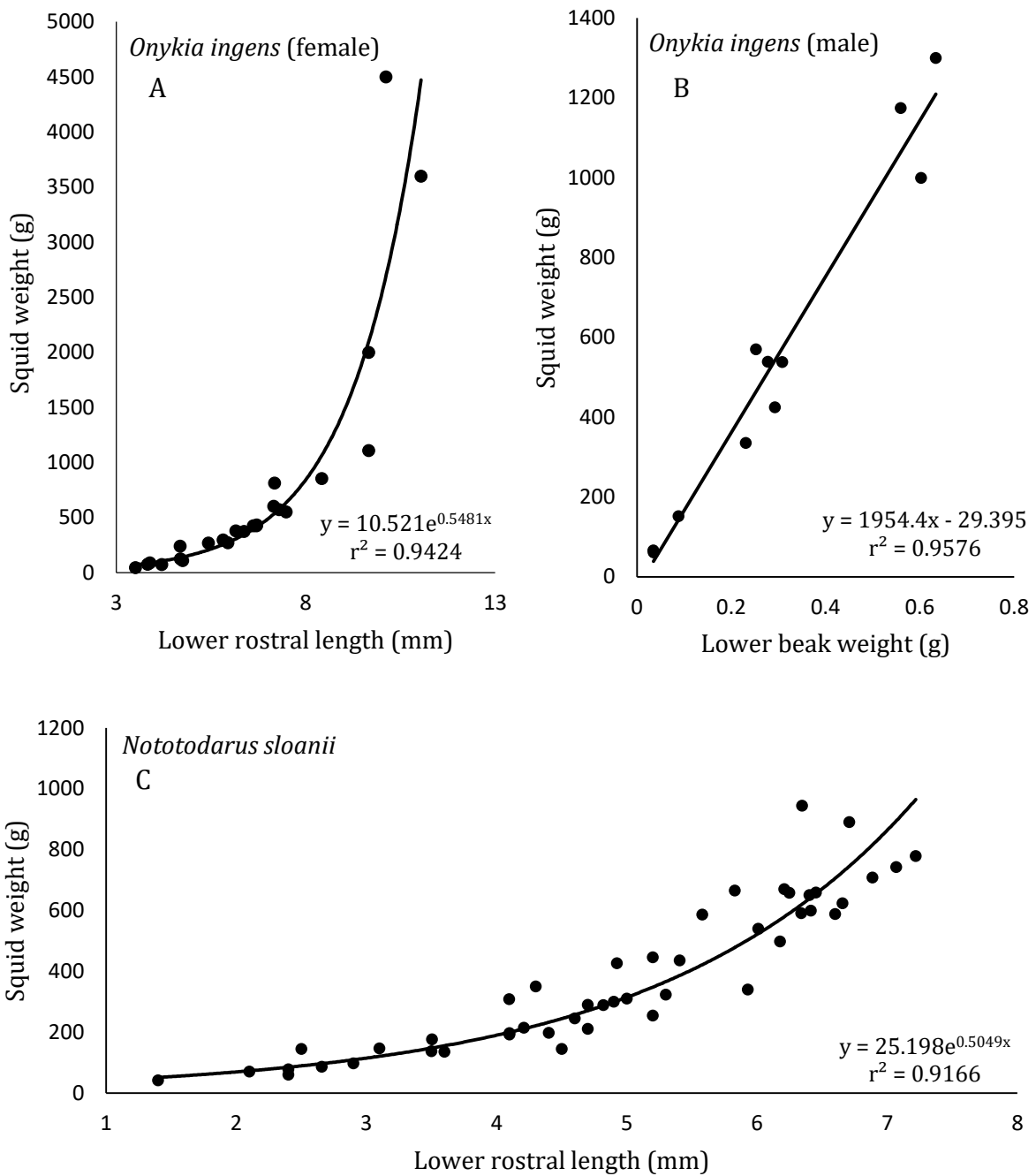


Figure 2.15: The best beak measurement predictors of squid weight for *O. ingens* and *N. sloanii*. A: squid weight versus lower rostral length for female *O. ingens* (n=24); B: squid weight versus lower beak weight for male *O. ingens* (n=11); C: squid weight versus lower rostral length for *N. sloanii* (n=47).

Table 2.4: The sample size, equation, r² and p value of the relationships between all measurements of

Species	Sex	BodyM*	BeakM**	n	Equation	r ²	p
<i>Onykia ingens</i>	F	W	LRL	25	$W=10.521e^{0.5481(LRL)}$	0.942	<0.001
			URL	24	$W=11.272e^{0.5483(URL)}$	0.905	<0.001
			LBW	23	$W=112.34e^{4.5923(LBW)}$	0.836	<0.001
			UBW	23	$W=106.91e^{4.518(UBW)}$	0.853	<0.001
			OBW	24	$W=108.81e^{2.2999(OBW)}$	0.851	<0.001
		ML	LRL	26	$ML=0.1955(LRL)+1.7868$	0.928	<0.001
			URL	26	$ML=0.1894(URL)+1.7948$	0.900	<0.001
			LBW	25	$ML=0.0216(LBW)-0.2533$	0.892	<0.001
			UBW	24	$ML=40.3(UBW)+12.683$	0.944	<0.001
			OBW	25	$ML=0.0455(OBW)-0.5219$	0.924	<0.001
	M	W	LRL	15	$W=152.55(LRL)-495.86$	0.899	<0.001
			URL	15	$W=213.9(URL)-763.57$	0.844	<0.001
			LBW	12	$W=1954.4(LBW)-29.395$	0.958	<0.001
			UBW	11	$W=2576.9(UBW)-74.178$	0.938	<0.001
			OBW	11	$W=1118.6(OBW)-50.789$	0.952	<0.001
ML		LRL	14	$ML=2.9891(LRL)+2.7614$	0.931	<0.001	
		URL	15	$ML=4.2954(URL)-3.0214$	0.935	<0.001	
		LBW	11	$ML=38.186(LBW)+12.343$	0.936	<0.001	
		UBW	11	$ML=0.0182(UBW)-0.1882$	0.916	<0.001	
		OBW	11	$ML=0.0426(OBW)-0.4696$	0.930	<0.001	
<i>Nototodarus sloanii</i>	W	LRL	47	$W=25.198e^{0.5049(LRL)}$	0.917	<0.001	
		URL	47	$W=19.053e^{0.53(URL)}$	0.883	<0.001	
		LBW	24	$W=3220(LBW)+22.896$	0.837	<0.001	
		UBW	24	$W=1908.7(UBW)+85.555$	0.888	<0.001	
		OBW	24	$W=1231.5(OBW)+48.904$	0.893	<0.001	
	ML	LRL	47	$ML=3.2702(LRL)+7.5137$	0.921	<0.001	
		URL	47	$ML=3.4379(URL)+5.6769$	0.889	<0.001	
		LBW	24	$ML=56.304(LBW)+17.406$	0.763	<0.001	
		UBW	24	$ML=32.395(UBW)+18.738$	0.762	<0.001	
		OBW	24	$ML=21.127(OBW)+18.024$	0.783	<0.001	

squid body size and all measurements of beak size.

*BodyM= measurements of body size: W= body weight, ML=Mantle length

**BeakM= measurements of beak size: LRL= lower rostral length, URL=Upper rostral length, LBW= lower beak weight, UBW= upper beak weight, OBW= overall beak weight

2.3.6 Eye lens growth in *Onykia ingens*

The relationship between eye lens weight and lens diameter is exponential for both sexes (Fig. 2.16). The relationship between eye lens diameter and mantle length is linear for both females ($ML=5.1864(LD)-10.887$, $r^2=0.80$) and males ($ML=3.2654(LD)+1.7254$, $r^2=0.77$) (Fig. 2.17A). The relationship between eye lens diameter and squid weight is exponential for females ($W=10.714e^{0.5187(LD)}$, $r^2=0.81$) and linear for males ($ML=170.06(LD)-590.15$, $r^2=0.73$) (Fig. 2.17B) when separated by sex.

The relationship between mantle length and lens weight is linear for both females ($ML=39.855(LW)+14.56$, $r^2=0.81$) and males ($ML=27.019(LW)+17.28$, $r^2=0.68$) (Fig. 2.18A). The relationship between squid weight and lens weight is exponential for females ($W=172.63e^{3.2174(LW)}$, $r^2=0.72$) and linear for males ($W=1460.5(LW)+196.67$, $r^2=0.70$). Lens weight is much more variable for females than males after lens weight is greater than 0.5g (Fig. 2.18B).

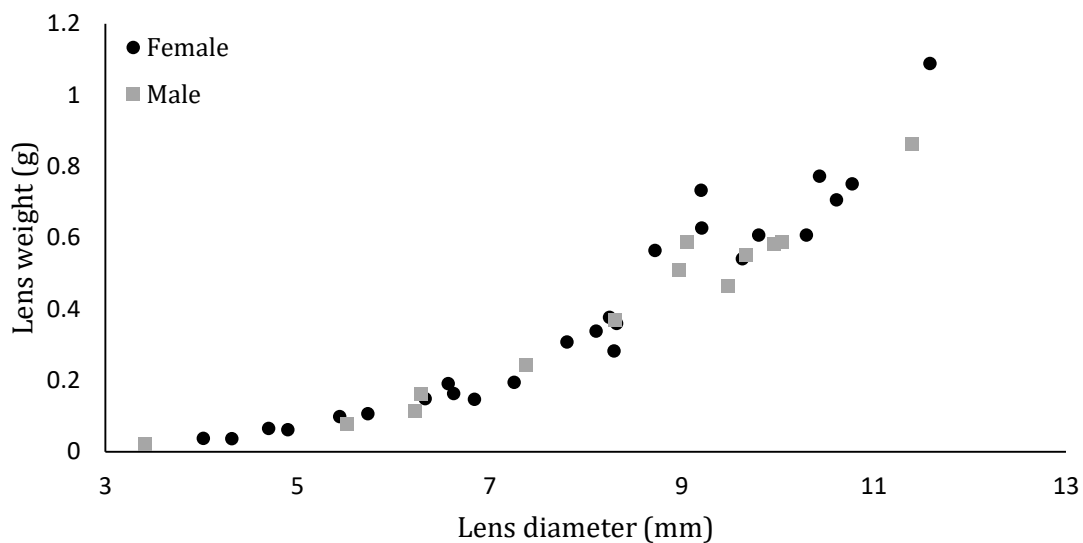


Figure 2.16: Eye lens weight versus diameter for *O. ingens* for females (black circles, $n=26$) and males (grey squares, $n=13$) separately.

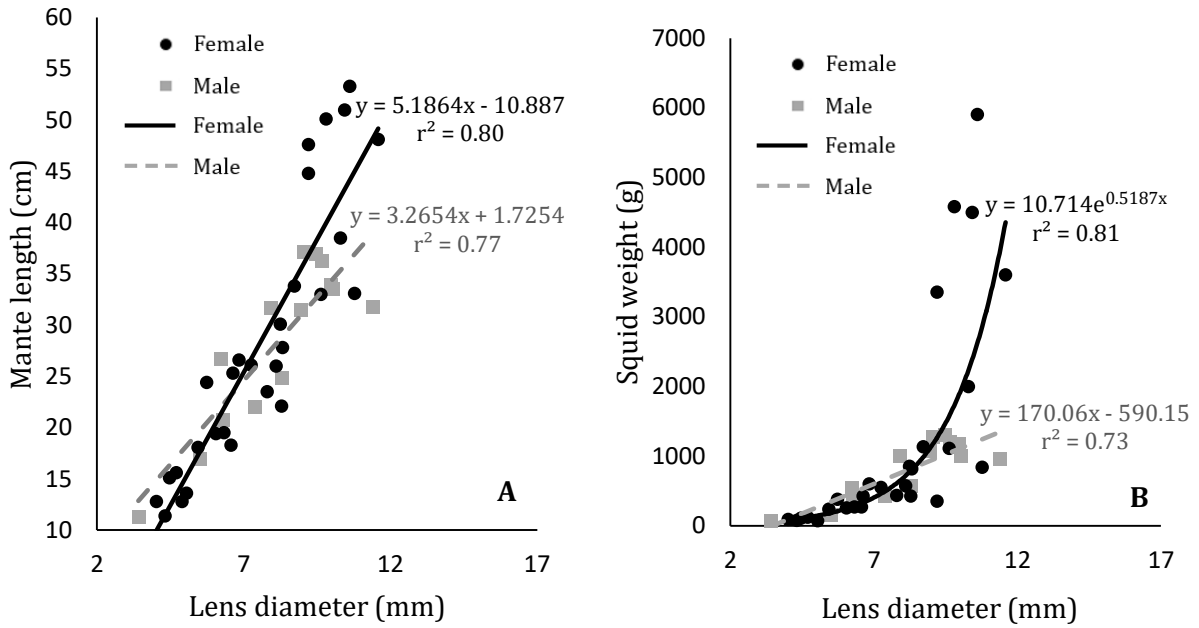


Figure 2.17: Squid size versus lens diameter in *O. ingens* for females (black circles and solid trendline, n=29) and males (grey squares and dashed trendline, n=16) separately; A: Mantle length versus lens diameter; B: squid weight versus lens diameter.

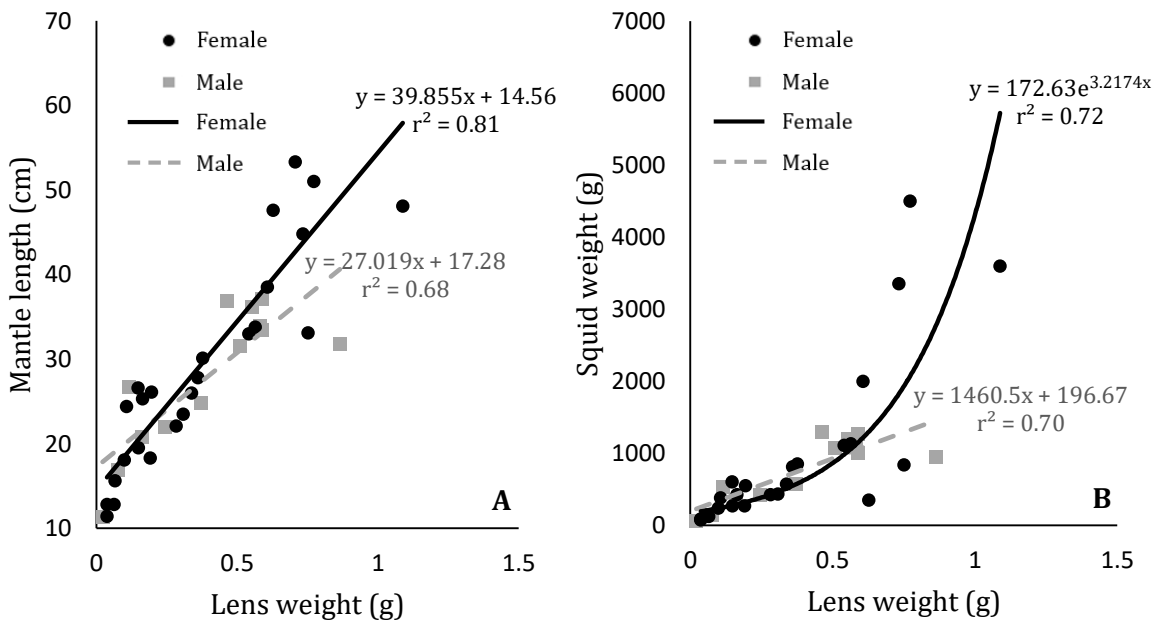


Figure 2.18: Squid size versus lens weight in *O. ingens* for females (black circles, n=23) and males (grey squares, n=13) separately; A: Mantle length versus lens diameter; B: squid weight versus lens diameter.

2.4 Discussion

2.4.1 Sex and size

The largest female of *Onykia ingens* in this sample reached a weight over three times that of the largest male *O. ingens* while only being 1.4 times the mantle length. The weight-to-mantle-length relationship is exponential in females. The most likely explanation for this relationship is that mantle length growth slows down as squid near the end of their life span, but weight gain does not, due to the increased production of eggs at maturity. Another plausible explanation is that mantle length does not slow down, but weight gain increases rapidly at the end of the squid's life due to reproductive organ growth (Laptikhovsky et al. 2007). Once females reach their exponential growth phase, their weight increases rapidly but their beak size does not, meaning that there is a large amount of variation when estimating the weight of these older females.

The weight-to-mantle-length relationship in male *O. ingens* is linear despite males also experiencing considerable reproductive organ growth (Arkhipkin & Laptikhovsky 2010). A possible explanation for this relationship is that males aren't able to feed at sexual maturity. This may be partially due to the fact that the terminal organ, when elongated, can protrude from the funnel making fast movement difficult (Fig. 1).



Figure 2.19: Sectioned mature male *O. ingens* with elongated terminal organ.

Nototodarus sloanii does not show the large degree of sexual dimorphism seen in *O. ingens*. Male and female *N. sloanii* in this sample obtained a similar overall size and their growth curves were not visually different. The relationship between body weight and mantle length in this species is exponential for both sexes. This relationship is probably due to the rapid growth of reproductive organs at maturity as with *O. ingens* females. As the growth curves are very similar it would seem that reproductive organ growth is similar in both sexes.

2.4.2 Best predictors of squid biomass

This is the first time beak weights have been investigated as predictors for squid size. Beak weights have been shown to be good predictors of squid size in *O. ingens*; however, rostral lengths are better predictors in *N. sloanii*. When estimating original squid biomass of *O. ingens* from a beak it is recommended to use the sex-specific relationships where possible. It is possible to sex *O. ingens* using the lower beak as males have a band of clear cartilage when they are maturing and a gap in the same place with a greatly eroded rostral edge when they are mature, while females have no band (Fig. 2.20) (Bolstad 2006).

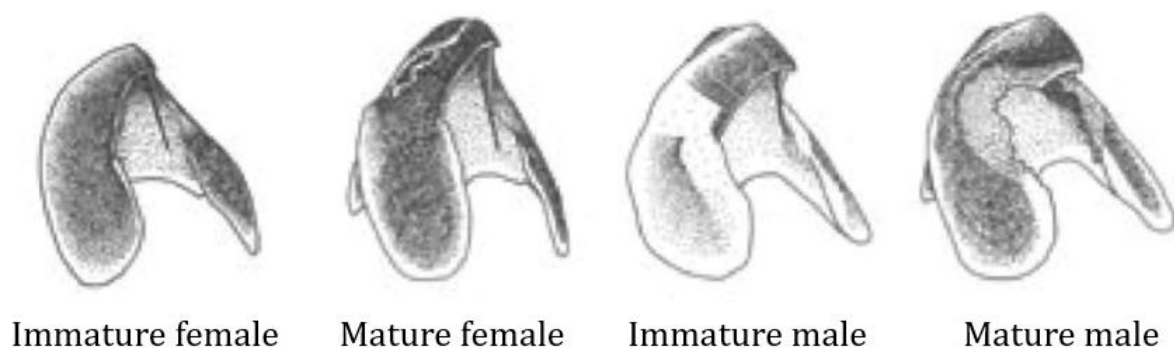


Figure 2.20: Comparison of immature and mature male and female beaks of *O. ingens* showing the band of cartilage, drawing from Bolstad 2006, p. 323, Table 1.

When estimating the original biomass of male *O. ingens* it is recommended to use the equation given for the relationship between lower beak weight and squid weight. I recommend using the relationship between upper beak weight and mantle length when estimating the biomass of female *O. ingens* if both halves of the beak are still connected. For female *O. ingens*, I recommend using the relationship between lower rostral length and squid weight when the two halves of the beaks are not connected. This second recommendation is so that the sex can be discerned and the estimate of biomass will be

accurate. The relationship between lower rostral length and mantle length is recommended when estimating the size of *N. sloanii*.

Beak weights may not be the most practical or accurate predictors of squid size under some circumstances. For example, beaks that have been in the stomach of a predator for a large period of time would have lost weight through the degradation of the outer surfaces of the beak. Rostral length measurements may not have been as badly affected. In these circumstances, the best rostral-length-to-body-size relationship should be considered. Beak weight as a predictor would, however, be useful in circumstances where the whole squid has been recovered but the body is not intact, making weight and mantle length measurements difficult.

2.4.3 Eye lens growth in *Onykia ingens*

The growth relationship between lens diameter and weight is exponential because the lens is a three-dimensional structure. This three-dimensionality means that, as the lens grows, layers are deposited that increase diameter slightly but increase the weight considerably. Lens weight and diameter have linear growth relationships with mantle length for both sexes of *O. ingens* and with squid weight for males. Females have an exponential growth relationship between lens size and squid weight. This exponential relationship is a result of the females growing heavier as they reach maturity and their hard structures not following the same trend.

2.4.4 Findings compared to other studies

General trends in allometric relationships and the methods utilised to collect the data should be compared within species where possible. Care must be taken when comparing and combining data sets between populations of species as growth rates, and other parameters, may differ. This warning is particularly valid for squid as the taxonomic position of species, and even different populations thought to be the same species, may change over time. An example of this unstable taxonomy is in the systematics of the commercially important *Nototodarus* genus around New Zealand. These two species (*N. sloanii* and *N. gouldi*) were once thought to be two populations of the same species, but were found to be two independent species (Smith et al. 1981, 1987).

All relationships between rostral lengths and squid size reported in this study for *O. ingens* support the relationships presented in both Bolstad (2006) and Jackson (1995). Regressions reported in this thesis have a better fit than those reported in Jackson (1995) and are similar to the fit of those reported in Bolstad (2006) (Fig. 2.21). Beaks analysed in Bolstad (2006) had been preserved before being measured, whereas the methods used to extract and measure beaks in Jackson (1995) are similar to those used in this study.

Another way to compare the results of allometric studies is to use the equations given for the relationships between a hard-part measurement and weight to estimate the overall weight of all animals in the data set. The actual combined weight of the *O. ingens* in this data set was 29.046kg, with males weighing 10.793kg and females weighing 18.253kg. Using the equations given for lower rostral length and weight, as this relationship was estimated in all previous studies, the present study estimated the combined weight of the males to be 10.305kg (95% of the actual value) and the females to be 18.089kg (99%); the equation for the same relationship given in Jackson (1995) gives estimates that are higher, with a combined male weight of 11.354kg (105%) and a combined female weight of 21.066kg (115%); the relationship presented in Bolstad (2006), who used preserved specimens, estimates the males and females to be 8.868kg (82%) and 14.007kg (76%) respectively, which is lower than the actual weight. The estimate of weight that was most accurate came from the relationships found in this study which is not surprising as it was calculated from this data. It is interesting to note that the difference in these estimates and relationships in each study is possibly due to different storage methods of beaks.

Raw data used to find allometric relationships for *O. ingens* in Bolstad (2006) were acquired and the total weight of the sample was estimated using the LRL to weight equations presented here, in Bolstad (2006) and in Jackson (1995) (Table 2.6). The actual combined weight of the females in the sample was 21.745kg, and 6.621kg for males. Equations from the present study produced elevated estimates of 34.020kg (156%) and 7.279 (109%) for females and males in the sample respectively. Equations from Jackson (1995) estimated even higher weights of 36.962kg (170%) and 9.331kg (141%) for females and males respectively. Equations presented in Bolstad (2006) gave the closest-to-actual weight estimates of 23.450kg (108%) and 6.235kg (94%) for

females and males respectively. The differences in accuracy between studies, and storage methods, further supports the need to state the type of beak storage method used as it likely has an effect on beak measurements.

The similar growth curves in both sexes of *N. sloanii* observed here support data presented by McKinnon (2006), as do the linear relationship between rostral lengths and mantle length and the exponential relationship between rostral length and squid weight. These beak-size-to-squid-size relationships, however, do not support the data presented in Jackson and McKinnon (1996), where the relationship between rostral length and squid weight was found to be linear for *N. sloanii*. The actual combined weight of all *N. sloanii* used in this study was 18.036kg, the equation for the relationship between lower rostral length and weight from each study was used to compare estimates of this overall weight between studies. The equation given in this study estimates that the overall weight is 17.812kg (99%), the equation from Jackson and McKinnon (1996) estimates the weight to be 30.099kg (169%) and the equation from McKinnon (2006) gives an estimate of 12.700kg (70%).

The beaks used to create the relationships in Jackson and McKinnon (1996) had been dried prior to measurements being taken which may have distorted measurements. The beaks McKinnon (2006) measured were stored in alcohol to prevent desiccation, in a similar way to those used in Bolstad (2006). This storage method probably kept the beaks a similar condition to the ones used in this study, which were frozen to prevent any desiccation. The difference in beak preparation methods might, however, explain the difference in growth relationships between studies.

The differences between studies for biomass estimate regression equations are likely to be due to the different beak preparation, storage and methods used and probably reflect differences in source material. The fact that these factors seem to make such a large difference means that preparation and preservation methods should always be clearly communicated in these types of studies (Bolstad 2006). When estimating biomass from a beak it is recommended that the beak storage method be taken into account when choosing which regression equations to use. This apparent effect of beak storage on regression equations further warrants a study of how 'storage' in stomach acids affects the beaks over time.

Squid rely on vision both to catch prey and avoid predation (Nilsson et al. 2012). The growth relationships between eye lens size and body size in squid show that the eye grows consistently over the life-time of the squid, except for females once they reach maturity. This continued, linear, growth rate of eye lenses suggests that squid rely on a consistent ratio between eye size and body size over their life history. Squid have much larger eyes, both in general and for their body size, than fish (Packard 1972, Nilsson et al. 2012). These larger eyes in squid may mean that squid depend more on vision as an indicator of food or danger than fish do, which may be due to fish having other extremely complex senses at their disposal, such as the lateral line. Further studies into the growth and development of cephalopod eyes over the life history of the animal are warranted.

Past studies (Parry 2003, Onthank & Lee 2013) have used eye lenses as archival tissues for stable isotope studies to trace migration in *Dosidicus gigas*. It is important to know the growth rate of eye lenses over the life history as it would affect the interpretation of the results of these stable isotope studies. Parry (2003) assumes constant growth of the lens over the life time of the squid to back calculate mantle length of squid at each layer of eye lens tissue. The data presented in this chapter support the assumption made by Parry (2003). The data here also give an equation that could be utilised in these types of studies in the future when estimating mantle length from eye lens diameter.

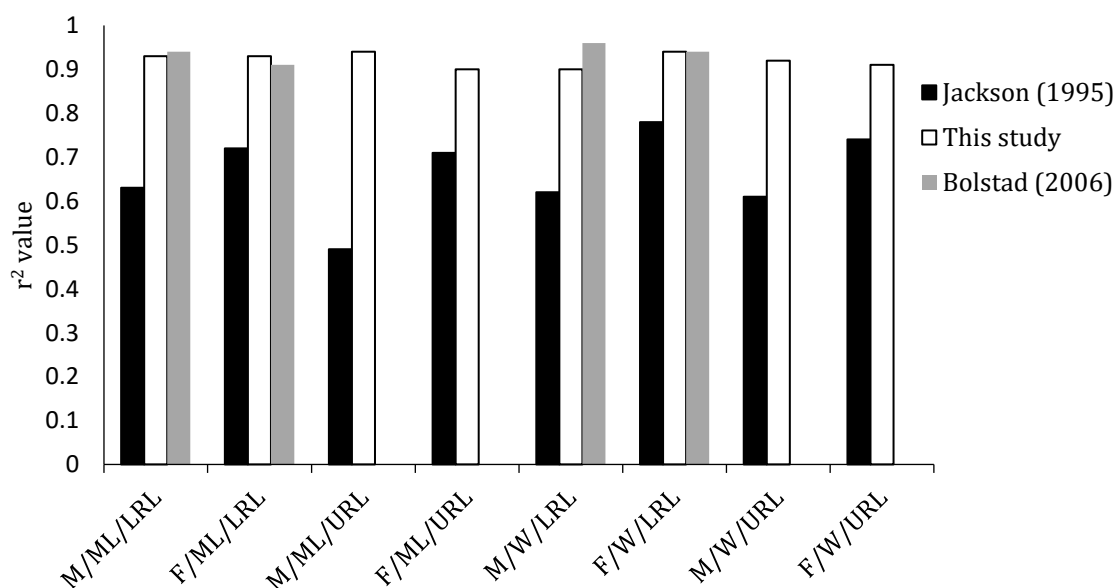


Figure 2.21: r^2 values of allometric relationships in studies of *Onykia ingens* in New Zealand waters.

Table 2.5: Actual and predicted combined weight (kg) of the squid used in this study using equations given in this chapter and other papers.

	Sex	Actual	P S*	J (1995)*	B (2006)*	J & M (1996)*	M (2006)*
<i>Onykia ingens</i>	M	10.793	10.305	11.354	8.868		
	F	18.253	18.089	21.066	14.007		
<i>Nototodarus sloanii</i>		18.036	17.812			30.099	12.700

* Papers equations were taken from: P S = present study J (1995) = Jackson (1995); B (2006) = Bolstad (2006); J & M (1996) = Jackson and McKinnon (1996); M (2006) = McKinnon (2006).

Table 2.6: Actual and predicted combined weight (kg) of the squid used in Bolstad (2006) using equations given in this chapter and other papers.

	Sex	Actual	Present study	Jackson (1995)	Bolstad (2006)
<i>Onykia ingens</i>	M	6.621	7.279	9.331	6.253
	F	21.745	34.020	36.962	23.450

2.4.5 Conclusions

Allometric relationships were found in this chapter for both *O. ingens* and *N. sloanii* that had very tight correlations. These relationship trends supported the majority of past studies that had analysed these relationships in these species. There was, however, some variation in relationships between studies which is probably due partially to differences in beak preparation methods and differences in squid source populations. These differences highlight the need for further study on the relationships between beak size and squid size between populations along with further research on the effects of beak preparation methods on beak parameters.

The use of beak weight to estimate original squid size has been trialled in this chapter and has been shown to give tight correlations in *O. ingens* but not *N. sloanii*. Beak weight should be further studied for its suitability as a predictor of squid biomass in diet analysis studies, in particular, how beak weight is affected over time in stomach acid compared to rostral length.

A preliminary study of eye lens growth over the life-history of *O. ingens* showed that these structures have a linear growth relationship with squid mantle length (except for females over a certain age). This relationship adds weight to the theory that squid

rely heavily on their vision for both prey capture and predator avoidance throughout their lives (Nilsson et al. 2012). The growth of hard parts is important to study as it allows researchers to infer information about the development of the animal, such as the development of eyesight in *Sepioteuthis lessoniana* (Sivak et al. 1994).

Naturally occurring allometric relationships can enable researchers to deduce the size of an animal armed only with a small portion of the animal. These allometric relationships are therefore important as biomass indicators, especially in species that are difficult to collect, such as deep water squid. Allometric equations allow the reconstruction of diets and the estimation of stock sizes of animals that are ecologically, or commercially, important in a relatively cheap, and easy, manner.

Chapter Three: Structure and Composition of
Statoliths of *Onykia ingens* and *Nototodarus*
sloanii

Table of Contents

3.1 Introduction	49
3.1.1 Structure and composition.....	49
3.1.2 Hard parts used to understand squid	50
3.1.3 Aims of this chapter	51
3.2. Review of methods	52
3.2.1 Common structural analysis methods	52
3.2.2 Common composition analysis methods	53
3.2.3 Methods used in this study	55
3.3 Methods.....	57
3.3.1 Squid collection and statolith extraction	57
3.3.2 Statolith preparation.....	57
3.3.3 Scanning electron microscopy (SEM).....	58
3.3.4 Raman Spectroscopy	58
3.3.5 LA-ICP-MS.....	59
3.4 Results.....	64
3.4.1 SEM.....	64
3.4.2 Raman spectra.....	66
3.4.3 LA-ICP-MS.....	70
3.4.3.1 Element concentrations	70
3.4.3.2 Differences between zones, location and sex.....	72
3.4.3.3 Differences between species.....	72
3.5 Discussion.....	78
3.5.1 Raman shifts and structure	78
3.5.2 Trace elements, what might they mean?	79
3.5.3 Overall statolith chemistry.....	81
3.5.4 Conclusions.....	86

3.1 Introduction

Both the structure and the composition of hard parts taken from an organism can be analysed by a variety of methods to study different aspects of the organism's life history. Information from hard parts can be used in a variety of ways ranging from taxon identification (e.g., Bolstad 2006) to complex analyses used to infer life history characteristics such as tracking ontogenetic migrations of animals (Arkhipkin et al. 2004). Knowing the structure and chemical composition of hard structures can also be very useful in the material sciences. The strength of chiton radulae (Weaver et al. 2010) and the combined strength and flexibility of squid beaks, despite having no mineralization (Miserez et al. 2008), provide two examples of hard parts that are of interest in biomaterials (Brooker & Shaw 2012).

Information on the structure and composition of hard parts is also useful in a fisheries context. This information can be used to both qualitatively and quantitatively analyse the diets of commercial fish species. These dietary analyses are carried out by matching hard parts found in the fish stomachs to prey animals (Hernández-García 1995, Stevens et al. 2012). Diet analyses using hard parts are also important in a conservation context. It is important to know the diets of large, charismatic megafauna, such as sperm whales (Gaskin & Cawthorn 1967), to conserve them. Knowledge of the hard parts of the prey of both economically and ecologically important animals allows researchers to decide the best way to manage ecosystem conservation.

3.1.1 Structure and composition

The structure of hard parts refers to both the size and shape of the overall hard part and the internal structure of the subunits from which it is made. The structure of a hard part can be used to infer information about the animal's life. For example, the growth rate in *Loligo vulgaris* and other coastal cephalopod species has been calculated using growth increments in statoliths (Natsukari & Komine 1992). The most common methods used in analysing structure are light microscopy and scanning electron microscopy (SEM).

The composition of hard parts, on the other hand, is the organic and inorganic components of a sample, including elements, major to trace, molecules, and polymorphs. The composition of a structure may be used as a proxy for aspects of an

animal's life, such as using stable isotope ratios in snail tissue to infer the snail's place in the food web (Post 2002). Soft tissues, such as muscle, are often used for the stable isotope studies that analyse these trophic relationships. Hard structures, however, have also been shown to provide information in analyses involving squid and are arguably more useful. Hard structures do not deteriorate as quickly as soft tissue, and some mineralised structures, such as beaks, can be recovered from predators' stomachs (Ruiz-Cooley et al. 2006). Hard parts are also often archival, growing over the life history of the squid, allowing information to be inferred about the whole life history of the animal (Onthank & Lee 2013). The composition of hard parts can be analysed using many different methods, including Raman spectroscopy, inductively coupled plasma mass spectrometry (ICP-MS), laser ablation ICP-MS (LA-ICP-MS) and energy dispersive X-ray spectroscopy (SEM-EDS).

3.1.2 Hard parts used to understand squid life history

Squid have several hard parts in their bodies that could shed light on the life history of the individual. The gladius has been used to estimate growth rates and trophic position (Perez et al. 2006, Lorrain et al. 2011). The beak is occasionally used in aging and growth studies and has been found to be very useful when investigating the trophic position of individuals (Cherel & Hobson 2005, Liu et al. 2015a). The hard structure that has received the most attention in global squid research for its use as an archival tissue are the statoliths (Dilly 1976, Radtke 1983, Arkhipkin 1993, Ikeda et al. 2003, Liu et al. 2011, Arkhipkin et al. 2015). Each of these structures are comprised primarily of polymers meaning that the properties of the hard parts can tell us a lot about their structure.

The structure of statoliths can be used to age individual squid (Arkhipkin & Shcherbich 2012) and their composition can be analysed using stable isotopes or trace elements over the life history to collect information about development (Zumholz et al. 2007b, Liu et al. 2011). It has been well documented in the past that statoliths of mature squid contain two major visually distinct zones: an inner, opaque, zone and an outer, translucent, one (Jackson 1993, Zumholz 2005). Jackson (1993) suggested that the difference in transparency between these zones in *Onykia ingens* is due to a difference in structure which reflects the ontogenetic migration that these squid undergo. While

statoliths are the most studied of the hard parts of squid, much remains unknown about them, particularly for certain taxa and geographic regions.

3.1.3 Aims of this chapter

This chapter provides an overview of the most commonly used methods of assessing the structure and composition of hard parts, then selects the methods that are the most useful for analysing squid hard parts for use in this study. The structure and mineral composition of squid statoliths from New Zealand will be analysed and compared with the literature. The trace element concentrations in statoliths will be analysed to gain a better understanding of squid life histories, habitat and taxonomy to explore the future possibilities of trace element data in tracing the geographical origin of individual squid.

Onykia ingens (warty squid) and *Nototodarus sloanii* (southern arrow squid) are two of the most abundant and ecologically important species of squid living in New Zealand's waters. These species have been studied to a sufficient level that the more in-depth methods of analysing structure and composition of their statoliths will be useful in further describing the life of these species.

3.2. Review of methods

3.2.1 Common structural analysis methods

Light microscopy allows the study of structure of large objects; the maximum resolution of a light microscope is 200nm and the maximum magnification is around x1500. The structure of small objects, such as statoliths, can be preliminarily observed by light microscopy, looking at light transmission and colour (Jackson 1993). This technique is used to identify species when only a hard part is found in dietary remains by analysing the overall structure of the hard part (McKinnon 2006). Light microscopy is the main method of visualising and counting the daily rings within squid statoliths to age individuals (Rodhouse & Hatfield 1990, Perez et al. 2006, Arkhipkin & Shcherbich 2012). Aging statoliths using a light microscope is destructive as they first need to be sectioned.

Scanning electron microscopy (SEM) provides better resolution (0.1nm) at higher magnification (up to x500000) than light microscopes. SEM is run in a vacuum and works by producing electrons from an 'electron gun' with a cathode and anode plate below the tip of the gun to 'shoot' the electrons in the right direction. These electrons are then focused through a condenser and objective lens onto the sample. On the way to the sample, the electron beam then passes through a series of scanning coils which control the beam's movement and make the beam scan across the sample. When the electrons make contact with the sample, one of three things can happen: 1: the electron passes through the sample without touching anything; 2: the electron hits an electron in the shell of an atom in the sample and ejects it creating a 'secondary electron'; 3: the electron hits the nucleus of an atom and bounces back and becomes a 'backscattered electron'. Due to these differences in how secondary and backscattered electrons are created, they can be used to elucidate different sample characteristics. Secondary electrons emitted from a sample change with surface topography, as more secondary electrons can escape from a bump on the sample surface than can escape from a low point. Backscattered electrons give information on the density of a sample. More electrons are backscattered from higher density material as the nuclei in the sample are closer together and electrons have a higher likelihood of hitting them (Welton 1984, McMullan 1995, Reed 2010).

3.2.2 Common composition analysis methods

X-ray diffraction (XRD) is an analytical chemistry technique for determining the composition of a crystalline sample and its structure. This technique is based on the idea that crystalline structures are arranged in layers that have spaces between them that are unique to each mineral. XRD utilises X-rays produced by bombarding a metal target with a beam of electrons to measure these spaces. The sample is exposed to X-rays at all possible angles of incidence; if the wavelength of the X-ray is the same as the distance between the layers in the sample, the angle of incidence and reflection of the X-ray are the same. These data are then used to calculate the space between layers in the sample which can then be identified by checking its spacings against a database of known minerals (Dutrow & Clark 2015). XRD is the only method, excluding electron backscatter diffraction (EBSD), that differentiates between polymorphs of the same compound (Dutrow & Clark 2015). XRD is non-destructive; however, it uses powdered solid samples, meaning that the average of the sample is obtained and uses around 0.5g of sample (Dutrow & Clark 2015).

Raman spectroscopy is one technique used in analytical chemistry to explore the molecular make-up of a sample, from exploring dyes in art (Leona et al. 2006) to determining calcite content in milk powder (Smith et al. 2013). This technique relies on the inelastic scattering of photons within monochromatic light. Inelastic scattering of light is when the energy of the light being emitted from a sample is different from the energy of the light going into it. Inelastic scattering occurs when a molecule absorbs the energy from the light causing the molecule to move to a different vibrational energy level. The light then stops and the molecule releases a photon which has a different energy from the light going in. This energy difference (or shift) is known as the Raman Effect. The shifted photons are then collected by a detector in the machine. The frequencies that each molecule vibrate at are called lattice modes and the position of these modes gives information on various properties of the molecules within the sample (Schrader et al. 2000). The light source is usually a laser (Princeton Instruments 2012). Raman spectroscopy is a valuable technique as it can be used when the sample is in a solid, liquid or gaseous state and it is fast and easy to use. Other advantages include that it is non-destructive when using solid samples meaning the same samples can be further analysed using different methods and only small amounts of samples are needed

(<0.1mg). Raman also gives a good qualitative description of the general make-up of the sample. The disadvantages of Raman spectroscopy are that, while it's easy and fast to get qualitative data, it is difficult and time-consuming to get quantitative data and it is not sensitive enough for trace element analyses.

Infrared spectroscopy (IR) is a method used in analytical chemistry to assess the structure and purity of a compound. IR makes use of infrared light to analyse a sample. Infrared light are the wavelengths of the electromagnetic spectrum that are between the visible and the microwave wavelengths. The infrared spectrum is split into three regions, near (which is closest in wavelength to visible light), mid and far; each of these regions can be used in IR depending on the molecules being analysed. Molecules naturally absorb infrared radiation and convert it into vibrational energy, when the energy of the infrared light is the same as a particular molecules vibrational mode, the light is absorbed by the molecule. This absorption of infrared radiation is utilised to analyse which molecules are in a sample by exposing it to infrared radiation and recording which wavelengths are absorbed. This data can then be analysed against the wavelengths absorbed by known materials and the material in question can be identified (University of Colorado 2002) (Reusch 2013a). IR detects molecules with more sensitivity than Raman as it can distinguish between different functional groups in a molecule however, more sample material is required (~2mg to 80mg depending on the exact method)(Department of Chemistry, UCLA 2003).

Inductively coupled plasma mass spectrometry (ICP-MS) is a powerful technique that is used to analyse the elemental content of a sample down to the parts per trillion level (Elmer 2001). A sample is introduced to the ICP-MS in aerosol form. This aerosol then passes through a plasma torch and undergoes a state change to gas (Wolf 2013). The gas is ionized and released into a mass spectrometer (MS) (Elmer 2001, Wolf 2013). Once in the MS the ions are accelerated into a tube by a negatively charged plate. The tube is bent and a quadrupole bends the ions through the tube. This bending via magnetic forces separates the ions based on their molecular weights as heavier ions bend less and lighter ions bend more. Ions then pass through a slit that only lets one mass through at a time, and hit a detector. The magnetic field is then varied so that all masses can be analysed and the composition of the sample can be defined. Mass

spectrometry is able to detect different isotopes of elements using this method (Reusch 2013b).

Gas samples can be introduced straight into the ICP-MS system, but liquid and solid samples must be turned into an aerosol first. For liquid samples this can be done using a nebulizer (Elmer 2001). Solid samples can either be digested into a liquid or ablated by a laser, then turned into an aerosol. Digesting solid samples takes the average trace element concentration of the structure (Liu et al. 2008) while laser ablation ICP-MS (LA-ICP-MS) allows researchers to compare parts of the sample. This ability to gain spatial resolution from a sample is one of the advantages of LA-ICP-MS; others include only needing small amounts of sample material (<0.1mg, compared to >0.5g for ICP-MS) and the speed at which analyses can be done. LA-ICP-MS is, however, a destructive method.

Scanning electron microscope - energy dispersive X-ray spectrometer (SEM-EDS) is another technique that can be used to analyse trace elements by mapping the surface and elemental structure of a sample (Welton 1984, Newbury & Ritchie 2013). As secondary electrons are ejected from the inner shell of atoms during SEM, the atom becomes unstable. When an atom is missing an electron from an inner shell, an electron from its outer shell drops into the inner shell to take the place of the missing electron. This electron shift releases energy in the form of X-rays. Each element emits its own X-ray signature when it loses an electron and these data can be utilized by an EDS unit to give information on the elements present in the sample being observed (Welton 1984, Newbury & Ritchie 2013). SEM-EDS has the advantage that it can take spatial data and can work with small samples (1-5µm across) (Goldstein et al. 2012). SEM-EDS is a destructive method as samples must be coated so that they are conductive. SEM-EDS is also less sensitive than LA-IPC-MS.

3.2.3 Methods used in this study

SEM was used to analyse the structure of statoliths as it gives better resolution than light microscopy and allows the structure and orientation of individual crystals to be analysed. Raman spectroscopy was selected to qualitatively analyse the mineral composition of statoliths as it is fast, readily available, and spatial resolution is fine, allowing information to be collected from each statolith. Other methods, such as XRD and IR require a large amount of sample material meaning more than one statolith

would need to be homogenised and analysed at once. Raman spectroscopy is also non-destructive meaning samples could be used again which is advantageous as there is a limited number of samples. LA-ICP-MS was selected for trace element analyses as it allows the spatial quantification of trace element data from a sample where most other methods do not. LA-ICP-MS also allows the analysis to be completed on single statolith rather than a homogenised powder. SEM-EDS does give spatial data from a single specimen; however, LA-ICP-MS is a more sensitive technique.

3.3 Methods

3.3.1 Squid collection and statolith extraction

Squid were collected and stored as described in section 2.2. Pairs of statoliths were dissected from 50 *Onykia ingens* specimens at the Auckland University of Technology (AUT) in June 2014. Statoliths from 50 *Nototodarus sloanii* specimens were dissected at the University of Otago in August 2015. Squid were defrosted on the day of statolith removal under running seawater. All statoliths were dissected using methods from Rodhouse & Hatfield (1990). Statoliths were removed from the statocysts using fine forceps and placed into small plastic vials so that they were not misplaced. Dissection of statoliths was undertaken in this research using the method outlined above as it was both the quickest method and gave the best statolith recovery rate in this study.

3.3.2 Statolith preparation

28 *O. ingens* and 30 *N. sloanii* statoliths were chosen to represent the full range of size, sexes and collection locations where possible. Statoliths were prepared for both Raman Spectroscopy and LA-ICP-MS. Each statolith was sectioned along the lateral axis so that the core and all of the rings were exposed allowing chemical analyses of the entire life history of the animal. Each statolith was mounted onto a microscope slide, concave side up, using a thermoplastic cement (Crystalbond[®]) heated to its melting point (150°C) then sanded using 1200grit Wet&Dry[®] sandpaper until the core of the statolith was visible. Statoliths were periodically checked under a light microscope so the core was not sanded through. Statoliths were then polished using 0.5µm alumina powder on a wet cloth to remove surface scratches so that structures were more visible. Sections from three cockles (*Austrovenus stutchburyii*) were also prepared in the same way to be analysed via Raman spectroscopy. This was done to make sure that the preparation method did not change the mineralogy of the samples as the cockles' shells are also made of aragonite. This preparation technique is similar to the preparation used when aging squid via their statoliths. When aging, the statolith is flipped over after this procedure and the process is repeated to give a very thin section of the statolith to better view the growth lines, I did this with the statoliths of *O. ingens* but not those of *N. sloanii*. I did not flip the *N. sloanii* statoliths over and sand the convex side as LA-ICP-MS

is a destructive method and it may have penetrated through the statolith if it was any thinner. I had already prepared the *O. ingens* statoliths for Raman Spectroscopy before I decided to utilise LA-ICP-MS which is why the statoliths were prepared differently.

Once each statolith was prepared, it was transferred onto a single slide with the other statoliths from the same species (Fig. 3.1). This combination of statoliths onto one slide was done so that the slide did not need to be changed between each sample while analyses were being carried out.

Six *O. ingens* and seven *N. sloanii* statoliths were chosen for examination by SEM. Sections already obtained for Raman spectroscopy and LA-ICP-MS would not work as the surface had been ground and polished, making them flat. Statoliths were sectioned by breaking them along the medial plane, across the core and perpendicular to growth rings. Statoliths were first placed convex side up on a microscope slide and fixed in place with a small amount of Crystalbond® around the base. The area of breakage was then determined and a scalpel was used to draw a line on the surface of the statolith along the plane of desired breakage. A very slight amount of pressure was then applied with the scalpel along this line until the statolith fractured. Statoliths were then moved to a SEM stub and secured using carbon tape with the fractured side of the statolith facing upwards. This work was carried out under a dissection microscope.

3.3.3 Scanning electron microscopy (SEM)

SEM work was carried out on a JEOL JSM-7500F scanning electron microscope (Fig. 3.2C) by the author with help from a technician. The SEM stub containing the sectioned statoliths was coated with a thin film of platinum palladium. The SEM stub was placed into the stub holder in the microscope and a vacuum was created. Photos were taken of the inside and outside surfaces of seven statoliths at 150x, 1000x, 3000x and 4500x magnifications.

3.3.4 Raman Spectroscopy

Raman spectroscopy was carried out using a Senterra Raman microscope (Fig. 3.2B) by the author, with help from Dr Geoff Smith of the University of Otago. Data was analysed using OPUS 6.5 software (Bruker Optics, Ettlingen, Germany). Samples mounted on slides were placed into the microscope. OPUS software was used to carry out transects across samples from the core to the outside edge perpendicular to growth

rings across the dorsal dome. The transect was made up of 20x50 μ m spots for *O. ingens* statoliths and 10x50 μ m spots for *N. sloanii* statoliths. Transects were shortened for *N. sloanii* statoliths due to time constraints and homogeneity of the samples. The laser setting were as follows: 785nm wavelength laser at 100mW with 20x50 μ m spots taken for 5s (10x50 μ m spots taken for 5s for *N. sloanii*) x6 co-additions. Calibration of the machine was undertaken at the start of each session using a polystyrene standard and an aragonite standard was used to calculate machine drift at the start and end of each session. The Crystalbond[®] mounting cement was analysed at the end of each sample run to compare its composition over a variety of samples. This was also done so that peaks related to the mounting media that are seen within the statolith samples can be explained.

The Raman peaks at 401 cm^{-1} , 649 cm^{-1} , 840 cm^{-1} , 1043 cm^{-1} , 1167 cm^{-1} , 1398 cm^{-1} , 1582 cm^{-1} , 1601 cm^{-1} , 1726 cm^{-1} and 1891 cm^{-1} are more prominent in the outer zone of the statolith as it is more transparent and thinner than the inner zone. This lets more light through the sample into the Crystalbond and glass slide, exciting this medium and thus producing photon shifts in the light that is picked up by the machine turned into peaks in the sample. This means that the peaks related to Crystalbond and glass appear more in the outer zone of the statolith because it is more transparent. The software that was used to analyse this data was not able to subtract these peaks; however, as the peaks are at known shift-values one can disregard them when analysing the sample for prominent structures and material.

Austrovenus stutchburyi (New Zealand cockle) is a bivalve with an aragonitic shell (Cummings 2014). The *A. stutchburyi* samples that were prepared and run in the same way as the statoliths of *O. ingens* and *N. sloanii* produced consistent Raman peaks at 151 cm^{-1} , 205 cm^{-1} , 250 cm^{-1} , 703 cm^{-1} , and 1085 cm^{-1} . These peaks are able to be attributed to aragonite (Frech et al. 1980, Gauldie et al. 1997). This consistency shows that the machine was calibrated correctly and the preparation methods used here did not alter the mineralogy of the minerals in the samples.

3.3.5 LA-ICP-MS

The laser ablation system used was a RESolution M-50 laser ablation system (Fig. 3.2A) attached to an Agilent 7500cs ICP-MS. This analysis was carried out by the author with the help of a technician (Malcolm Reid). 10 elements were analysed for in

the statoliths, they were: Be, Mg, Mn, Cu, Zn, Sr, Y, Zr, Ba and U. These elements were analysed for as they have been previously found in statoliths (Zumholz et al. 2007b, Liu et al. 2011) with the exception of Be which was suggested by the head technician. The slides with the samples mounted onto them were placed inside a cell that was directly under the laser. A microscope was set up to view the samples using a mirror so that the microscope lens would not interfere with the laser. The cell was then purged with pure N₂ gas which increases the system sensitivity to trace elements. The laser settings were as follows: 75µm spots used to run a transect between 400–600µm long, data acquisition time of 135 seconds which was made up of a 20-second gas blank then 115 seconds of ablation as 115 seconds was the time taken for the longest transect. There was a 5-second cleaning run prior to data acquisition to take the surface off the transect to avoid contamination via sample handling. The 20-second gas blank at the start of data acquisition was a time where no laser ablation occurred but the gas that is used to purge the cell is flowing and being analysed by the ICP-MS. This analysis of gas also occurs during the laser ablation stage of data acquisition. By running a gas blank at the start of each data acquisition period the traces picked up in the gas can be subtracted from the data acquired during ablation so that the data is representative of the sample and not the gas in the cell.

Three calibration materials were used during laser ablation: NIST610, NIST 612 and MACS (homogenised otolith). NIST610 and NIST 612 are standard reference materials (SRMs) made of glass support matrices with known quantities of known trace elements added to them. The two SRMs differ in the exact trace elements embedded in the matrix and the concentrations of each element (Reed 1992a, b). Normally the SRM with the closest concentrations of trace elements to the samples being analysed is used; we used both as we were uncertain which would be closest. MACS is a SRM made of calcium carbonate (Strnad et al. 2009), homogenised otoliths in this case. Calibration transects were run at the start and end of each slide being analysed and between every 8–10 samples to account for machine drift. Calibration transects had a 5-second cleaning run then a 60-second data acquisition period which included a 20-second gas blank and 40 seconds of ablation.

Data were analysed using Iolite version 2.5 on Igor Pro version 6.37. The software analysed the trace element concentrations in the statoliths by first subtracting

the background signals of the gas in the cell. The calibration standard material that was closest to the samples (NIST610) was then chosen. The software was then used to isolate the areas of interest in the analyses, which were the transects of the statoliths. The amount of each trace element in the transect was quantified by setting calcium as the internal standard at 40%wt as this value has been used in other studies (Zumholz et al. 2007b) and has been found for Humboldt squid (Chen, B unpublished data). The resulting data were expressed as amount of trace elements in parts per million (ppm) at time slices, where time zero is the start of the transect. Data were then exported to Microsoft Excel (2013) where each element was converted to a ratio of the element to calcium and expressed in mmol of the element per mol of calcium. 50 μ m-long sections of the transects were then chosen to represent the inner and outer zones of the statoliths. Graphs were created in Excel and ANOVAs were run in R (v2.15.3) to test for statistical significance.

All of the specimens that I was able to prepare for LA-ICP-MS from the Pukaki Rise location were females. To test whether there was a difference in trace element concentrations between sexes I used only statoliths from squid collected on the Chatham Rise as this sample contained both males and females. When I compared *O. ingens* statoliths between geographical regions I only included females from both regions. This sex selection is because the results of analysis on sex effect in the Chatham Rise cannot be extrapolated to the Pukaki Rise as the squid may be from different populations. When comparing statoliths of different sexes or regions, the outer zone readings were used as they better reflect the environment in which the squid was caught and its recent life history.

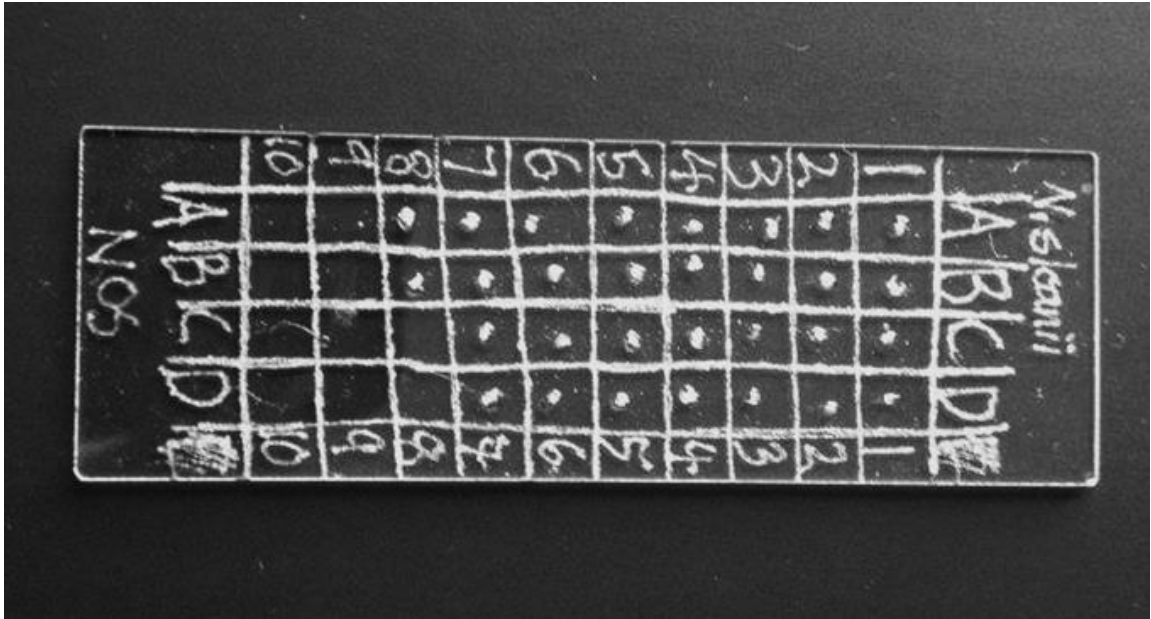


Figure 3.1: Slide with *N. sloanii* statoliths prepared for LA-ICP-MS.

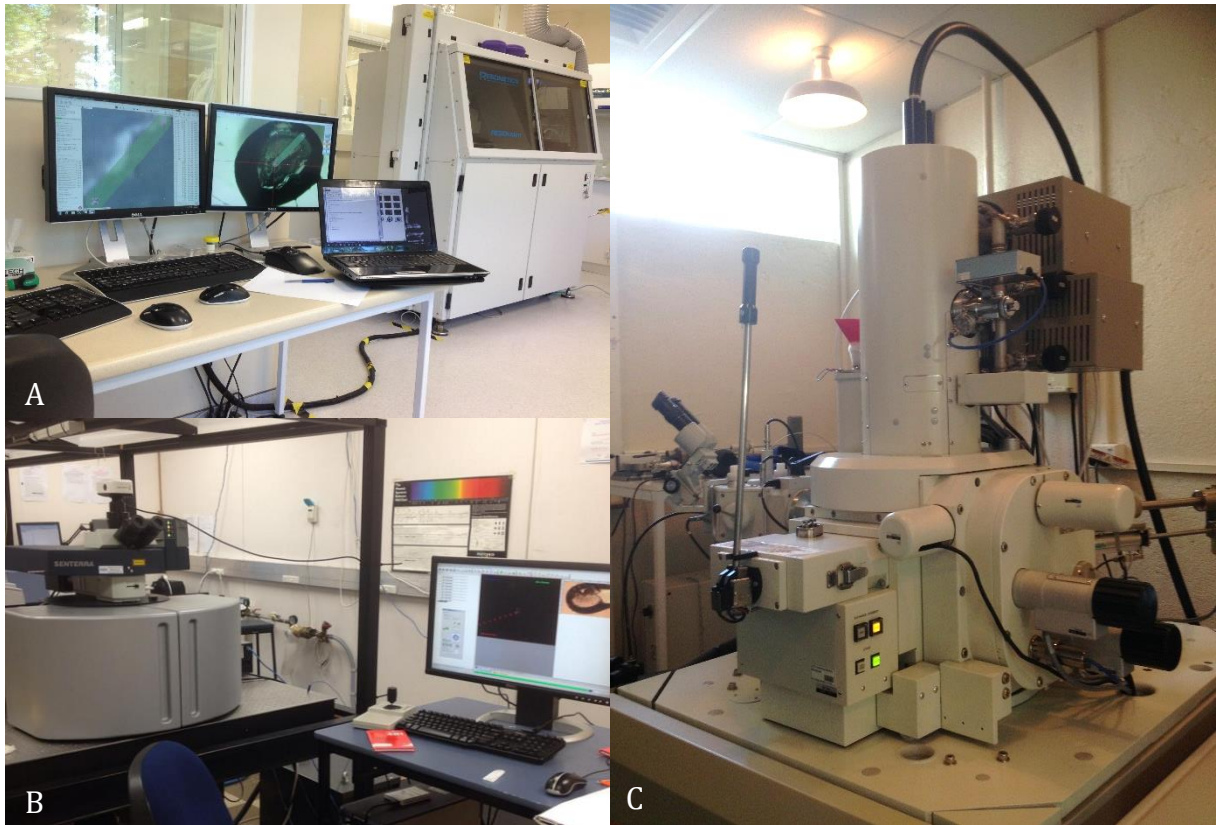


Figure 3.2: The instruments used to analyse structure and composition in this chapter. A: RESolution laser ablation system; B: Senterra Raman spectrometer; C: JEOL scanning electron microscope.

3.4 Results

3.4.1 SEM

The outer crystalline structure of statoliths from both *Onykia ingens* and *Nototodarus sloanii* is very similar, having a botryoidal structure, which is porous in places, made up of the ends of aragonite crystals (Boggild 1930) (Fig. 3.3A, 3.4C & D). Likewise, the internal crystal structure of the statoliths is similar between the two species (Fig. 3.3 & 3.4). The internal crystal structure is that of regularly placed, tightly packed elongated columnar crystals radiating outward from the core, appearing to have three-dimensional rotational symmetry (Fig. 3.3A & B). The wing of the statolith is made up of irregularly packed statoconia that are hexagonal and consist of many columnar crystals as the ends are rough (Fig. 3.5).

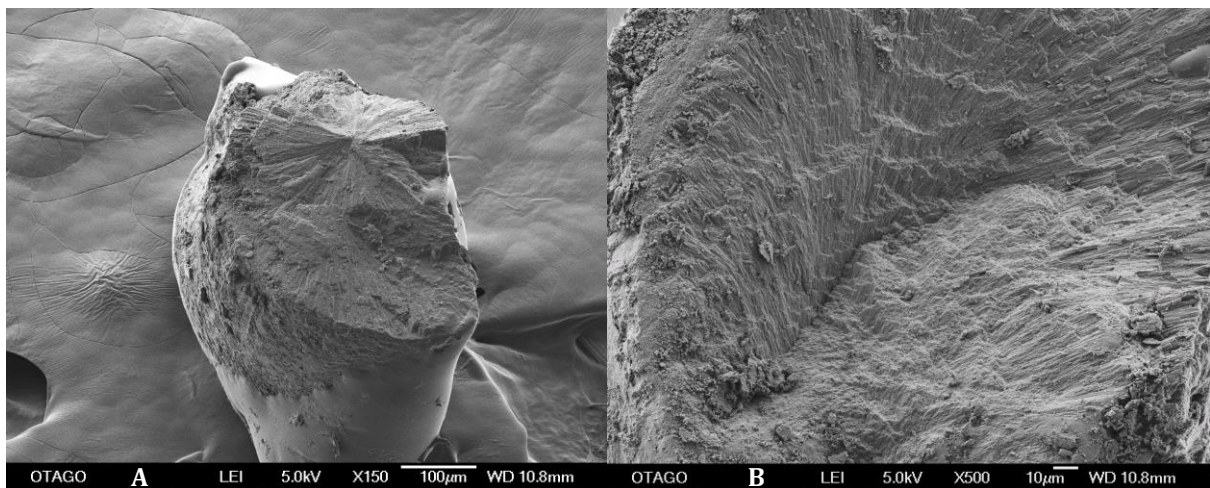


Figure 3.3: SEM images of fractioned statoliths from *N. sloanii* (A) and *O. ingens* (B). A: overall statolith magnified 150x. B: fractioned surface of a statolith magnified 500x.

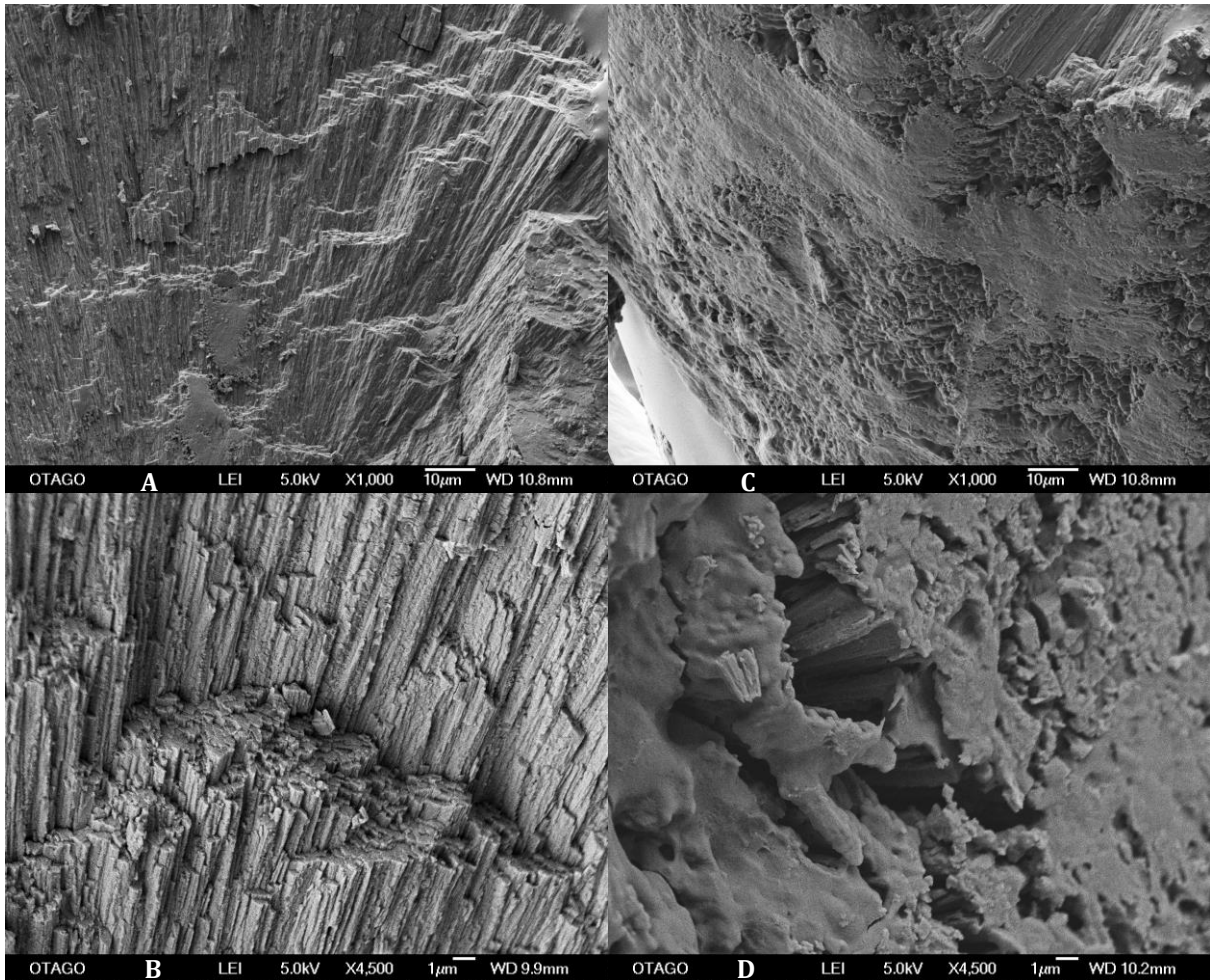


Figure 3.4: SEM images of statoliths from *O. ingens* (A & C) and *N. sloanii* (B&D). A: fractioned surface of a statolith at 1000x magnification. B: the outside of a statolith at 1000x magnification. C: fractioned surface of a statolith at 4,500x magnification. D: the outside of a statolith at 4,500x magnification.

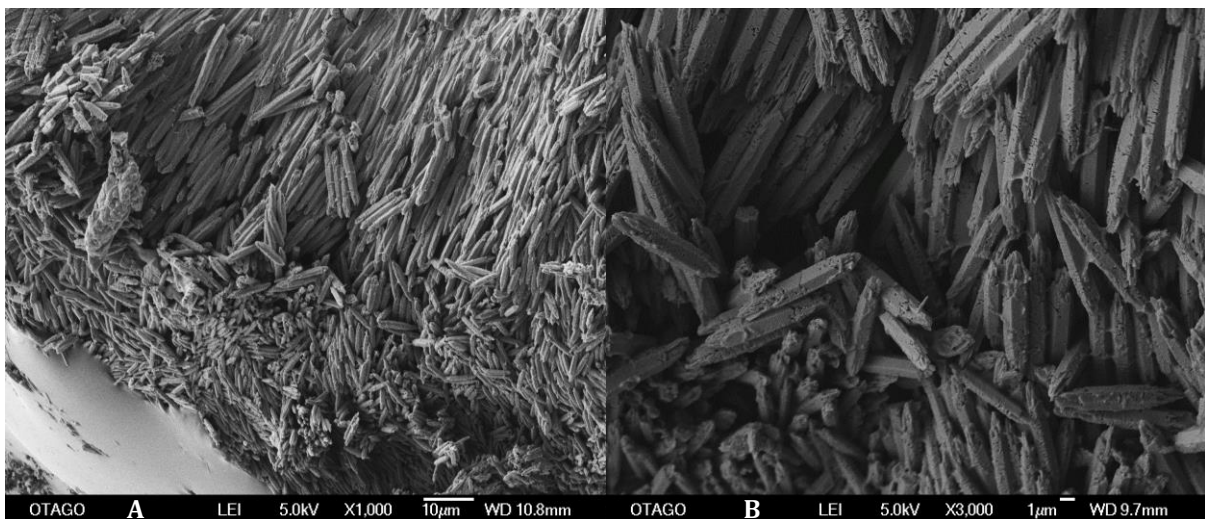


Figure 3.5: SEM images of the outside surface from the wing of a statolith from *O. ingens*. A: outside surface of the wing at 1000x magnification. B: outside surface of the wing at 3000x magnification.

3.4.2 Raman spectra

Spectra of Crystalbond® over glass had peaks at the following Raman shift frequencies: 98cm⁻¹, 402cm⁻¹, 649cm⁻¹, 812cm⁻¹, 840cm⁻¹, 877cm⁻¹, 1043cm⁻¹, 1167cm⁻¹, 1396cm⁻¹, 1582cm⁻¹, 1601cm⁻¹, 1726cm⁻¹ and 1892cm⁻¹ (Fig. 3.6).

Spectra of *Austrovenus stutchburyi* aragonite standards had peaks consistently at 151cm⁻¹, 205cm⁻¹, 250cm⁻¹, 703cm⁻¹ and 1085cm⁻¹ (Fig. 3.6) (Table 3.1).

Spectra of *O. ingens* statoliths exhibited consistent peaks at 150cm⁻¹, 204cm⁻¹, 704cm⁻¹, 1085cm⁻¹, 1398cm⁻¹, 1582cm⁻¹, 1601cm⁻¹, 1726cm⁻¹ and 1891cm⁻¹ over the entire structure (Fig. 3.7) (Table 3.1). Peaks corresponding to peaks from Crystalbond® and glass were more prominent in spectra taken from the inner zone of the statolith. The peak at 272cm⁻¹ in the inner zone shifted to 255cm⁻¹ in the outer zone in some samples (Fig. 3.8); however, this did not occur in all samples and did not appear specific to location of squid capture or sex. Sex or location of capture had no apparent effect on the location of peaks (Table 3.1).

Spectra of *N. sloanii* statoliths exhibited consistent peaks at 150cm⁻¹, 204cm⁻¹, 704cm⁻¹ and 1085cm⁻¹ regardless of the position on the statolith from which the spectrum was taken (Fig. 3.9) (Table 3.1). There were two main differences between the peaks of the inner and outer zone. The first difference was the occurrence and strength of peaks at 401cm⁻¹, 649cm⁻¹, 840cm⁻¹, 1043cm⁻¹, 1167cm⁻¹, 1398cm⁻¹, 1582cm⁻¹, 1601cm⁻¹, 1726cm⁻¹ and 1891cm⁻¹. The core of the statoliths consistently showed fewer of these peaks than the outer zone. The second difference between the two zones was a peak shift. There was a peak at around 272cm⁻¹ present in the core sites that consistently shifted to around 250cm⁻¹, at the outer edge of the statolith (Fig. 3.10). Sex had no apparent effect on the location of peaks (Table 3.1).

Spectra of *O. ingens* and *N. sloanii* exhibited the same consistent peaks at 150cm⁻¹, 204cm⁻¹, 704cm⁻¹ and 1085cm⁻¹ (Table 3.1). There was, however, a higher occurrence of the peak shift from 272cm⁻¹ to 250cm⁻¹ in the samples from *N. sloanii*.

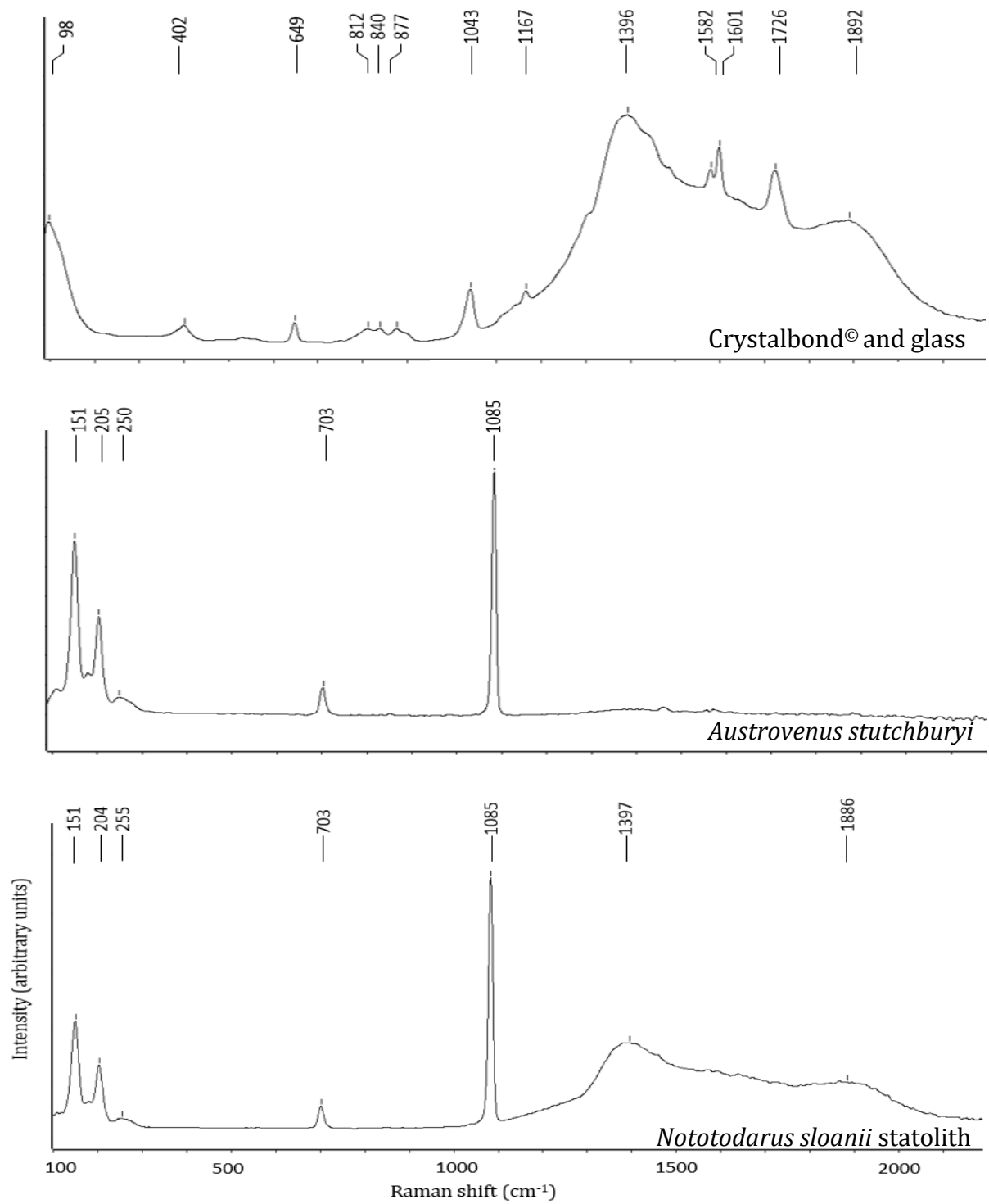


Figure 3.6: Typical Raman spectra of Crystalbond® mounting media over glass, *A. stutchburyi* shell (aragonite) and *N. sloanii* statolith. Peaks are marked and labelled giving exact locations.

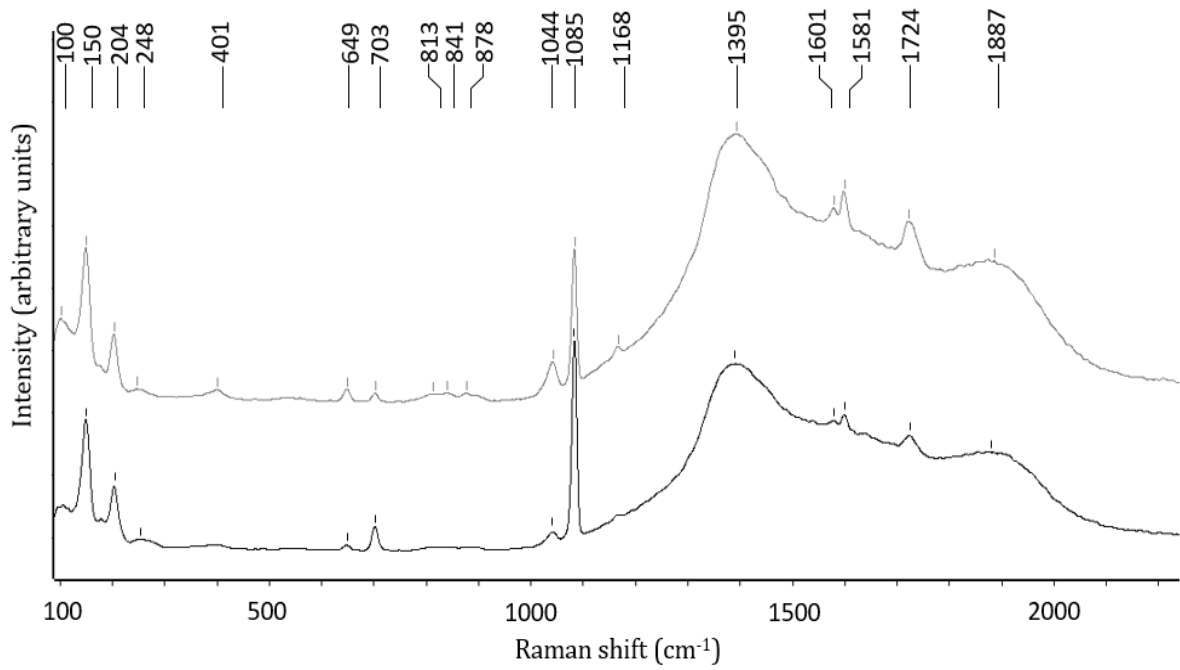


Figure 3.7: Raman spectra of typical *O. ingens* statolith, inner zone in black, outer zone in grey. Peaks are marked by lines giving exact locations.

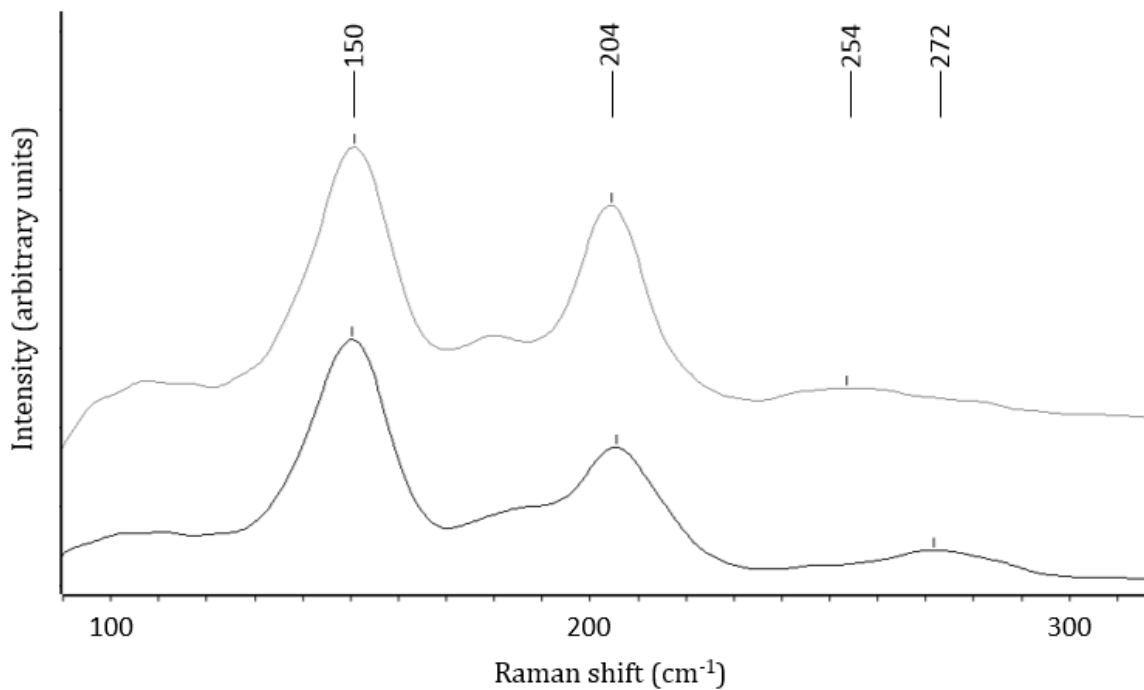


Figure 3.8: Low-end Raman spectra of *O. ingens* statolith showing the shift of the peak from 272cm^{-1} to 254cm^{-1} . Inner zone in black, outer zone in grey, peaks are marked by lines giving exact locations.

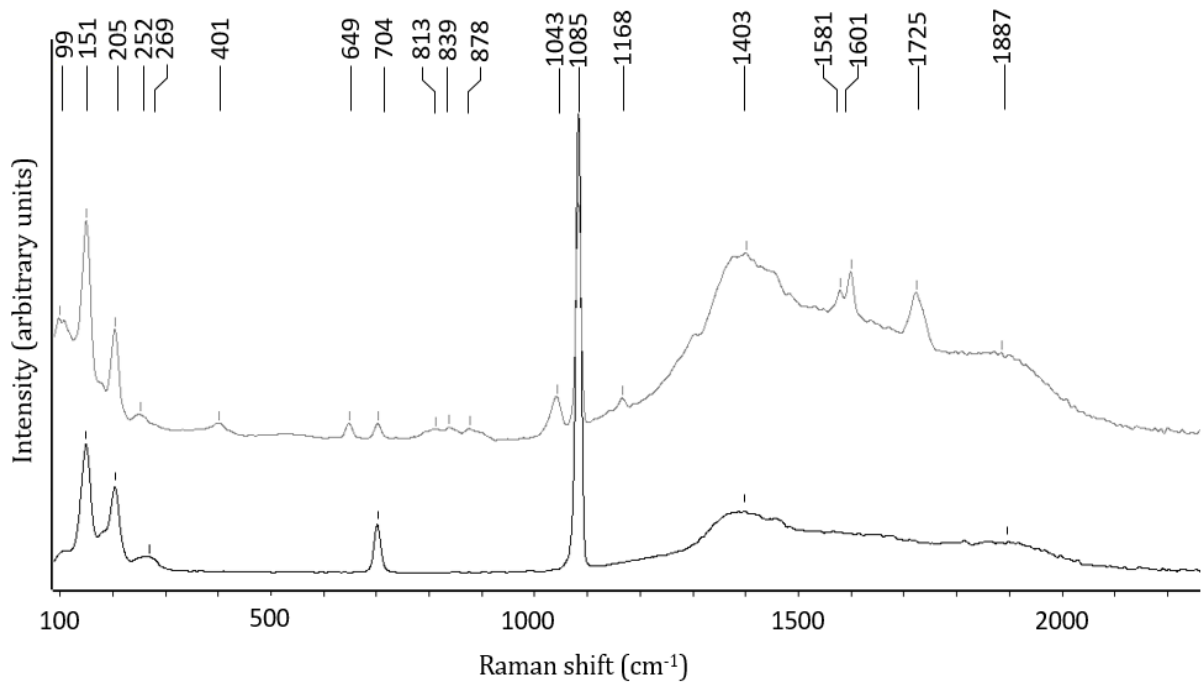


Figure 3.9: Raman spectra of typical *N. sloanii* statolith showing difference in peaks between zones. Inner zone in black, outer zone in grey, peaks are marked by lines giving exact locations.

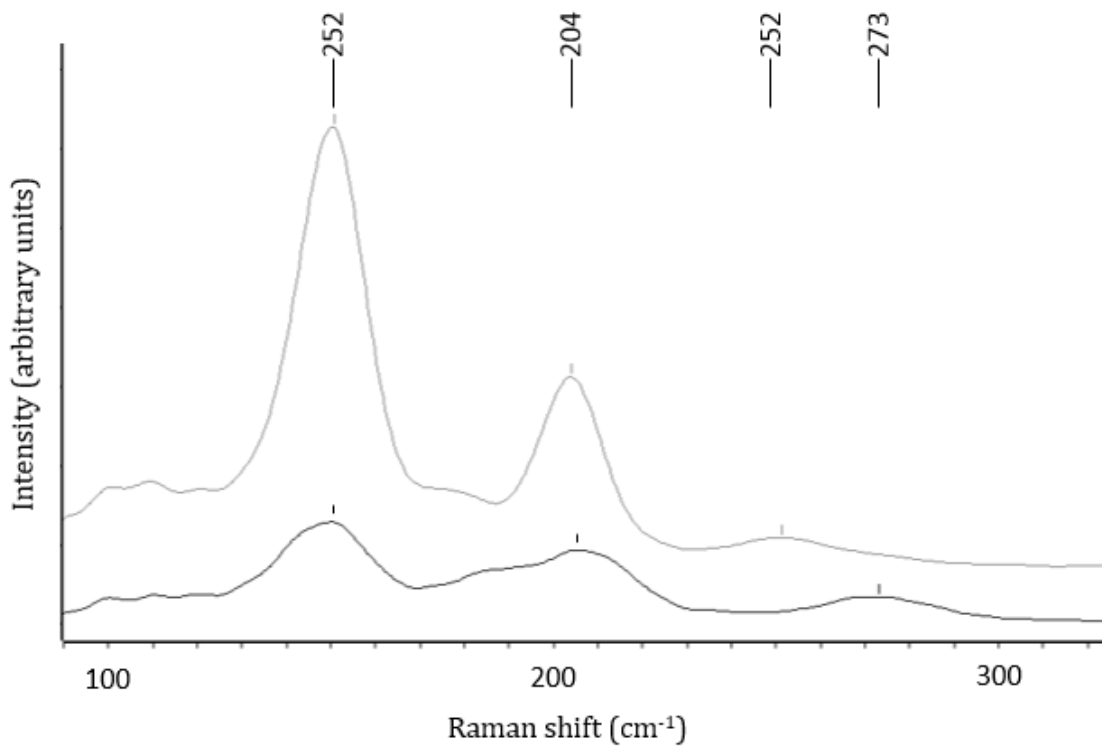


Figure 3.10: Low-end Raman spectra of *N. sloanii* statolith showing the shift of the peak from 273 cm^{-1} to 252 cm^{-1} . Inner zone in black, outer zone in grey, peaks are marked by lines giving exact locations.

Table 3.1: Raman frequencies for statoliths and the cockle standard excluding peaks from Crystalbond® and glass.

Sample	Location	Sex	n	Lattice modes			v4	v1
<i>Onykia ingens</i>	Chatham Rise	Male	11	150cm ⁻¹	204cm ⁻¹	250-270 cm ⁻¹	704cm ⁻¹	1085cm ⁻¹
		Female	8	150cm ⁻¹	204cm ⁻¹	250-270 cm ⁻¹	704cm ⁻¹	1085cm ⁻¹
	Pukaki Rise	Male		150cm ⁻¹	204cm ⁻¹	250-270 cm ⁻¹	704cm ⁻¹	1085cm ⁻¹
		Female	9	150cm ⁻¹	204cm ⁻¹	250-270 cm ⁻¹	704cm ⁻¹	1085cm ⁻¹
<i>Nototodarus sloanii</i>	Chaslands	Male	17	150cm ⁻¹	204cm ⁻¹	250-270 cm ⁻¹	704cm ⁻¹	1085cm ⁻¹
		Female	13	150cm ⁻¹	204cm ⁻¹	250-270 cm ⁻¹	704cm ⁻¹	1085cm ⁻¹
<i>Austrovenus stutchburyi</i>	Portobello		3	150cm ⁻¹	204cm ⁻¹	250cm ⁻¹	704cm ⁻¹	1085cm ⁻¹

3.4.3 LA-ICP-MS

3.4.3.1 Element concentrations

Statoliths of both *O. ingens* and *N. sloanii* contained trace levels of all ten trace elements that were analysed (Table 3.2). In *O. ingens*, the highest concentration of the trace elements measured in the statoliths was in strontium, ranging from 5946 to 10709ppm with a mean value of 7244ppm. The ratio Sr: Ca had a range of 6.8 to 12.25mmol mol⁻¹ with a mean value of 8.29 mmol mol⁻¹ (Table 3.2). Zirconium, beryllium and yttrium were present in the lowest concentrations of the trace elements measured with means of, 0.018, 0.025 and 0.026ppm respectively (Table 3.2). The concentrations and element: Ca ratios of all elements analysed in *O. ingens* statoliths are given in Table 3.2.

Strontium also had the highest concentration of measured trace elements in *N. sloanii* statoliths with a range of 6074 to 9466ppm and a mean of 7590ppm (Table 3.3). The Sr: Ca ratio has a range of 6.95 to 10.83 mmol mol⁻¹ with a mean of 8.68 mmol mol⁻¹ (Table 3.3). Zirconium, yttrium and uranium were present in the lowest concentrations of the trace elements analysed in *N. sloanii* statoliths, with means of 0.011, 0.018 and 0.019ppm respectively (Table 3.3). The concentrations and element: Ca ratios of all elements analysed in *N. sloanii* statoliths are expressed in Table 3.3.

Table 3.2: The range, mean and standard deviation of all trace elements analysed in the statoliths of *O. ingens* expressed as concentrations and ratios to calcium (n=28).

Element	Concentration (ppm)			Element: Ca (mmol mol ⁻¹)		
	Range	Mean	Std dev	Range	Mean	Std dev
Beryllium	BDL* - 0.51	0.02523	0.05967	BDL* - 0.0056	0.00027800	0.000663
Magnesium	21.66 - 1873	55.85	107.8	0.089 - 7.72	0.2298	0.4442
Manganese	0.78 - 18.51	4.431	1.787	0.0014 - 0.0338	0.008077	0.003254
Copper	BDL* - 116.2	1.317	5.574	BDL* - 0.18	0.002073	0.008792
Zinc	BDL* - 50.92	2.087	5.326	BDL* - 0.078	0.003194	0.008163
Strontium	5946 - 10709	7244	601.9	6.80 - 12.25	8.285	0.6885
Yttrium	BDL* - 0.57	0.02609	0.04128	BDL* - 0.0006	2.919E-05	4.58E-05
Zirconium	BDL* - 5.60	0.0178	0.1217	BDL* - 0.0061	1.952E-05	0.000134
Barium	BDL* - 150	9.558	3.698	BDL* - 0.1095	0.006971	0.002698
Uranium	BDL* - 0.60	0.03763	0.04575	BDL* - 0.0003	1.623E-05	1.98E-05

*BDL = below detectable level

Table 3.3: The range, mean and standard deviation of all trace elements analysed in the statoliths of *N. sloanii* expressed as concentrations and ratios to calcium (n=30).

Element	Concentration (ppm)			Element: Ca (mmol mol ⁻¹)		
	Range	Mean	Std dev	Range	Mean	Std dev
Beryllium	BDL* - 0.3954	0.03234	0.06740	BDL* - 0.0044	0.00036	0.00075
Magnesium	19.21 - 2349.6	50.14	73.53	0.07902 - 9.685	0.2067	0.3031
Manganese	BDL* - 44.20	0.6701	0.8237	BDL* - 0.0807	0.001222	0.001502
Copper	BDL* - 96.27	0.8857	4.800	BDL* - 0.1518	0.001396	0.007569
Zinc	BDL* - 108.7	0.9035	4.287	BDL* - 0.1665	0.001385	0.00657
Strontium	6074 - 9466	7590	540.6	6.946 - 10.83	8.680	0.6182
Yttrium	BDL* - 0.1266	0.01783	0.01919	BDL* - 0.0001	2.01E-05	2.16E-05
Zirconium	BDL* - 2.802	0.01092	0.07368	BDL* - 0.0031	1.20E-05	8.09E-05
Barium	4.616 - 11.55	7.026	0.9182	0.0034 - 0.0084	0.005126	0.00067
Uranium	BDL* - 0.3137	0.01863	0.02185	BDL* - 0.0001	7.84E-06	9.20E-06

*BDL = below detectable level

3.4.3.2 Differences between zones, location and sex

There was no significant difference in the element: Ca ratios for any trace elements measured between sexes in the specimens of *O. ingens* caught on the Chatham Rise ($p>0.05$) (Table 3.4) There was also no significant difference in the element: Ca ratios for any trace elements measured between the sexes in *N. sloanii* ($p>0.05$) (Table 3.5).

The statoliths of *O. ingens* showed a clear pattern in trace element: Ca shifts between the inner and outer zones for seven out of the ten elements measured. Copper, zinc, magnesium, yttrium, zirconium, barium and uranium all occurred in significantly higher concentrations in the inner zone than in the outer zone of the statoliths ($p<0.05$) (Fig 3.11). Strontium, manganese and beryllium showed no significant difference between the two zones of the statolith ($p>0.05$).

Statoliths of female *O. ingens* from the Pukaki Rise had significantly higher element: Ca ratios of copper, zinc, barium and uranium than statoliths of females from the Chatham Rise ($p<0.05$) (Fig. 3.12). There was no significant difference in the element: Ca ratios between locations for the other six elements analysed ($p>0.05$).

Seven out of ten of the elements measured in the statoliths of *N. sloanii* showed a significant difference in their element: Ca ratios between zones of the statolith ($p<0.05$). Beryllium, copper, zinc, yttrium and zirconium all had significantly higher ratios in the outer zone than in the inner zone (Fig. 3.13). Barium and strontium had significantly higher ratios in the inner zone than the outer zone (Fig. 3.13). Magnesium, manganese and uranium had no significant difference between zones ($p>0.05$).

3.4.3.3 Differences between species

Six out of the ten trace elements measured had significantly different ratios in the outer zone of statoliths between the two species ($p<0.01$). Barium, manganese, strontium, uranium and yttrium all had higher element: Ca ratios in the outer zone of *O. ingens* than in *N. sloanii* (Fig. 3.14). Beryllium had a higher ratio in the outer zone of *N. sloanii* than in *O. ingens* (Fig. 3.14) Magnesium, copper, zinc and zirconium had no significant difference in element: Ca ratio between species.

Table 3.4: ANOVAs of trace element: Ca ratios in male versus female *O. ingens*. df= degrees of freedom;

Element	df	SS	MS	F-value	p-value
Beryllium	1	0	4.00E-12	0	0.99
Magnesium	1	9.90E-03	9.00E-03	0.13	0.72
Manganese	1	7.29E-06	7.29E-06	0.48	0.50
Copper	1	1.09E-06	1.09E-06	0.10	0.76
Zinc	1	4.00E-07	3.50E-07	0.01	0.93
Strontium	1	1.75E-01	1.75E-01	0.48	0.50
Yttrium	1	1.14E-09	1.14E-09	0.30	0.59
Zirconium	1	2.80E-10	2.76E-10	0.06	0.81
Barium	1	7.48E-06	7.48E-06	1.17	0.30
Uranium	1	3.24E-10	3.24E-10	1.25	0.28

SS= sum of squares; MS= mean square.

Table 3.5: ANOVAs of trace element: Ca ratios in male versus female *N. sloanii*.

Element	df	SS	MS	F-value	p-value
Beryllium	1	9.00E-10	9.10E-10	0.02	0.90
Magnesium	1	4.87E-01	4.87E-01	2.77	0.11
Manganese	1	1.67E-06	1.67E-06	1.42	0.24
Copper	1	1.07E-04	1.07E-03	0.84	0.37
Zinc	1	3.28E-04	3.28E-04	1.94	0.18
Strontium	1	1.01E-01	1.01E-01	1.15	0.29
Yttrium	1	3.64E-11	3.64E-11	0.42	0.52
Zirconium	1	1.00E-10	1.01E-10	0.02	0.91
Barium	1	1.10E-08	1.08E-08	0.03	0.86
Uranium	1	3.57E-10	3.57E-10	1.70	0.20

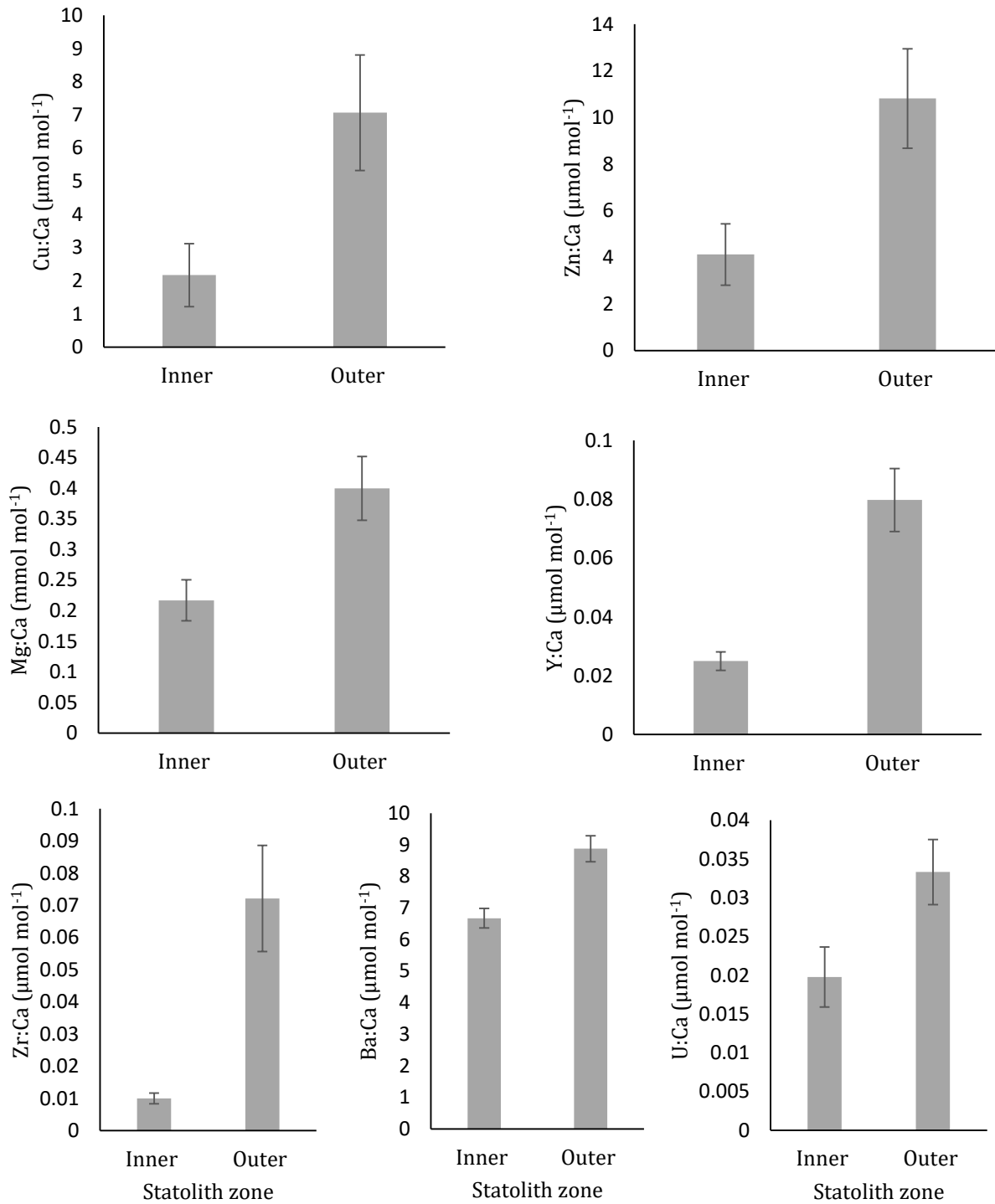


Figure 3.11: Trace element:Ca ratios in the two zones of *O. ingens* statoliths. Only the seven trace elements that had significant differences between zones are shown (n=28 for each column).

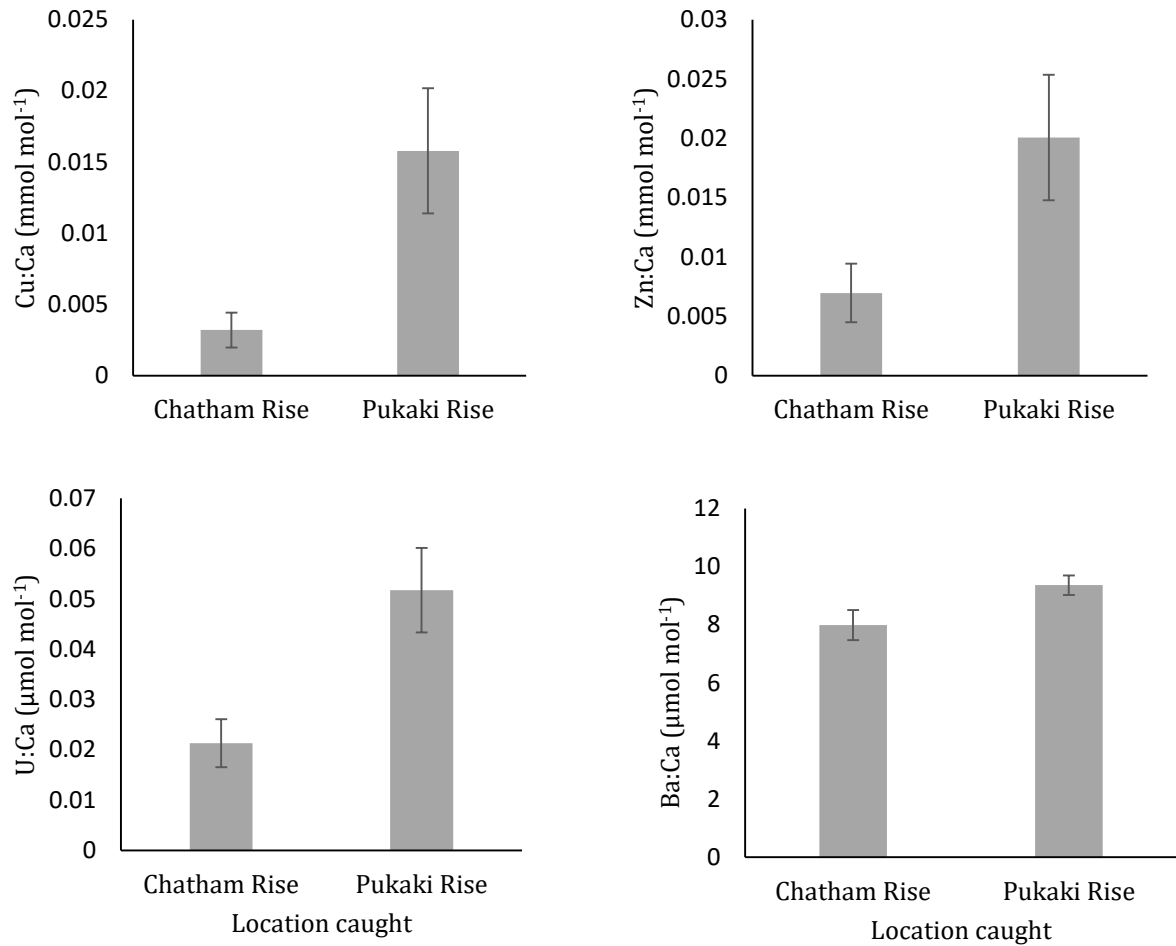


Figure 3.12: Trace element:Ca ratios in the statoliths of female *O. ingens* caught at two different locations. Only the four trace elements that had significant differences between locations are shown (n=16 for each column).

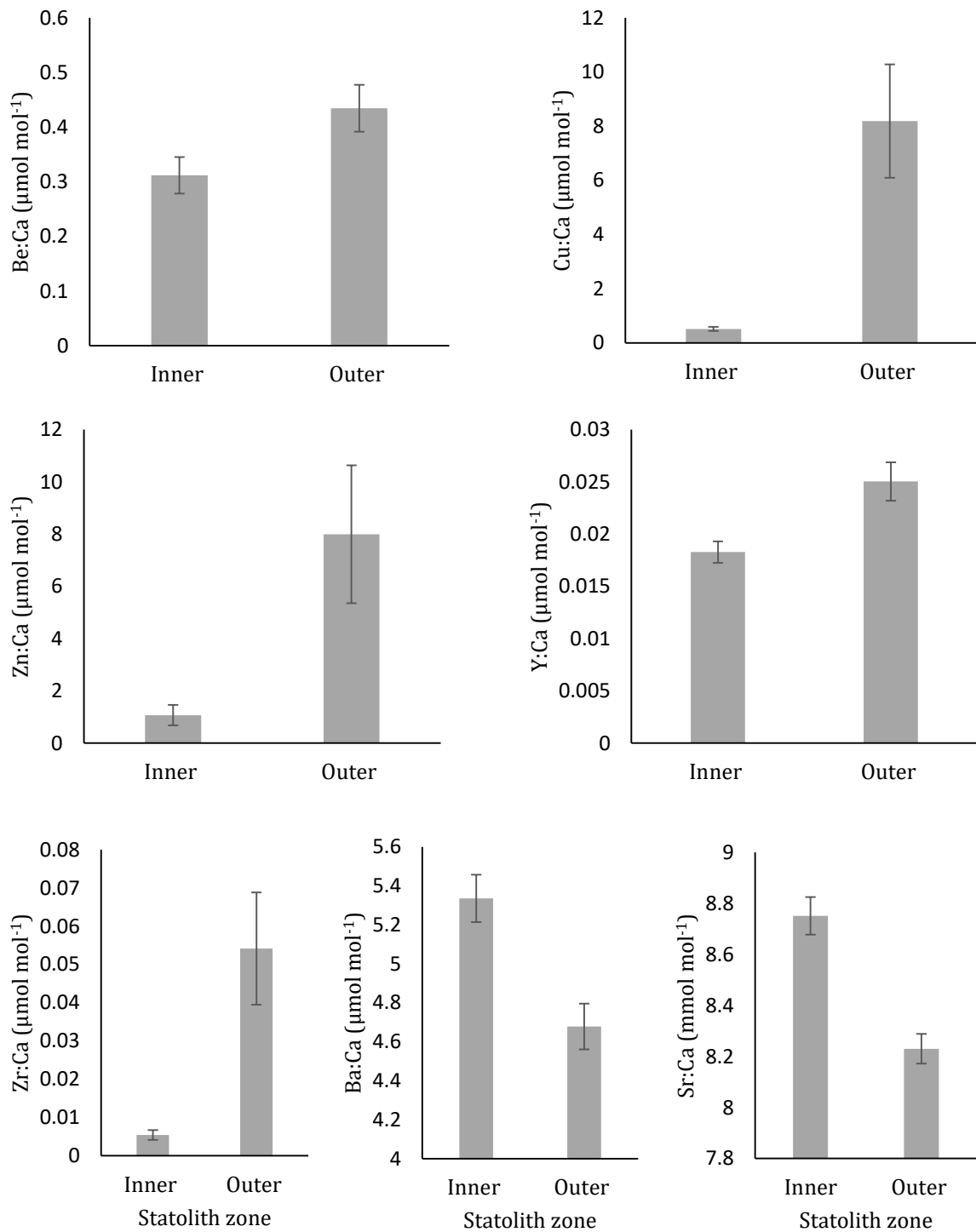


Figure 3.13: Trace element:Ca ratios in the two zones of *N. sloanii* statoliths. Only the seven trace elements that had significant differences between zones are shown (n=30 for each column).

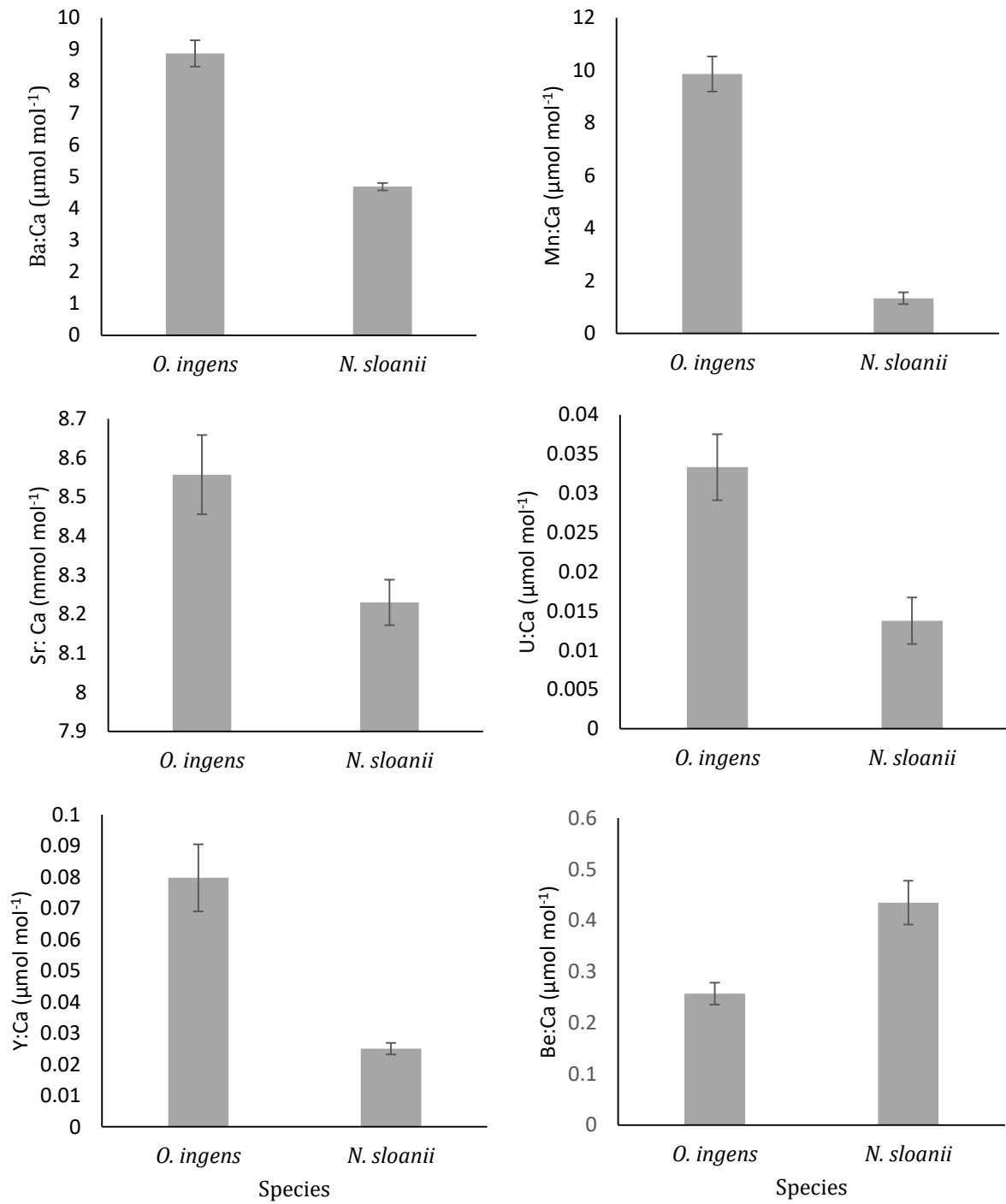


Figure 3.14: Trace element:Ca ratios in the statoliths of the two species of squid analysed. Only the six trace elements that had significant differences between species are shown (n=57 for each column).

3.5 Discussion

This is the first time Raman spectroscopy has been used to analyse the mineralogy of squid statoliths. The shift of the low-frequency peak from 270cm^{-1} in the inner zone of the statoliths to 250cm^{-1} in the outer zone has, therefore, never been seen before. This shift in peak is not attributed to mounting media as it is not a peak that is present in the control curves, meaning that the shift is attributable to the samples themselves.

This is not the first study to analyse trace elements in statoliths; however, it is the first to do so in squid from New Zealand waters and it is the first to analyse for and find beryllium in statoliths (Table 3.6). Overall, ten trace elements were measured (Be, Mn, Mg, Cu, Zn, Sr, Y, Zr, Ba, U) in the statoliths and all were found at some level in some part of each statolith. Seven trace elements measured by LA-ICP-MS had significantly different concentrations between the inner zone and the outer zone in statoliths of *Onykia ingens* and *Nototodarus sloanii*. There was a significant difference for four trace elements in *O. ingens* statoliths from the Chatham Rise and Pukaki Rise and six trace elements were significantly different between the two species. These significant differences in trace element concentrations are probably due to differences in environmental conditions experienced by the squid in their different locations as trace element concentrations are known to fluctuate with location and abiotic factors (Ikeda et al. 1996, Arkhipkin et al. 2004, Zumholz et al. 2007a). There was no difference in trace element concentrations between sexes within locations.

3.5.1 Raman shifts and structure

The mineral composition of squid statoliths has been consistently aragonite in the species studied, which come from a large array of families and locations around the world (Clarke 1978, Hurley & Beck 1979, Radtke 1983). These aragonitic statoliths puts squid in a group with teleosts and amphibians as they also have aragonitic otoliths, whereas cartilaginous fishes, mammals and birds all have calcitic otoliths (Dilly 1976).

It is known that the modes in the low frequency region (100cm^{-1} to 350cm^{-1}) of the Raman spectra of aragonite correspond to the translational and rotational lattice of the structure. The Raman spectra of the internal fundamental modes of carbonate are between 600cm^{-1} and 1800cm^{-1} (Urmos et al. 1991). The shift in the low frequency

Raman peak from 270cm⁻¹ to 250cm⁻¹ between the two statolith zones shows that there is a change in the crystal structure between zones. This change in crystal structure has been hypothesised in the past, but was not seen under SEM (Jackson 1993). The shift in transparency between the two zones seen in statoliths is likely due to the difference in lattice structure between the zones. This shift occurred in all of the *N. sloanii* samples but only in some of the *O. ingens* samples, which may be due to the difference in preparation methods between the statoliths of the two species which gave less material in the *O. ingens* specimens. It has been hypothesised that the difference in structure between zones in *O. ingens* is due to an ontogenetic migration (Jackson 1993), this suggests that there may be a similar migration in *N. sloanii* that has yet to be observed.

Dilly (1976) published the first SEM pictures of squid statoliths and reported the same crystal structures for the statoliths of *Sepia officinalis* and *Taonius megalops* that were present here for *O. ingens* and *N. sloanii*. Villanueva (2000a, b) used SEM imaging to examine the deposition rate of growth rings in larval statoliths and observed a similar internal radiating crystal structure. Methods used in Villanueva (2000a, b) to visualise internal crystals gave a much more ordered and controlled view of the crystal structure than is seen in this study. The structures observed here aid in the function of the statoliths as a gravity and acceleration indicator, for example, the porous nature of the outer surface is thought to allow for the anchoring filaments in the surrounding tissue to hold the statolith in place (Dilly 1976).

3.5.2 Trace elements: what might they mean?

The means of all trace elements that have been measured in this study, for *O. ingens* and *N. sloanii*, are within the ranges of values reported in past studies (excluding beryllium as it has not been reported before) (Ikeda et al. 2003, Arkhipkin et al. 2004, Zumholz et al. 2007b, Warner et al. 2009, Liu et al. 2011, 2013, 2016, Arbuckle & Wormuth 2014, Green et al. 2015, Liu, Chen, & Chen 2015) (Table 3.7). The trace element with the highest concentration in statoliths from both *O. ingens* and *N. sloanii* was strontium. This pattern supports that from all other studies excluding Liu et al. (2016) and Liu et al. (2015b). The Sr: Ca reading for *D. gigas* in Liu et al. (2016) is three orders of magnitude lower than the others; however, the data was probably mis-reported as it was expressed $\mu\text{mol/mol}$ when it was likely mmol/mol . In Liu et al. (2015b), all elements excluding strontium are three orders of magnitude higher than in

other studies. In Liu et al. (2015b) the data were all reported as mmol/mol, when it was likely $\mu\text{mol/mol}$ for all elements excluding strontium (Table 3.7).

The average strontium concentration in the outer zone of the statoliths, which corresponds to the time closest to the capture of these squid, was higher in *O. ingens* than in *N. sloanii*. This difference in strontium concentration supports the idea that strontium concentration is lower in species that are coastal, such as *N. sloanii* (Ikeda et al. 1997). The Sr:Ca ratio has been shown to be an useful tool to reconstruct the temperature over the life history of an animal in otoliths of fish (Campana 1999), skeletons of corals (Swart et al. 2002) and statoliths of marine gastropods (Zacherl 2005). In squid, the Sr:Ca ratio is thought to have a negative correlation with temperature (Ikeda et al. 1996, Arkhipkin et al. 2004). The strontium concentrations in the statoliths of *O. ingens* showed no significant difference between zones or geographical location. This lack of difference suggests that either temperatures over the life-span, and geographic range, of the *O. ingens* used in this study did not differ or that strontium is not only linked to temperature but to other environmental factors in this species. *Nototodarus sloanii* statoliths contained a significantly higher concentration of strontium in their inner zone than in their outer zone. This difference in *N. sloanii* statoliths may be driven, at least partly, by temperature and therefore, may be further evidence for an ontogenetic migration within the species. The difference in strontium could also be due to the squid being caught directly after summer meaning that the squid would have spent the last part of their life in warmer waters, thus having a lower uptake of strontium according to the relationships proposed in Ikeda et al. (1996) and Arkhipkin et al. (2004).

Uranium, zinc, magnesium, manganese and copper incorporation into squid statoliths has been suggested to be dependent on temperature (Ikeda et al. 1996, Zumholz et al. 2007b, Liu et al. 2013). The lack of specific temperature data collected with the samples in this study does not allow this link to be evaluated for *O. ingens* and *N. sloanii*. The link between these elements and temperature may also be species dependent, or it may also be dependent on other factors, such as nutrient availability or salinity, which confound data (Ikeda et al. 1997, 2002, Zumholz et al. 2006).

There has been evidence in previous studies to suggest that barium incorporation into statoliths is positively correlated to depth and upwelling (Arkhipkin

et al. 2004, Zumholz, et al. 2007b). The distribution of barium in the ocean is lower in surface waters than in deeper waters (Zumholz et al. 2007a). Both species of squid had levels of barium that were higher in the inner zone of the statolith than the outer zone. This difference between zones shows the opposite distribution to what would be expected for *O. ingens* due to their ontogenetic migration to deeper waters. Individuals of *O. ingens* from the Chatham Rise and the squid from the Pukaki Rise were collected at very similar depths and they had different levels of barium. The data presented here suggests that, while depth may play a role in barium incorporation, there is another mechanism of barium incorporation into the statoliths that is not reliant on passive intake.

In past studies, yttrium and zirconium has been found in higher concentrations in the core of the statolith than the outer zone (Zumholz et al. 2007b). The opposite distribution was found here for *O. ingens* and *N. sloanii*. No explanation for the incorporation pattern of these elements into squid statoliths has been suggested. Beryllium was found to be significantly lower in the inner zone of *N. sloanii* statoliths than the outer zone but showed no difference within statoliths of *O. ingens*. Beryllium concentration was also significantly higher in *N. sloanii* than in *O. ingens*. The difference between species suggests that the uptake of beryllium into statoliths is active.

Onykia ingens live a pelagic life in the water column while the inner zone of their statolith is being laid down, as they mature they shift to a demersal life. *Nototodarus sloanii*, on the other hand, are a pelagic species throughout their life history, but it has been noted that they move from shallow water to slightly deeper water as they mature (Dunn 2009). *Nototodarus sloanii* undergo a diurnal migration to surface waters each night to feed. The diet of both *O. ingens* and *N. sloanii* change as they mature, with smaller squid eating more crustaceans and larger squid consuming more fish and other squid (Uozumi 1998, Phillips et al. 2003, Dunn 2009). Many different abiotic factors, such as habitat and diet may play a role in the differences between, and within, statoliths of these two species.

3.5.3 Overall statolith chemistry

The analysis of the mineral composition of statoliths of *O. ingens* and *N. sloanii* concluded that they are made primarily of aragonite. Aragonite is less stable than calcite and will slowly change form to calcite over time in the sediment after the animal has

died (Jamieson 1953). The rate of state change of aragonite to calcite has been suggested for use in aging when aragonite structures are found in the fossil record (Dilly 1976); however there has not been enough research on this rate in statoliths to validate this suggestion. As more and more CO₂ dissolves into the oceans, the saturation point of CaCO₃ in the oceans decreases which makes it harder for animals that mineralise to make and maintain calcium carbonate structures (Doney et al. 2009). As squid have calcium carbonate statoliths, it is reasonable to assume that their statoliths will be affected by the increasing atmospheric CO₂. Along with the decrease in CaCO₃, there is an increase in H⁺ ions in the water, which makes the oceans more acidic (Doney et al. 2009). The lower stability of aragonite means that ocean acidification may affect the retention time of aragonitic statoliths and otoliths in the sediment, however, this is only speculation at this time. A lower retention time would mean that squid, and other taxa with aragonitic otoliths, could be under represented in the future fossil record.

Table 3.6: Comparison of trace elements found in squid statoliths between studies.

	Species	Location	Technique	Be	Mg	Mn	Cu	Zn	Sr	Y	Zr	Ba	U	Ca	Fe	Pb	Na	Ni	Al	Cr	Co
This study	<i>Onykia ingens</i>	SP	LA-ICP-MS	✓	✓	✓	✓	✓	✓	✓	✓	✓	✓								
This study	<i>Nototodarus sloanii</i>	SP	LA-ICP-MS	✓	✓	✓	✓	✓	✓	✓	✓	✓	✓								
Arbuckle & Wormuth 2014	<i>Dosidicus gigas</i>	GI, CA and WS	LA-ICP-MS	✓	✓	✓	✓	✓	✓	✓	✓	✓	✓	✓	✓	✓					
Arkhipkin et al. 2004	<i>Loligo gahi</i>	FI	ICP-MS	✓	✓	✓	✓	✓	✓	✓	✓	✓	✓	✓	✓	✓					
Green et al. 2015	<i>Nototodarus gouldi</i>	AU	LA-ICP-MS	✓	✓	✓	✓	✓	✓	✓	✓	✓	✓	✓	✓	✓					
Ikeda et al. 1995	<i>Todarodes pacificus</i>	SoJ	PIXIE	✓										✓	✓						
Ikeda et al. 1996	<i>Todarodes pacificus</i>	SoJ	PIXIE		✓	✓	✓	✓	✓	✓	✓	✓	✓	✓	✓	✓					
Ikeda et al. 1997	14 species*	NP	PIXIE	✓	✓	✓	✓	✓	✓	✓	✓	✓	✓	✓	✓	✓					
Ikeda et al. 2002a	<i>Todarodes pacificus</i>	SoJ	EMP	✓										✓	✓						
Ikeda et al. 2002b	<i>Dosidicus gigas</i>	EP	PIXIE	✓	✓	✓	✓	✓	✓	✓	✓	✓	✓	✓	✓	✓					
Ikeda et al. 2003	<i>Todarodes pacificus</i>	SoJ	EMP	✓										✓	✓						
ξ Liu et al. 2011	<i>Dosidicus gigas</i>	Ch and Pe	LA-ICP-MS	✓	✓	✓	✓	✓	✓	✓	✓	✓	✓	✓	✓	✓					
Liu et al. 2013	<i>Dosidicus gigas</i>	Ch, Pe and CR	ICP-MS	✓	✓	✓	✓	✓	✓	✓	✓	✓	✓	✓	✓	✓					✓
Liu et al. 2015a	<i>Dosidicus gigas</i>	Ch	ICP-MS	✓	✓	✓	✓	✓	✓	✓	✓	✓	✓	✓	✓	✓					✓
Liu et al. 2015b	<i>Dosidicus gigas</i>	Ch	ICP-MS	✓	✓	✓	✓	✓	✓	✓	✓	✓	✓	✓	✓	✓					✓
Liu et al. 2016	<i>Dosidicus gigas</i>	Ch	LA-ICP-MS	✓	✓	✓	✓	✓	✓	✓	✓	✓	✓	✓	✓	✓					✓
Warner et al. 2009	<i>Doryteuthis opalescens</i>	SCA	LA-ICP-MS	✓	✓	✓	✓	✓	✓	✓	✓	✓	✓	✓	✓	✓					✓
Zumholz et al. 2007a	<i>Gonatus fabricii</i>	DB	LA-ICP-MS	✓	✓	✓	✓	✓	✓	✓	✓	✓	✓	✓	✓	✓					✓
Zumholz et al. 2007b	<i>Gonatus fabricii</i>	DB	NanoSIMS	✓										✓	✓						✓

*The fourteen species examined were *Ommastrephes bartamii*, *D. gigas*, *Stenoteuthis oualaniensis*, *Gonatopsis makko*, *Gonatopsis borealis*, *Beryteuthis magister*, *Loligo bleekeri*, *Loligo duravicelli*, *Loligo chinensis*, *Loligo edulis*, *Sepioteuthis lessoniana*, *Sepia aculeata*, *Sepiella inermis* and *Rossia pacifica*. All fourteen species contained all trace elements measured in that study.

*** Locations are as follows: SP= South Pacific; SoJ= Sea of Japan; FI= Falkland Islands; NP= North Pacific; Ch= Chile; Pe= Peru; CR= Costa Rica; DB= Disko Bay, Greenland; GI= Galapagos Islands; Ca= California; WS= Washington State; Au= Australia.

Table 3.7: Comparison of means (or ranges if no means were reported) of trace element ratios between studies. Blank spaces are where the element was not analysed

Species	Be/Ca umol/mol	Mg/Ca mmol/mol	Mn/Ca umol/mol	Cu/Ca umol/mol	Zn/Ca umol/mol	Sr/Ca mmol/mol	Y/Ca umol/mol	Zr/Ca umol/mol	Ba/Ca umol/mol	U/Ca umol/mol
This study	0.280	0.230	8.077	2.073	3.194	8.284	0.029	0.020	6.971	0.016
This study	0.360	0.207	1.222	1.396	1.385	8.680	0.020	0.012	5.126	0.008
Arbuckle & Wormuth 2014		0.158	1.186	0.195	0.487	6.642	0.043	0.035	9.08	0.022
Arkhipkin et al. 2004		0.07-0.17	1.0-3.0			~8			3.0-8.0	
Green et al. 2015*		~0.15-0.17	~0.3-0.6			~7.6-8.1			~4.5-5.2	
Ikeda et al. 1995			0.022-0.035							
Ikeda et al. 1997**						ND				
Ikeda et al. 2002a			ND	ND	ND	ND				
Ikeda et al. 2002b										
Ikeda et al. 2003						17-24?				
Liu et al. 2011		0.154				15.6			16.8	
Liu et al. 2013		0.9	3.86	15.4	70	15.8			22.2	0.049
Liu et al. 2015a		0.194-0.249	3.15-4.73	0.91-1.06	2.46-7.63	15.7-16.3			12.4-24.4	0.020-0.15
Liu et al. 2015b		342	2950	27900	85700	16.4			23600	
Liu et al. 2016		ND	ND	ND	ND	0.014-0.018			8.34-35.37	
Warner et al. 2009		2.4	18.6			10.4			7.3	
Zumholz et al. 2007a		0.110-0.590	3.2-6.8		0.9-4.5	6.3-8.1	0.056-0.081	0.012-0.029	5.7-8.2	0.002-0.009
Zumholz et al. 2007b						ND				

ND= Data either not reported, reported in different units or not found

*= Means not reported, estimated from graph

**= 14 species were the same as in table 3.6

The significant differences in chemistry between zones within statoliths observed for both *O. ingens* and *N. sloanii* could be used to track individual squid over their life history if they have unique signatures. This difference between zones could be combined with the differences found between locations to trace ontogenetic migrations within locations and the amount of mixing between locations. The significant differences statoliths of different species could be used to help identify species when statoliths are recovered.

It has been suggested that trace element incorporation into statoliths is dependent on the niche that the squid occupy, taking into account parameters such as habitat and diet, which changes with location and age of the animal (Ikeda et al. 2003, Arkhipkin et al. 2004). This idea is suggested for two main reasons, the first being that trace elements in the surrounding water change in response to many different abiotic factors, such as temperature and depth (Arbuckle & Wormuth 2014). The second reason that the niche may affect trace element incorporation is that the prey composition is often different between locations and squid age. These changes in water and prey type are important to keep in mind when studying squid as ontogenetic shifts in habitat, as seen in *O. ingens* (Jackson et al. 2000a), or prey, as seen in *N. sloanii* (Dunn 2009), is prolific within the taxa.

The correlation found between geographic location and trace element incorporation do not implicitly mean that the abiotic and biotic factors are the cause of the shift in element incorporation. The current lack of data on causative relationships between trace element incorporation and environment means that data cannot yet be extrapolated to different species and different locations. Experimental data collected by manipulating one, or more, of these variables at a time, and analysing the trace element incorporation response could help shed light on what factors cause the shift. Experimental data are difficult to obtain for squid, especially large, deep sea ones, like *O. ingens*, as they are difficult to keep in captivity. These types of experiments could be undertaken on smaller squid that are easier to keep in captivity. Ikeda et al. (2002) carried out one of these manipulative investigations to study the cause of the daily pattern of strontium incorporation in *Todarodes pacificus* in an experimental setting. This daily variation was hypothesised to be related to the daily vertical migrations that *T. pacificus* underwent. Ikeda et al. (2002) found that these strontium variations

occurred even when *T. pacificus* was kept at a constant depth in an aquarium setting and concluded that the variations may be due to a natural variation in feeding habits. More experiments like the one carried out by Ikeda et al. (2002) are warranted to extend our knowledge of the causes of trace element incorporation in squid.

Regardless of the cause, the difference in trace element incorporation between geographically separate locations has been observed in many species of squid (Ikeda et al. 2003, Arkhipkin et al. 2004, Zumholz et al. 2007b, Warner et al. 2009, Wang et al. 2012, Liu et al. 2013, 2016, Arbuckle & Wormuth 2014, Green et al. 2015, Liu, Chen, & Chen 2015, Liu et al. 2015b). This difference means that trace element 'fingerprints' could be established of squid from each location and a library of these fingerprints could be built over time. These fingerprints could then be used in fisheries and conservation research to bring better resolution to food webs and help influence management decisions by producing a better understanding of population structure and migration patterns. Ideally, a methodological standard for testing statoliths should be developed and used to create the fingerprints to counter any inter-method discrepancies. A large amount of work would need to be undertaken for this fingerprinting to become viable. For example, each species, and population would need to be investigated separately to discern if the variability between individuals is smaller than the variability between populations, among other variables.

3.5.4 Conclusions

Onykia ingens and *N. sloanii* statoliths are aragonitic, with two major zones that have a significant structural and chemical change between them. These differences between zones suggest an ontogenetic shift in niche during the life of both of these squid. The use of geochemical markers in hard structures of animals to gain information about their life history is an expanding field that promises to have many uses (Campana 1999). The applications of trace element analyses of these hard parts in the fisheries range from aiding in stock assessment in fisheries via the identification of separate stocks (Liu et al. 2011) to analysing the otoliths of escaped salmon to trace where they escaped from (Hansen et al. 2015). These trace element analyses of animal structures also have wide-ranging applications in marine conservation, such as tracing prey origin, and biomaterials.

Chapter Four: Trace Element Composition of Beaks of *Onykia ingens*

Table of Contents

4.1 Introduction	89
4.1.1 Aims of this chapter	91
4.2 Methods.....	92
4.2.1 Squid collection	92
4.2.2 Beak collection	92
4.2.3 ICP-MS preparation	94
4.2.4 Laser ablation preparation	94
4.2.5 Solution based ICP-MS	95
4.2.6 LA-ICP-MS spot ablation.....	95
4.2.7 Data analyses.....	96
4.3 Results.....	97
4.3.1 Solution based ICP-MS	97
4.3.2 LA-ICP-MS.....	97
4.4 Discussion.....	104
4.4.1 Conclusion	106

4.1 Introduction

Cephalopod beaks are among the most impressive hard structures in the animal kingdom. The cephalopod beak is both hard and sharp enough to cut through the tissue and bone of prey, yet soft enough to be held in place by the muscular buccal mass (Fig. 4.1) (Miserez et al. 2010). Cephalopod beaks are also durable enough to withstand digestion in stomach acids for long periods of time, allowing for their recovery in diet analysis studies (Gaskin & Cawthorn 1967, VanHeezik & Seddon 1989, Cherel et al. 2002). Cephalopod beaks possess these properties without having any mineralisation within the beak, meaning that their structure and composition is of particular interest in the materials industry (Broomell et al. 2007, Miserez et al. 2010).



Figure 4.1: The beak of a colossal squid (*Mesonychoteuthis hamiltoni*) in the buccal mass. Photo courtesy of: Norm Heke, Te Papa.

Squid beaks are sclerotised, meaning they consist of a composite of chitin and proteins rather than minerals (Broomell et al. 2007, Miserez et al. 2010). This sclerotisation is in contrast to many other hard parts in the animal kingdom, such as abalone shells, which are composed of up to 95% mineral by volume (Meyers et al. 2006). Chitin exists in three forms: alpha (α), beta (β) and gamma (γ), with α being the most abundant in the natural world (Rudall 1969, Rinaudo 2006). These forms can be differentiated using nuclear magnetic resonance spectroscopy (NMR) alongside X-ray powder diffraction (XRD) (Rinaudo 2006). It is important to know what form of chitin the structure being analysed is as each form has different properties. β -chitin is more reactive than γ -chitin which in turn is more reactive than α -chitin; however, all three

forms are relatively non-reactive when compared to mineralised materials (Kurita et al. 1993a, Jang et al. 2004). Squid beaks are made of α -chitin (Hudson & Smith 2013), which helps to explain why beaks last for a long time in predator's stomachs. Squid contain another sclerotised structure: the gladius. The gladius is made of β -chitin (Lavall et al. 2007) and therefore does not persist as long as beaks after the squid has died.

Squid beaks have a gradient of stiffness, from being stiff at the tip, which is the part that cuts prey, to being pliable at the base which connects to the buccal mass (Miserez et al. 2008). The gradient of stiffness allows the beak to be held in place by soft tissue, yet still slice through the flesh and bone of prey. The gradient is governed by the content of water, protein, tanning pigment and chitin in the respective areas of the beak (Miserez et al. 2008). Hardening in non-mineralised structures is often connected to the presence of metals, such as Zn, which makes up around 3% of the weight of the structure in *Nereis* jaws (Miserez et al. 2007). The difference in composition and physical properties of the beak over its length may influence, or be influenced by, the trace element chemistry of the beak.

Squid gladii and beaks are large reservoirs of chitin, which can be processed into chitosan. Chitosan is a polysaccharide that has many different uses in medicine, water treatment, and the cosmetic industry (Jang et al. 2004). Gladii have been analysed for trace elements to make sure chitosan made from them is fit for human consumption. One study by Chandumpai et al. (2004) found that the chitin that makes up the gladius contains low levels of Ca, Mg, Cu, Fe and Cd. Another study of trace elements in squid gladii by Kurita et al. (1993b) found Na, Mg, P, K, Ca and Fe in gladii of *Ommastrephes bartrami*. Squid beaks have been the subject of at least two trace element studies in the past. These two studies identified no metal ions, minerals or halogens in squid beaks using SEM-EDS (Broomell et al. 2007, Miserez et al. 2007). It is important to know the full chemical composition of materials of interest as this broadens our understanding of how the material is made and how it functions. The trace element composition of a structure can also provide information on aspects of the life of the animal which it came from, for example, tracking escaped salmon back to their original farm (Hansen et al. 2015).

Trace elements in statoliths of squid have been shown to depend on the location in which the squid lived (Ikeda et al. 2003a, Arkhipkin et al. 2004, Zumholz et al. 2007a, Warner et al. 2009, Wang et al. 2012, Liu et al. 2013, 2016, Arbuckle & Wormuth 2014, Green et al. 2015, Liu, Chen, & Chen 2015). In fact, multivariate trace element ‘fingerprints’ have been hypothesised and made for hard parts from squid to correspond with geographic location (Liu et al. 2013). If trace element composition in squid beaks is dependent on location, geographic fingerprinting could be used to investigate where squid came from when only their beaks are recovered. Back-tracking of squid could be useful in diet analysis studies where squid are prey (Gaskin & Cawthorn 1967, Boren 2008). Tracing the original location of squid via their beaks would increase our knowledge of the feeding habits of the commercially and ecologically important predators of squid, such as sperm whales (*Physeter macrocephalus*) (Gaskin & Cawthorn 1967) and swordfish (*Xiphus gladius*) (Hernández-García 1995).

4.1.1 Aims of this chapter

This chapter will describe the trace element composition of beaks from *Onykia ingens* using solution-based and laser ablation ICP-MS, giving a preliminary analysis of the variation within beaks of squid from two different locations. This chapter will then discuss the potential future use of trace element concentrations in squid beaks as geographic tracers.

4.2 Methods

Beaks of *Onykia ingens* were extracted, prepared and analysed using analytical chemistry methods to determine their trace element contents. 10 beaks were prepared and mounted for analysis in LA-ICP-MS to analyse trace element incorporation over the squid's life-history. Six beaks were digested and analysed using ICP-MS to quantify trace elements in the beaks after LA-ICP-MS analysis. ICP-MS was done to obtain the concentration of one element to use as a normalising element, thus allowing the quantification of all other elements.

4.2.1 Squid collection

Onykia ingens were collected as in section 2.2; however, squid used from TAN1401 were collected from 4, rather than 11, different stations over the Chatham Rise (Fig 4.2). Squid were collected from depths ranging from 726m to 1222m with a temperature range of 5°C to 8°C (Stevens et al. 2015).

4.2.2 Beak collection

Beaks were extracted from frozen *O. ingens* at AUT University in Auckland in June 2015 then shipped to the University of Otago lab at Portobello, Dunedin. Most of the beaks came out of the buccal mass that was holding them in place after the squid was frozen, but some had to be cut out with a scalpel. The beaks were stored in a -20°C freezer to reduce desiccation. In total, sixteen beaks were analysed, eight from the Chatham Rise group and eight from the Pukaki Rise group. Beaks were soaked in 10% bleach for three hours to remove the film of organic matter left on them. Beaks were then removed from the bleach solution and rinsed thoroughly, first with reverse osmosis water then with Milli-q[®] de-ionised water to remove the bleach from the surface of the beak.

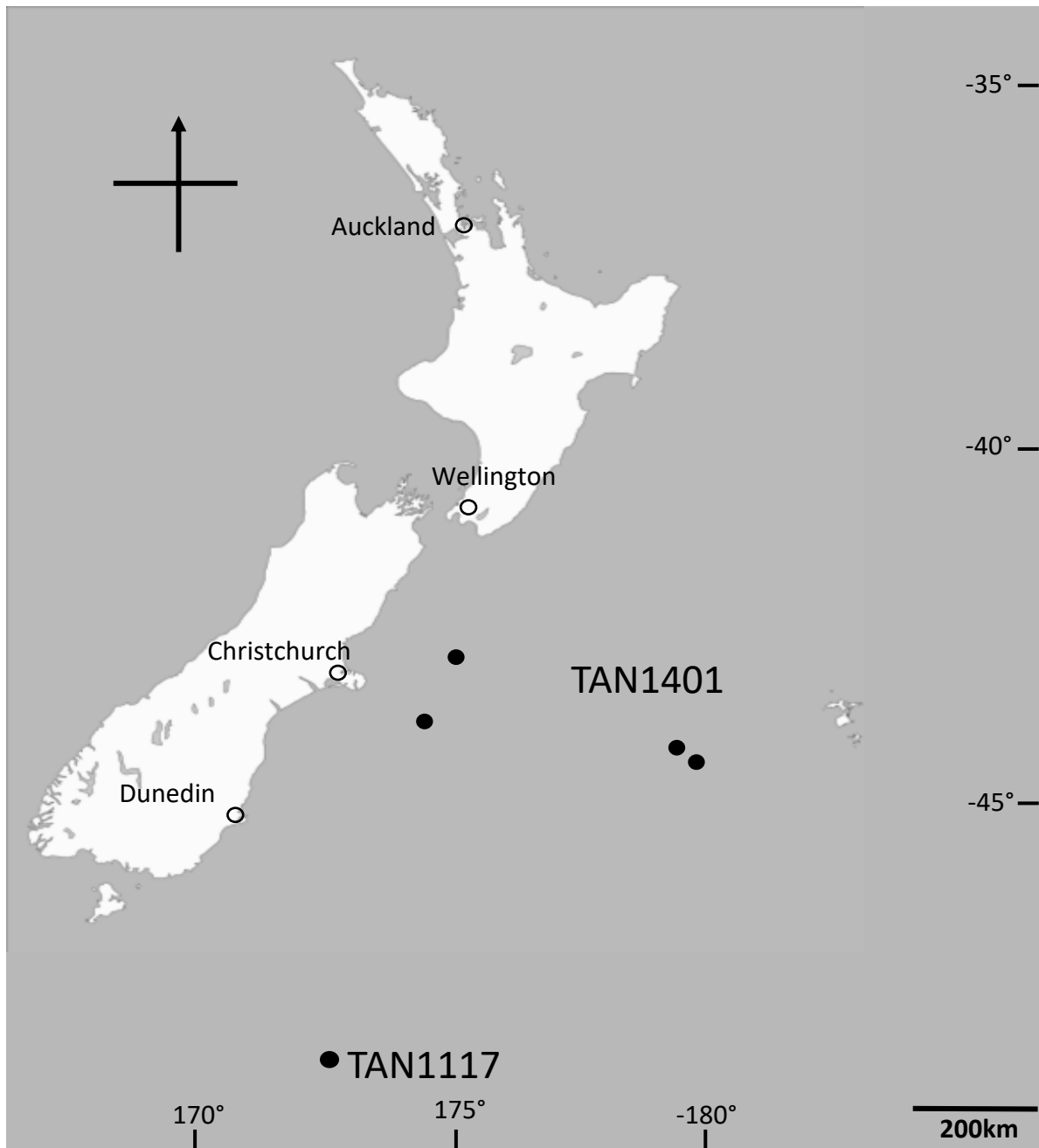


Figure 4.2: Locations where squid *O. ingens* were caught: TAN1401 and TAN1117.

4.2.3 ICP-MS preparation

Six lower beaks and four upper beaks were prepared for ICP-MS analysis. Three lower beaks and two upper beaks were from the Chatham Rise group and three lower beaks and two upper beaks were from the Pukaki Rise. Both upper and lower beaks from the same individuals were used to give an idea of the total trace element incorporation in whole squid beaks. Before solid samples are introduced into a trace element analysis system that requires liquid samples, such as ICP-MS, the samples must be digested (Milestone Science 2001). Beaks were digested using a MARS 6 microwave digestion system (CEM Corporation) in the chemistry department at the University of Otago by David Barr. Each beak was cut into small pieces using sterile dissection scissors by the author to aid with the digestion, then washed, first with reverse osmosis water then with Milli-q[®] de-ionised water.

Microwave digestion heats samples in a closed PTFE vessels along with nitric acid. These closed vessels create a pressurised environment that increases the boiling point of the nitric acid. The higher temperature means that the reaction between the acid and the sample material is more energetic. With the reaction taking place with a higher energy, materials that have a high resistance to acid dissolution, such as squid beaks, are able to be digested. Microwaves are used as they heat the sample in a more controlled manner than hot plate methods (Hoenig & De Kersabiec 1996).

4.2.4 Laser ablation preparation

Three small pieces were removed from the lower beak from each beak pair to be analysed. Only lower beaks were used here so that more individuals could be analysed to give a better indication of the variation between individuals. The three pieces were chosen to represent three separate stages of life-history and to analyse the trace element variation within an individual's life history. The three places that were sampled were the left wing tip (LLW), the top right corner of the left wing (LLUW) and rostral beak tip (LRBT) (Fig. 4.3). Each piece of beak was then mounted onto a glass microscope slide using a thermoplastic cement (Crystalbond[®]) heated to its melting point (150°C) using a heat pad. Mounting was carried out under a dissection microscope. Pieces from all 10 beaks were mounted on the same slide so that the slide didn't have to be changed between each sample.

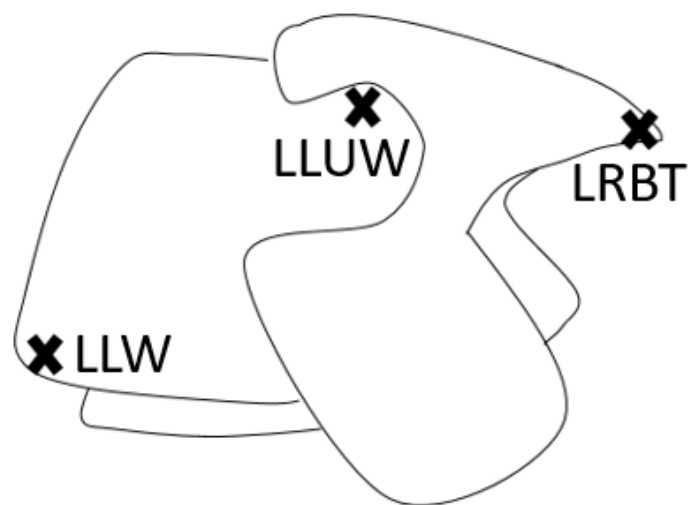


Figure 4.3: The three sites where samples were taken from each lower beak.

4.2.5 Solution-based ICP-MS

Samples were digested using a microwave-digestion system then introduced into an Agilent 7500cs ICP-MS system as an aerosol in the chemistry department at the University of Otago. Both the microwave digestion and subsequent ICP-MS analyses were undertaken by David Barr from the University of Otago. The aerosol was then vaporised and turned into gas, which was ionised and introduced into the mass spectrometer. The mass spectrometer quantitatively determined the elemental composition of the sample and the output was in parts per million (ppm).

4.2.6 LA-ICP-MS spot ablation

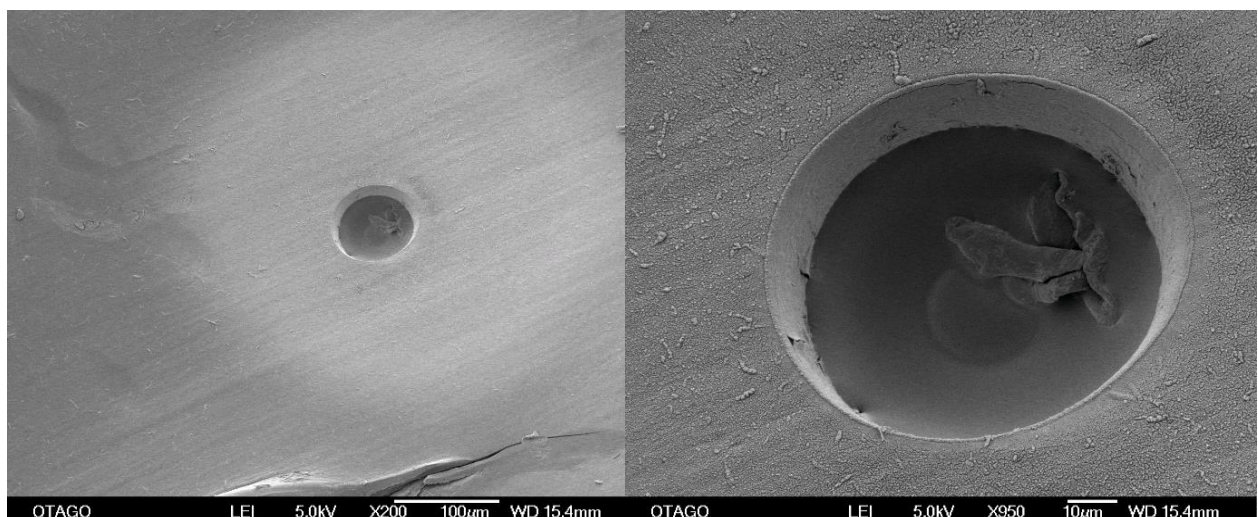
The laser ablation system was a RESOLUTION M-50 laser ablation system (Fig. 3.1A) attached to an Agilent 7500cs ICP-MS. The LA-ICP-MS analyses were undertaken by the author. The slide with the samples was placed inside a cell that was directly under the laser. A microscope was set up to view the samples using a mirror so that the microscope lens would not get in the way of the laser. The cell was then purged with pure N₂ gas which increases the system sensitivity to trace elements. The laser settings were as follows: 75µm spot sample, data acquisition time of 60 seconds which was made up of a 20 second gas blank then 40 seconds of ablation in a single spot, drilling a hole (Fig 4.4). The 20 second gas blank at the start of data acquisition was a time where

no laser ablation occurred but the gas that is used to purge the cell is flowing and being analysed by the ICP-MS. This analysis of gas also occurs during the laser ablation stage of data acquisition. By running a gas blank at the start of each data acquisition period the traces picked up in the gas can be subtracted from the data acquired during ablation so that the data is representative of the sample and not the gas in the cell. 11 elements were analysed: Mg, Mn, Cu, Zn, Sr, Be, Ca, Y, Zr, Ba and U.

Three calibration materials were used during laser ablation: NIST610, NIST 612 and MACS (homogenised otolith). NIST610 and NIST 612 are standard reference materials (SRMs) made of glass support matrices with known quantities of known trace elements added to them. The two SRMs differ in the exact trace elements embedded in the matrix and the concentrations of each element (Reed 1992a, b). Normally the SRM with the closest concentrations of trace elements to the samples being analysed is used, we used both as we were uncertain which would be closest. MACS is a SRM made of calcium carbonate (Strnad et al. 2009), homogenised otoliths in this case. Calibration transects were run at the start and end of each slide being analysed and between every 10 samples to account for machine drift. Calibration spots had the same ablation methods as the samples.

4.2.7 Data analyses

With LA-ICP-MS data, to quantify trace elements and compare between beaks, there must be one element that is fairly stable between samples, in statoliths this is Ca, which is around 40%. As the levels of every element varied among beaks (in the ICP-MS results), LA-ICP-MS data could only be compared within, not between beaks. LA-ICP-MS data was analysed using a worksheet designed to run in Microsoft Excel (2010). The



worksheet uses the calibration materials to adjust traces in each sample for machine drift. ICP-MS data was visualised and plotted in Microsoft Excel (2010).

Figure 4.4: Scanning electron micrographs of holes made in pieces of *O. ingens* beak with laser ablation ICP-MS.

4.3 Results

4.3.1 Solution based ICP-MS

23 trace elements were found in beaks of *Onykia ingens* analysed by solution-based ICP-MS, together making up an average of 3773ppm. All 23 elements were found in all ten beaks, excluding Li, which was below the limit of detection (0.0015ppm) in two of the beaks. Na had the highest average concentration in the beaks, having a concentration around three times higher than the second highest, K. Co had the lowest average concentration of 0.01ppm (Table 4.1) (Fig. 4.1).

4.3.2 LA-ICP-MS

11 trace elements were analysed in the beaks of *O. ingens*, they were: Mg, Mn, Cu, Zn, Sr, Be, Ca, Y, Zr, Ba and U. Seven of these trace elements analysed using LA-ICP-MS were present at all three sites on all 10 beaks analysed (Table 4.2). Of the remaining four, barium was found in all beaks at all sites excluding the LLUW of one beak; Y was present in the LLW of seven beaks and the LLUW and LRBT of six; Zr was seen in the LLW of seven beaks and the LLUW and LRBT of two; finally, Be was found in only the LLW of three beaks, the LLUW of two and the LRBT of none.

The levels of most trace elements present in each beak varied between sites sampled within beaks (Fig. 4.6, 7, 8 & 9). There are no overall trends within or between sex or site.

Table 4.1: The range, average and standard deviation and machine error of all of the trace elements found in *O. ingens* beaks analysed in order of highest to lowest average concentration (n=6).

Element	Range (ppm)	Average (ppm)	Std Dev (ppm)	Machine Error (%)
Na	1210.10 - 2141.18	1637.25	286.27	5
K	388.89 - 931.81	568.95	157.50	5
P	248.55 - 1569.72	560.58	398.76	6
Ca	215.17 - 915.92	403.82	213.17	9
Mg	104.83 - 1110.11	364.93	340.91	8
B	93.70 - 179.60	138.32	30.17	8
Zn	37.53 - 106.63	69.26	28.02	9
Fe	6.08 - 12.29	8.57	1.92	10
Cu	3.55 - 7.78	5.87	1.39	7
Se	1.68 - 6.62	3.71	1.45	8
Mo	2.26 - 6.43	3.68	1.35	6
Sr	2.57 - 4.53	3.46	0.64	9
Mn	0.70 - 2.59	1.33	0.50	15
As	0.83 - 2.36	1.31	0.43	11
Cd	0.04 - 2.62	0.60	0.92	7
Cr	0.30 - 1.33	0.51	0.30	25
U	0.12 - 0.62	0.36	0.17	4
Rb	0.24 - 0.54	0.34	0.10	6
Ni	0.20 - 0.39	0.26	0.06	23
Pb	0.05 - 0.14	0.09	0.03	22
Ba	0.04 - 0.07	0.05	0.01	33
Li	BLD* - 0.060	0.03	0.01	22
Co	0.01 - 0.02	0.01	0.00	7

*BLD = below limit of detection

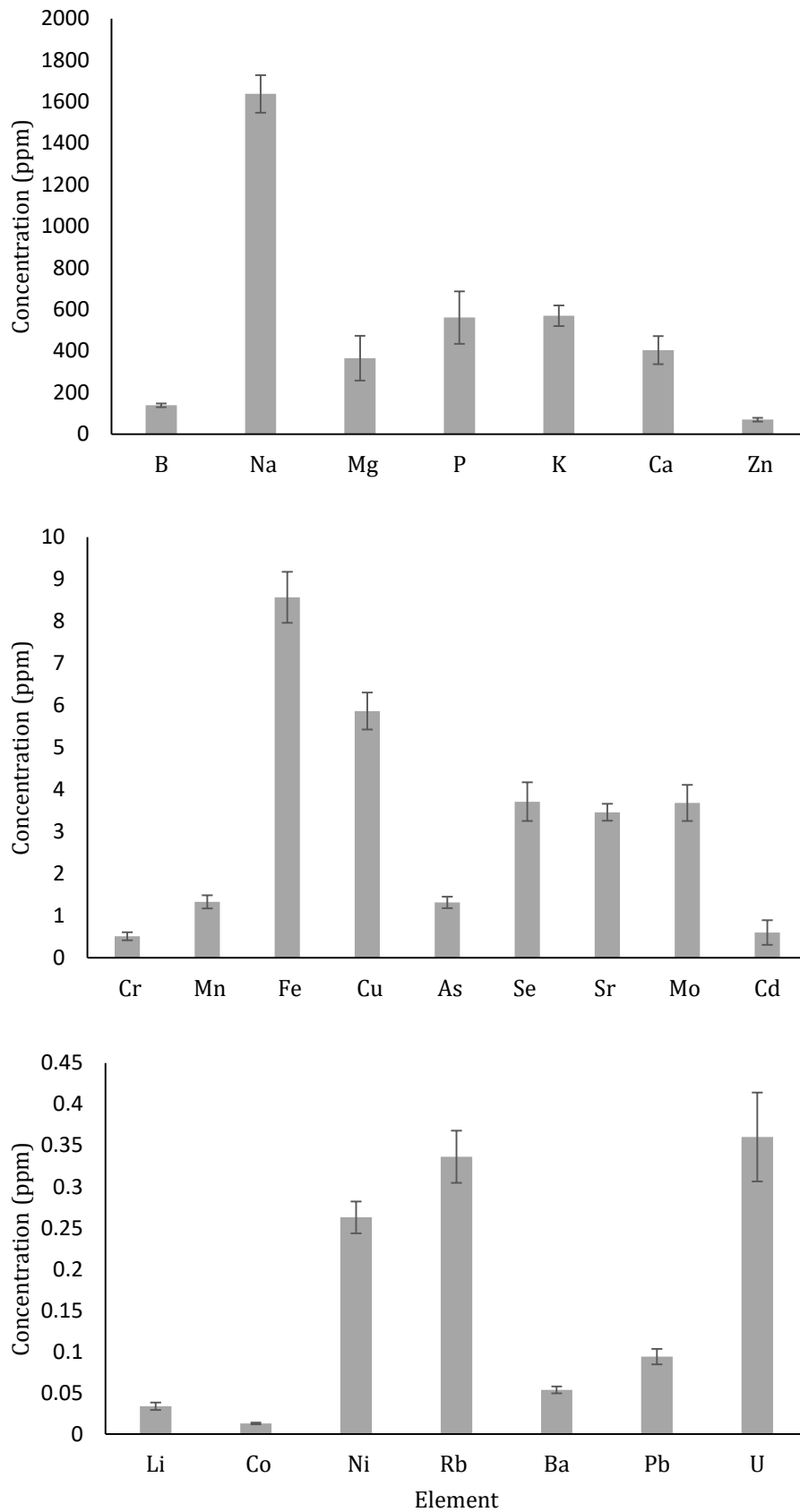


Figure 4.5: The average concentration of the 23 trace elements found in *O. ingens* beaks. (n=6). Elements are on three separate graphs so that all averages can be visualised. Error bars are $\pm 1SE$.

Table 4.2: Number of beaks, out of 10, that contained each element above the detectable level at each site

Beak site	Element										
	Mg	Mn	Cu	Zn	Sr	Be	Ca	Y	Zr	Ba	U
LLW	10	10	10	10	10	3	10	7	7	10	10
LLUW	10	10	10	10	10	2	10	6	2	9	10
LRBT	10	10	10	10	10	0	10	6	2	10	10

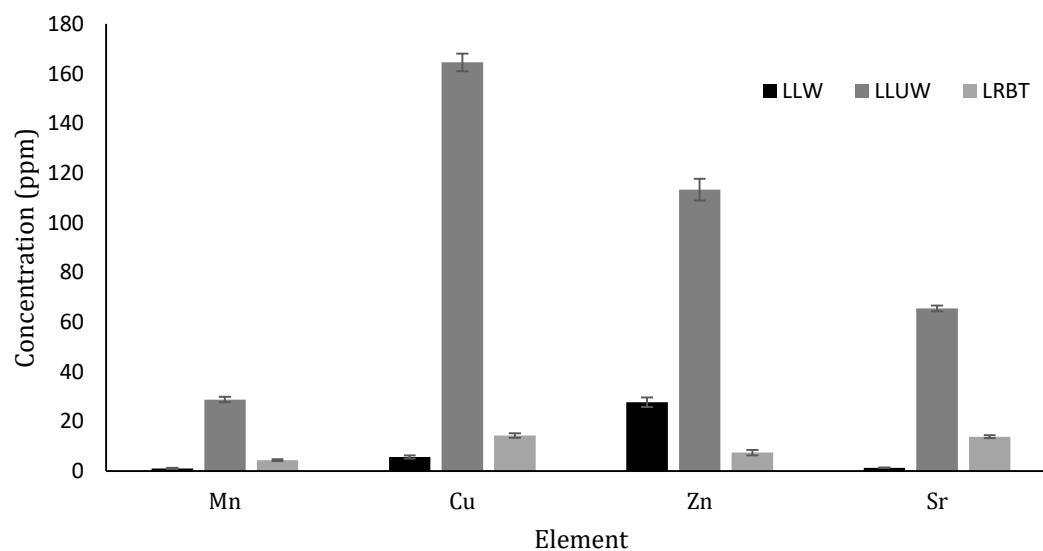
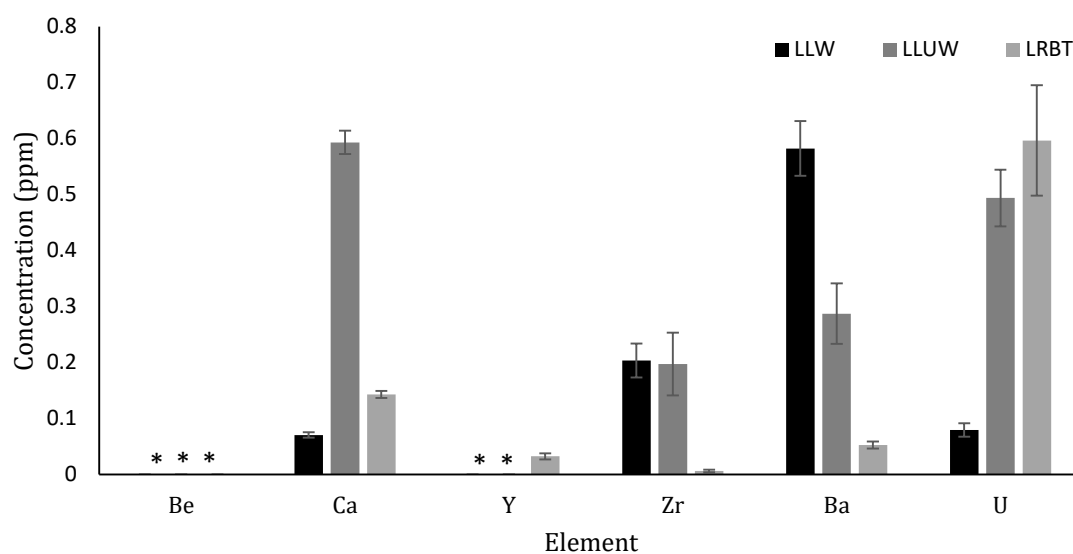


Figure 4.6: Concentration of all trace elements measured, normalised to 365ppm Mg at each site in one beak (Chatham Rise male, ML: 37.4cm, W: 1375g). Bars are ± 1 the estimate of the total error (standard error within sample and machine error). * = element not present in sample.

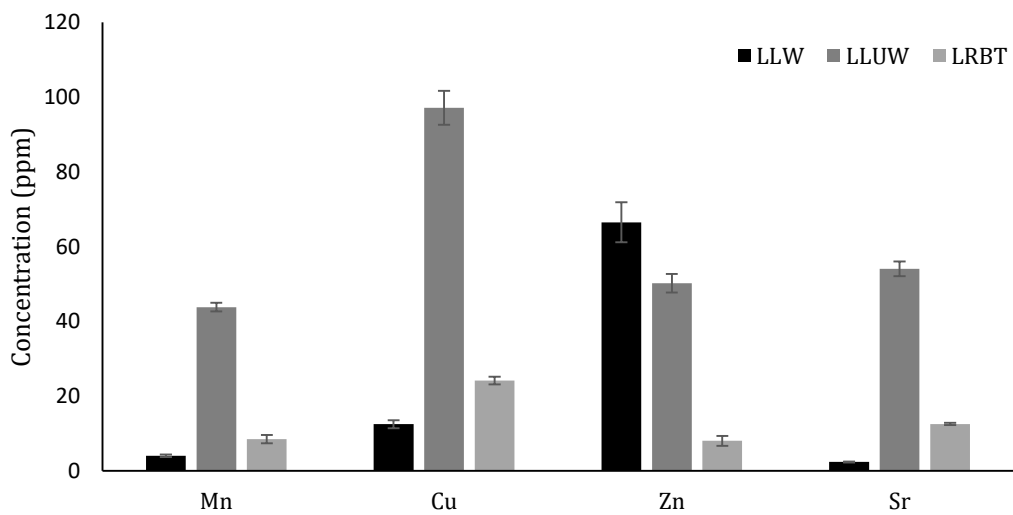
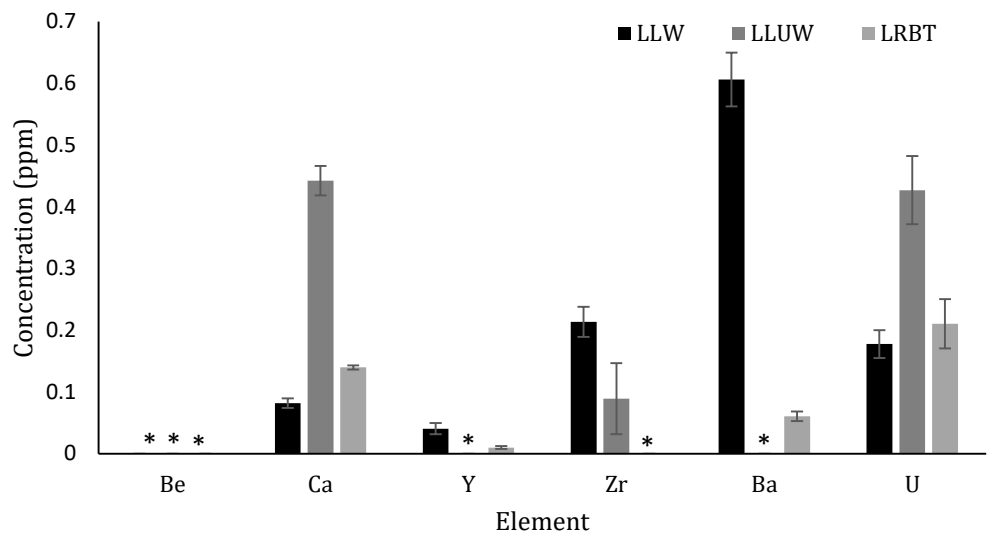


Figure 4.7: Concentration of all trace elements measured, normalised to 365ppm Mg at each site in one beak (Chatham Rise female, ML: 38.5cm, W: 2000g). Bars are ± 1 the estimate of the total error (standard error within sample and machine error). * = element not present in sample.

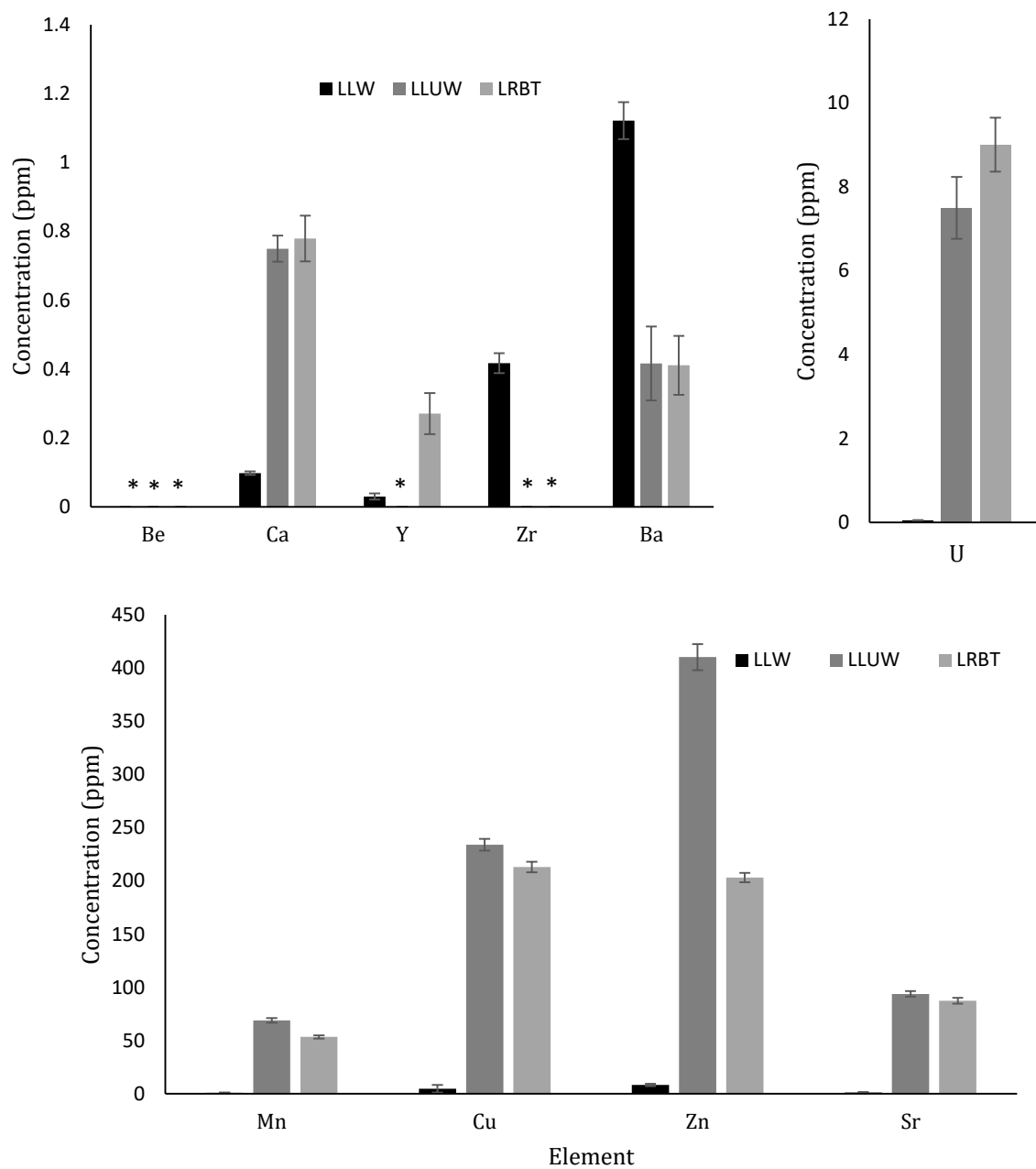


Figure 4.8: Concentration of all trace elements measured, normalised to 365ppm Mg at each site in one beak (Pukaki Rise female, ML: 23.5cm, W: 434.4g). Bars are ± 1 the estimate of the total error (standard error within sample and machine error). * = element not present in sample.

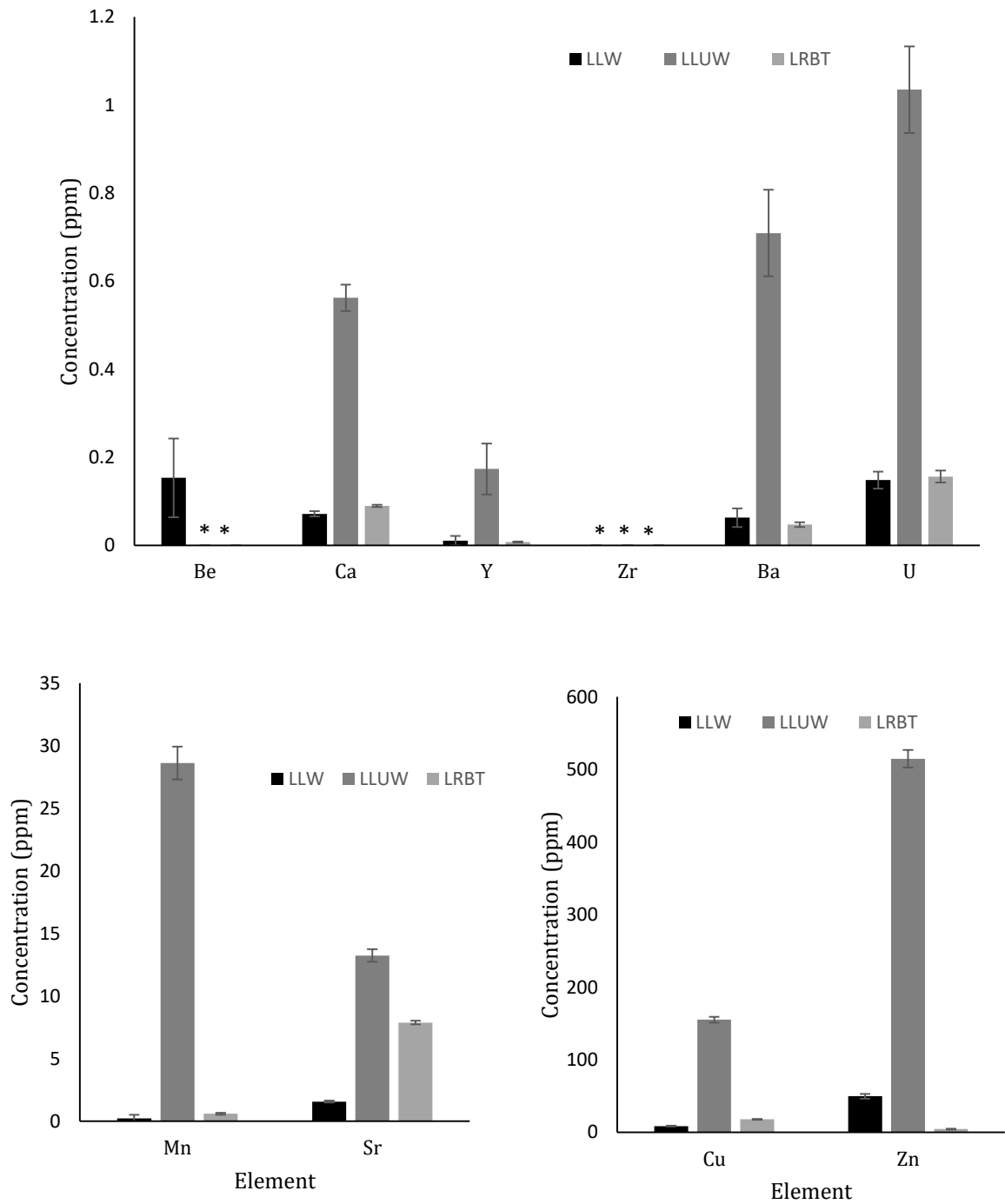


Figure 4.9: Concentration of all trace elements measured, normalised to 365ppm Mg at each site in one beak (Pukaki Rise male, ML: 26.7cm, W: 538g). Bars are ± 1 the estimate of the total error (standard error within sample and machine error). * = element not present in sample.

4.4 Discussion

This is the first time squid beaks have been analysed for their trace elements using either solution based, or laser ablation, ICP-MS. Data collected and reported here show that beaks of *Onykia ingens* contain trace elements (Na, K, P, Ca, Mg, B, Zn, Fe, Cu, Se, Mo, Sr, Mn, As, Cd, Cr, U, Rb, Ni, Pb, Ba, Li, Co, Y, Zr and Be) and that both methods used in this study are capable of resolving those trace elements.

This is the first time trace elements in squid beaks have been described. It was found, using ICP-MS, that beaks of *O. ingens* contain, on average, 3.7% trace elements by mass. The element with the highest concentration, almost half of the trace element mass, is sodium. Over 99% of the trace element mass found in beaks of *O. ingens* is made up of Na, K, P, Ca, Mn, B and Zn. The other sixteen elements found using ICP-MS compose less than 1% of the beak mass attributable to trace elements meaning that these sixteen elements make up, on average, only 0.03% of the beaks' overall mass.

LA-ICP-MS on the smaller beak fragments found a further three trace elements that were not discovered by the solution based ICP-MS; these elements were Be, Y and Zr. These three elements were not found in all beaks, and not in all sections of beaks in which they were found, but, there is no obvious pattern for incorporation. As these elements were not found in all beaks, and only in some sections in those beaks that contained them, it is not surprising that they were not found via solution based ICP-MS. LA-ICP-MS carried out on smaller sections of the beaks also revealed a large degree of within beak variation that had no obvious trend between beaks.

Two previous studies found no evidence of any trace elements in beaks of *Dosidicus gigas* (Table 4.3) (Broomell et al. 2007, Miserez et al. 2007). The major difference between these two studies and the current study is the method used to analyse the squid beaks. Both Broomell et al. (2007) and Miserez et al. (2007) used SEM-EDS to analyse the beaks, whereas the current study used the more sensitive ICP-MS. The difference in trace elements between studies is probably attributable to the different analysis method, though the different species may have also made a difference (Table 4.3).

Chandumpai et al. (2004) and Kurita et al. (1993b) analysed the trace element composition of three different species of squid gladii using ICP-MS. Both found trace

levels of Ca, Mg and Fe in the squid gladii, one study also found Cd and the other found K and P. The concentrations of Ca and Mg that were found in the beaks of *O. ingens* were higher than those found in the gladii of *Loligo lessoniana*, *Loligo formosana* and *Ommastrephes bartrami*. The concentration of Fe found in the beaks of *O. ingens* was similar to that found in the gladii of *L. lessoniana*, but half the value of that found in *L. formosana* and twice that found in *O. bartrami*. Both the K and P concentrations from the beaks of *O. ingens* were higher than those in *O. bartrami*. Cd concentrations were a lot higher in gladii of *L. formosana* than beaks of *O. ingens* (Table 4.3). It is not surprising that trace element values between squid gladii and beaks vary as, despite both being made of chitin, these structures are dissimilar. Beaks are exposed to the water, while gladii are inside the animal; beaks are made of α -chitin whilst gladii are made of β -chitin; lastly they are structurally different, beaks are short, wide and hard to cut prey, gladii are long and thin to provide rigidity to the body.

Miserez et al. (2009) detected both Cl and S in the non-chitinous sucker rings of *D. gigas*; neither element was detected in the beaks of *O. ingens* (Table 4.3). This difference may be due to differing trace metal incorporation between substances, as beaks are made of chitin and sucker rings are made primarily of proteins. The difference may indicate that both Cl and S lend some sort of structural support to the sucker rings which is not used in beaks.

The variation seen here within beaks shows that analyses that can pinpoint small areas of squid beaks, such as LA-ICP-MS, have advantages over methods that homogenise the entire sample, such as solution-based ICP-MS. Variation over the length of the squid beak may be due to the age of the section as the beak grows in length as the squid ages. However, the beak also grows in thickness so the outer layers would be younger than the middle layers, therefore, even the beak tip would have young layers. Another possible cause of the within beak variation is the difference in water, tanning pigment, protein and chitin content along the length of the beak which, in turn, causes the difference in stiffness.

The values reported for the elements found using ICP-MS show that there is a large amount of variation between beaks. Data reported for LA-ICP-MS show that there is also a large variation of all elements investigated within individual beaks. The high

variability in all of the elements measured by both methods suggests that none of the elements measured would make good normalisation elements for LA-ICP-MS.

As squid beaks contain trace elements, there is the possibility that they are different between species and populations, as they are in statoliths (Arkhipkin et al. 2004, Green et al. 2015). If there is a difference between species and populations, trace element analyses could be used when a beak is recovered from a predators stomach to help identify the species and even track which population it came from. Geographic tracking would aid in the management of squid populations as predators can act as biological sampling units and it could be used in fisheries forensics to confirm the location of capture of market squid. Populations of important squid predators, such as New Zealand fur seals (*Arctocephalus fosteri*) (Boren 2008) and hoki (*Macruronus novaezelandiae*) (Clark 1985) would also benefit from this beak trace element tracking system. The squid predator's movements could be traced via the original location of the squid in their stomachs. For the use of predators as biological sampling units for this beak trace element tracking system to become a possibility, data on the effect of stomach acid on the trace element composition over time would need to be gathered. There needs to be far more research and data collected on squid beak trace elements for this "fingerprinting" technique to be possible. This preliminary analysis has shown that there are elements present in beaks which acts as a proof of concept for the idea and highlights methods that could be used in future studies to further analyse the variation within, and among squid beaks.

4.4.1 Conclusion

Beaks of *O. ingens* incorporate trace elements into their structure which possibly helps increase their structural stiffness and complexity as they do in structures of other animals, such as the incorporation of Zn into the jaws of *Neris virens* (Broomell et al. 2008). This hypothesis could be tested using the methods outlined in Broomell et al. (2008) to test the hardness and stiffness before and after trace elements are removed from the sample. These trace elements, regardless of their origin, mode of incorporation or applications in the structure of the beak itself, may one day prove to be useful indicators of geographic movement and origin in squid.

Table 4.3: Comparison of mean trace element concentrations from squid hard parts in all past studies. Brackets are $\pm 1SD$ where given

Paper	Hard part	Species	Method	n	Element (ppm)									
					Ca	Mg	Cu	Fe	Na	K	P	Cd	Cl	S
This study	Beak	<i>O. ingens</i>	ICP-MS	6	403.8 (± 213.2)	364.9 (± 340.9)	5.9 (± 1.4)	8.6 (± 1.9)	1637 (± 286.3)	569.0 (± 157.55)	560.6 (± 398.8)	0.6 (± 0.9)		
Miserez et al. 2007	Beak	<i>D. gigas</i>	EDS	NR										
Broomell et al. 2007	Beak	<i>D. gigas</i>	EDS & X-ray	NR										
Chandumpai et al. 2004	Pen	<i>L. lessoniana</i>	AA & ICP-MS	4	17.7 (± 3.3)	3.3 (± 0.8)	0.9 (± 0.3)	7.7 (± 0.3)						
Kurita et al. 1993	Pen	<i>L. formosana</i>	AA & ICP-MS	4	24.2 (± 5.8)	5.5 (± 1.0)	16.2 (± 5.7)	17.2 (± 2.8)				8.1 (± 0.2)		
Miserez et al. 2009	Pen	<i>O. bartramii</i>	ICP-MS		344	121		4		19	287			
	Sucker rings	<i>D. gigas</i>	EDS										* *	

Blank space = elements were not found

* = Element found but not quantified

NR = not reported

Chapter Five: General Conclusions

Figure 1 shows a conceptual framework of the scope of this thesis. Squid are born and age over time. At any point in their life history, squid may be eaten or suffer mortality by other means; the hard parts then go on to either another animal's stomach, are caught in fisheries, or go to the sea floor. The structure and composition of the squid's hard parts are affected by both the environment that the squid inhabits and its life-history stage. In this thesis, hard parts of two common species of squid from southern New Zealand, *Onykia ingens* and *Nototodarus sloanii*, were identified, analysed and then reviewed for their potential effectiveness as tools to explore the life history of the animal, and its environment, post-mortem. These initial studies, alongside evaluation of current literature on the use of squid hard parts, informed the decision to focus on two hard parts: beaks and statoliths.

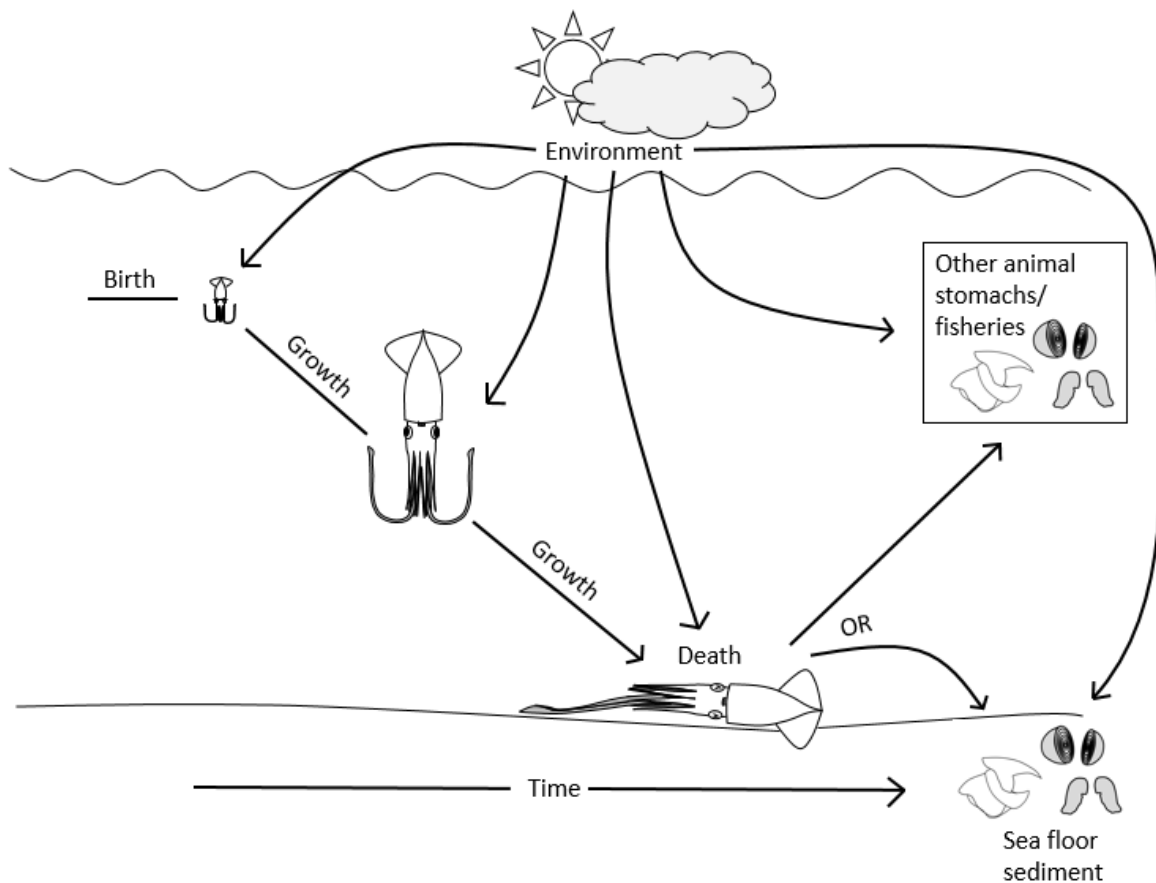


Figure 5.1: A generalised diagram of the major factors (environment and life history stage) that affect the structure and composition of hard parts. Death can occur at any point along the squid's life history.

Allometric relationships between beak size and body size were examined and beak weight was investigated as a predictor of squid size for the first time. Beak weights were found to be the best predictors for squid size in *O. ingens* while rostral lengths were the best predictors of squid size in *N. sloanii*. Beak weights have been shown here

to be accurate predictors of squid size in *O. ingens* (r^2 from 0.84 to 0.96) and should be used as a predictor in scenarios where the whole squid is recovered but mantle length and weight measurements cannot be taken. This scenario could occur due to factors such as a loss of arms, tentacles or mantle pieces in trawls. However, beak weight may have limited applications in diet analysis studies as it may be affected by dissolution in stomach acid at a faster rate than rostral lengths are. Due to its high accuracy as a predictor, it is recommended that beak weight be further studied for its suitability as a predictor of squid biomass in these diet studies. Future tests should include investigating how beak weight changes over time in stomach acid compared to rostral length measurements.

This study built on allometric relationships and equations between beaks and squid size explained in past studies via the addition of new data and gave new, accurate equations for squid size estimation. The allometric trends found in this study broadly supported growth trends found in the majority of past studies that had analysed these relationships in these species (Jackson 1995, Bolstad 2006, McKinnon 2006). There was, however, some disagreement in specific relationships and equations between studies; for example, Jackson & McKinnon (1996) found a linear relationship between rostral length and squid weight, whereas this study found this relationship to be exponential. Different beak storage methods can change the dimensions of the beak (Jackson et al. 1997) and the differences seen between studies are likely due to the differing beak storage between studies. These discrepancies highlight the need for further study of the effect of beak storage and preparation methods on beak dimensions.

Methods of exploring statolith structure and composition were reviewed and SEM, Raman spectroscopy and LA-ICP-MS were used to carry out these analyses. It was shown that statoliths of both *O. ingens* and *N. sloanii* are made of calcium carbonate in the aragonite polymorph, much like other squid species (Radtke 1983, Zumholz et al. 2007a, Wang et al. 2012). Raman spectroscopy showed that the crystal structure of the aragonite changed between the inner and outer zone of the statolith as theorised by Jackson (1993). The difference in structure between these zones has been suggested to be due to a habitat shift in *O. ingens* (Jackson 1993). The presence of the structural shift in *N. sloanii* suggests that they also undergo an ontogenetic migration, as theorised by McKinnon (2006). Understanding the reason for this zonation would give a better

insight into statolith formation and therefore help the interpretation of statoliths trace element and stable isotope data. Interestingly, the structural change is not manifested under SEM. Statolith preparation methods used by Kristensen (1980) and Radtke (1983), and higher magnifications using the SEM might enable visualisation of this difference in structure in the future.

Analysis using LA-ICP-MS found a significant difference in trace element incorporation between the two zones within statoliths of both species. Trace element incorporation also significantly differed among two source locations of *O. ingens* and between *O. ingens* and *N. sloanii*. These differences suggest a difference in lifestyle between the two species which is detectable by trace element analysis. For example, Sr was higher in *O. ingens* than in *N. sloanii* which suggests that *N. sloanii* live in shallower waters that are closer to the coast (Ikeda et al. 1997), which supports the real life distribution of these species (Jackson et al. 2000a). Further investigation into the influence of abiotic and biotic factors on the trace element incorporation into statoliths are warranted. Finding out how environmental factors affect trace element incorporation into statoliths would be useful in the reconstruction of individual squid life history. The possible future applications of this information range from paleo-climate reconstruction using squid statoliths from the fossil record, to tracing ontogenetic migrations in individuals.

Beaks of *O. ingens* were analysed for trace elements using solution-based and laser-ablation ICP-MS for the first time. Data collected and reported here show that beaks of *O. ingens* contain trace elements and that both methods used in this study are capable of identifying these trace elements. Past studies looking for trace metals in beaks of other species of squid using SEM-EDS found none (Broomell et al. 2007, Miserez et al. 2007), making this the first time that trace metals have been quantified in squid beaks. It was found that beaks of *O. ingens* contain, on average, 3.7% trace elements by mass. Over 99% of the trace element mass found in beaks of *O. ingens* is made up of Na (~45%), K, P, Ca, Mg, B and Zn. The other sixteen elements found using ICP-MS together consist of, on average, only 0.03% of the beaks' overall mass.

There is a large amount of variation (see table 4.1) of trace elements within, and among, beaks of *O. ingens*. This variation means that quantification of minerals using LA-ICP-MS is difficult as there needs to be an element that is stable (at the same

quantity) between beaks for normal quantification methods. Further investigation of different methods of quantifying beak elements on an intra-beak scale is needed.

It has been suggested that incorporation of trace elements into hard structures of animals increases their stiffness and complexity, such as the incorporation of Zn into the jaws of the polychaete worm *Neris virens* (Broomell et al. 2008). It is likely that this is also the case for squid as they need very hard beaks to cut up prey. The elements incorporated into the beak may also interact with the gradient of physical and chemical variables along the beak which contribute to the gradient of stiff to pliable from the tip to the wings of the beak (Miserez et al. 2008). This hypothesis could be tested using the methods outlined in Broomell et al. (2008) to test the hardness and stiffness before and after trace elements are removed from the sample.

Beak trace element trends may be different between species and populations, as they are in statoliths (Arkhipkin et al. 2004, Green et al. 2015). If these differences occur consistently, trace element analyses could potentially be used when a beak is recovered from a predator's stomach to identify the species and track which population it came from; however, the effect of stomach acid on elemental composition would need to be investigated. This tracking would revolutionise management of squid populations as predators could act as biological sampling units. Tracking could be used in fisheries forensics to confirm the location of capture of market squid. Migrations of predators that eat squid could also be traced via the original location of the squid in their stomachs to aid in their management.

To get beak trace element data to this “fingerprinting-and-tracking” stage will require a large amount of research, but the presence of trace elements as shown here confirms the potential. There is a need for quantitative analyses of trace elements within squid beaks, possibly using solution-based ICP-MS, with a large sample size to further assess the amount of intra-beak variation. If consistency within beaks can be found, beaks of individuals within a population, or geographic location, could be compared to examine how much they vary. Groups of beaks from different locations could then be compared; if there is consistent variation of beaks between locations that is higher than the variance within beaks and locations, trace element fingerprinting could take place.

Final conclusion

Identifying and describing naturally occurring allometric relationships can allow researchers to extrapolate the size of an animal from a single hard part. The resulting equations allow the reconstruction of diets of animals that are ecologically, or commercially, important in a relatively cheap and easy manner, and can provide useful insights for prey species that are normally difficult to sample, such as deep-sea squid. The relationships presented here expand on those in the literature and offer an insight into a novel method of beak size measurement.

Trace elements in hard parts have the potential capability to expose many aspects of the life history of an animal; for example their larval geographic origin (Zacherl 2005). The potential for the use of trace elements from a hard part as a geographical marker adds another layer to post-mortem research in diet studies and fisheries forensics in fisheries management. Statoliths are shown here to have differing trace element concentrations between life-history stages, geographic areas and species, which supports the literature and the idea of using these elements as a natural tag in the future. Beaks are shown to contain trace elements which vary to a large degree between, and within, beaks. The presence of trace elements in squid beaks establishes the grounds for further research to help identify the significance of the variations seen here.

References

- Aguiar D, Rossi-Wongtschowski C, Perez J (2012) Validation of daily growth increments of statoliths of Brazilian squid. *Bioikos* 26:13–21
- Arbuckle NSM, Wormuth JH (2014) Trace elemental patterns in Humboldt squid statoliths from three geographic regions. *Hydrobiologia* 725:115–123
- Arkhipkin AI (1993) Age, growth, stock structure and migratory rate of pre-spawning short-finned squid *Illex argentinus* based on statolith ageing investigations. *Fisheries Research* 16:313–338
- Arkhipkin AI, Campana SE, FitzGerald J, Thorrold SR (2004) Spatial and temporal variation in elemental signatures of statoliths from the Patagonian longfin squid (*Loligo gahi*). *Canadian Journal of Fisheries and Aquatic Sciences* 61:1212–1224
- Arkhipkin AI, Laptikhovskiy V V. (2010) Observation of penis elongation in *Onykia ingens*: implications for spermatophore transfer in deep-water squid. *Journal of Molluscan Studies* 76:299–300
- Arkhipkin AI, Perez JAA (1998) Life history reconstruction. In: Rodhouse PG, Dawe EG, O'Dor RK (eds) *Squid Recruitment Dynamics: The Genus Illex as a Model, the Commercial Illex Species and Influence on Variability*. Food & Agriculture Org., p 273
- Arkhipkin AI, Rodhouse PGK, Pierce GJ, Sauer W, Sakai M, Allcock L, Arguelles J, Bower JR, Castillo G, Ceriola L, Chen C-S, Chen X, Diaz-Santana M, Downey N, González AF, Granados Amores J, Green CP, Guerra A, Hendrickson LC, Ibáñez C, Ito K, Jereb P, Kato Y, Katugin ON, Kawano M, Kidokoro H, Kulik V V., Laptikhovskiy V V., Lipinski MR, Liu B, Mariátegui L, Marin W, Medina A, Miki K, Miyahara K, Moltschaniwskyj N, Moustahfid H, Nabhitabhata J, Nanjo N, Nigmatullin CM, Ohtani T, Pecl G, Perez JA a., Piatkowski U, Saikliang P, Salinas-Zavala C a., Steer M, Tian Y, Ueta Y, Vijai D, Wakabayashi T, Yamaguchi T, Yamashiro C, Yamashita N, Zeidberg LD (2015) World squid fisheries. *Reviews in Fisheries Science & Aquaculture* 23:92–252
- Arkhipkin AI, Shcherbich ZN (2012) Thirty years' progress in age determination of squid using statoliths. *Journal of the Marine Biological Association of the United Kingdom* 92:1389–1398

- Bagley NW, O'Driscoll R, Oeffner J (2013) Trawl survey of hoki and middle-depth species in the Southland and Sub-Antarctic areas , November – December 2011 (TAN1117).
- Baum JK, Worm B (2009) Cascading top-down effects of changing oceanic predator abundances. *Journal of Animal Ecology* 78:699–714
- Boggild O (1930) The shell structure of the mollusks. Kjobenhavn
- Bolstad KS (2006) Sexual dimorphism in the beaks of *Moroteuthis ingens* Smith, 1881 (Cephalopoda: Oegopsida: Onychoteuthidae). *New Zealand Journal of Zoology* 33:317–327
- Bolstad KS (2010) Systematics of the Onychoteuthidae Gray, 1847 (Cephalopoda: Oegopsida). *Zootaxa* 186:1–186
- Boren L (2008) Diet of New Zealand fur seals (*Arctocephalus forsteri*): a summary. *Doc Research and Development Series* 319:19p
- Brooker L, Shaw J (2012) The chiton radula: a unique model for biomineralization studies. *Advanced Topics in Biomineralization*: 65–84
- Broomell CC, Khan RK, Moses DN, Miserez A, Pontin MG, Stucky GD, Zok FW, Waite JH (2007) Mineral minimization in nature's alternative teeth. *Journal of the Royal Society Interface* 4:19–31
- Broomell CC, Zok FW, Waite JH (2008) Role of transition metals in sclerotization of biological tissue. *Acta Biomaterialia* 4:2045–2051
- Budelmann BU (1988) Morphological diversity of equilibrium receptor systems in aquatic invertebrates. *Sensory biology of aquatic animals*:757–782
- Budelmann BU (1990) The statocysts of squid. In: *Squid as Experimental Animals*. p 421–439
- Campana SE (1999) Chemistry and composition of fish otoliths: pathways, mechanisms and applications. *Marine ecology Progress series* 188:263–297
- Chandumpai A, Singhpibulporn N, Faroongsarng D, Sornprasit P (2004) Preparation and physico-chemical characterization of chitin and chitosan from the pens of the squid species , *Loligo lessoniana* and *Loligo formosana*. *Carbohydrate Polymers* 58:467–474
- Chen, B (2011) LA-ICP-MS of *Dosidicus gigas* statoliths. Unpublished data.
- Cherel Y, Hobson KA (2005) Stable isotopes, beaks and predators: a new tool to study the trophic ecology of cephalopods, including giant and colossal squids. *Proceedings of the Royal Society B* 272:1601–1607

- Cherel Y, Pütz K, Hobson K (2002) Summer diet of king penguins (*Aptenodytes patagonicus*) at the Falkland Islands, southern Atlantic Ocean. *Polar Biology* 25:898–906
- Cherel Y, Ridoux V, Spitz J, Richard P (2009) Stable isotopes document the trophic structure of a deep-sea cephalopod assemblage including giant octopod and giant squid. *Biology letters* 5:364–367
- Clarke MR (1985) The food and feeding of seven fish species from the Campbell Plateau, New Zealand. *New Zealand Journal of Marine and Freshwater Research* 19:339–363
- Clarke MR (1978) The cephalopod statolith - an introduction to its form. *Journal of the Marine Biological Association of the United Kingdom* 58:701–712
- Clarke MR (1986) *A handbook for the identification of cephalopod beaks*. Clarendon Press, Oxford
- Clarke MR (1996) Cephalopods as prey III cetaceans. *Philosophical Transactions of the Royal Society of London B: Biological Sciences* 351:1053–1065
- Clarke MR, Roper CFE (1998) Cephalopods represented by beaks in the stomach of a sperm whale stranded at Paekakariki, North Island, New Zealand. *South African Journal of Marine Science* 20:129–133
- Cummings V (2014) Ocean acidification impacts on New Zealand abalone, cockle and flat oyster. In: *Future proofing New Zealand's shellfish aquaculture: monitoring and adaptation to ocean acidification*.p 28–29
- Department of Chemistry UCLA (2003) *Practical aspects of Infrared Spectroscopy or "how to get a good IR spectrum."* :1
- Dilly DPN (1976) The structure of some cephalopod statoliths. *Cell and Tissue Research* 175:147–163
- Doney SC, Fabry VJ, Feely RA, Kleypas JA (2009) Ocean acidification: the other CO₂ problem. *Annual Review of Marine Science* 1:169–192
- Dunn MR (2009) Feeding habits of the ommastrephid squid *Nototodarus sloanii* on the Chatham Rise, New Zealand. *New Zealand Journal of Marine and Freshwater Research* 43:1103–1113
- Dutrow B, Clark C (2015) *X-ray powder diffraction (XRD)*. Science Education Resource Center at Carleton College
- Elmer P (2001) *The 30-minute Guide to ICP-MS*. Perkin Elmer, Shelton CT:1–8

- Fea NI, Harcourt R, Lalas C (1999) Seasonal variation in the diet of New Zealand fur seals (*Arctocephalus forsteri*) at Otago Peninsula, New Zealand. *Wildlife Research* 26:147–160
- Frech R, Wang C, Bates J (1980) The i.r. and Raman spectra of CaCO₃ (aragonite). *Spectrochimica Acta* 36:915–919
- Gaskin DE, Cawthorn MW (1967) Diet and feeding habits of the sperm whale (*Physeter Catodon L.*) in the Cook Strait region of New Zealand. *New Zealand Journal of Marine and Freshwater Research* 1:156–179
- Gauldie RW, Sharma SK, Volk E (1997) Micro-Raman spectral study of vaterite and aragonite otoliths of the coho salmon, *Oncorhynchus kisutch*. *Comparative Biochemistry and Physiology - A Physiology* 118:753–757
- Goldstein J, Newbury D, Joy D, Lyman C, Echlin P, Lifshin E, Sawyer L, Michael J (2012) *Scanning electron microscopy and X-ray microanalysis*, 3rd edn. Springer Science & Business Media, New York
- Green CP, Robertson SG, Hamer PA, Virtue P, Jackson GD, Moltschanivskyj NA (2015) Combining statolith element composition and Fourier shape data allows discrimination of spatial and temporal stock structure of arrow squid (*Nototodarus gouldi*). *Canadian Journal of Fisheries and Aquatic Sciences* 1618:1–37
- Hansen T, Fjelldal P, Myers FW, Swearer S, Dempster T (2015) Detecting and tracing farmed salmon with natural geo-element otolith “fingerprint” tags: developing and validating tag delivery techniques.
- Hernández-García V (1995) The diet of the swordfish *Xiphias gladius* Linnaeus, 1758, in the central east Atlantic, with emphasis on the role of cephalopods. *Fishery Bulletin* 93:403–411
- Hoening M, Kersabiec AM De (1996) Sample preparation steps for analysis by atomic spectroscopy methods: Present status. *Spectrochimica Acta - Part B Atomic Spectroscopy* 51:1297–1307
- Hudson S, Smith C (2013) Polysaccharides: chitin and chitosan: chemistry and technology. In: Kaplan D (ed) *Biopolymers from renewable resources*. Springer Science & Business Media, p 420
- Hunt S, Nixon M (1981) A comparative study of protein composition in the chitin-protein complexes of the beak, pen, sucker disc, radula and oesophageal cuticle of cephalopods. *Comparative Biochemistry and Physiology Part B: Comparative Biochemistry* 68:535–546

- Hunter S, Brooke ML (1992) The diet of giant petrels *Macronectes* spp. at Marion Island, Southern Indian Ocean. *Colonial Waterbirds* 15:56–65
- Hurley G, Beck P (1979) The observation of growth rings in the statoliths from the Ommastrephid squid, *Illex illecebrosus*. Northwest Atlantic Fisheries Organisation:1–14
- Hurley G, Odense PH, O’Dor RKO, Dawe E (1985) Strontium labelling for verifying daily growth increments in the statolith of the short-finned squid (*Illex illecebrosus*). *Canadian Journal of Fisheries and Aquatic Sciences* 42:380–383
- Ikeda Y, Arai N, Kidokoro H, Sakamoto W (2003) Strontium:calcium ratios in statoliths of Japanese common squid *Todarodes pacificus* (Cephalopoda: Ommastrephidae) as indicators of migratory behavior. *Marine Ecology Progress Series* 251:169–179
- Ikeda Y, Arai N, Sakamoto W, Kidokoro H, Yatsu A, Nateewathana A, Yoshida K (1997) Comparison on trace elements in squid statoliths of different species’ origin: as available key for taxonomic and phylogenetic study. *International Journal of PIXE* 7:141–146
- Ikeda Y, Arai N, Sakamoto W, Yoshida K (1996) Relationship between statoliths and environmental variables in cephalopod. *International Journal of PIXE* 6:339–345
- Ikeda Y, Okazaki J, Sakurai Y, Sakamoto W (2002a) Periodic variation in Sr/Ca ratios in statoliths of the Japanese common squid *Todarodes pacificus* Steenstrup, 1880 (cephalopoda: Ommastrephidae) maintained under constant water temperature. *Journal of Experimental Marine Biology and Ecology* 273:161–170
- Ikeda Y, Yatsu A, Arai N, Sakamoto W (2002b) Concentration of statolith trace elements in the jumbo flying squid during El Nino and non-El Nino years in the eastern Pacific. *Journal of the Marine Biological Association of the UK* 82:863-866
- Jackson GD (1993) Growth zones within the statolith microstructure of the deepwater squid *Moroteuthis ingens* (Cephalopoda:Onychoteuthidae) evidence for a habitat shift? *Canadian Journal of Fisheries and Aquatic Science* 50:2366–2374
- Jackson GD (1994) Statolith age estimates of the loliginid squid *Loligo opalescens* (Mollusca: Cephalopoda): corroboration with culture data. *Bulletin of Marine Science* 54:554–557
- Jackson G (1995) The use of beaks as tools for biomass estimation in the deepwater squid *Moroteuthis ingens* (Cephalopoda: Onychoteuthidae) in New Zealand waters. *Polar Biology* 15:9–14

- Jackson GD (1997) Age, growth and maturation of the deepwater squid *Moroteuthis ingens* (Cephalopoda: Onychoteuthidae) in New Zealand waters. *Polar Biology* 17:268–274
- Jackson GD (2001) Confirmation of winter spawning of *Moroteuthis ingens* (Cephalopoda: Onychoteuthidae) in the Chatham Rise region of New Zealand. *Polar Biology* 24:97–100
- Jackson GD, Buxton NG, George MJA (1997) Beak length analysis of *Moroteuthis ingens* (Cephalopoda: Onychoteuthidae) from the Falkland Islands region of the Patagonian shelf. *Journal of the Marine Biological Association of the United Kingdom* 77:1235–1238
- Jackson GD, Choat IH (1992) Growth in tropical cephalopods: an analysis based on statolith microstructure. *Canadian Journal of Fisheries and Aquatic Sciences* 49:218–228
- Jackson GD, Forsythe JW (2002) Statolith age validation and growth of *Loligo plei* (Cephalopoda: Loliginidae) in the north-west Gulf of Mexico during spring/summer. *Journal of the Marine Biological Association of the UK* 82:677–678
- Jackson GD, George MJA, Buxton NG (1998a) Distribution and abundance of the squid *Moroteuthis ingens* (Cephalopoda: Onychoteuthidae) in the Falkland Islands region of the South Atlantic. *Polar Biology* 20:161–169
- Jackson GD, McKinnon JF (1996) Beak length analysis of arrow squid *Nototodarus sloanii* (Cephalopoda: Ommastrephidae) in southern New Zealand waters. *Polar Biology* 16:227–230
- Jackson GD, McKinnon JF, Lalas C, Arden R, Buxton NG (1998b) Food spectrum of the deepwater squid *Moroteuthis ingens* (Cephalopoda: Onychoteuthidae) in New Zealand waters. *Polar Biology* 20:56–65
- Jackson GD, O'Shea S (2003) Unique hooks in the male scaled squid *Lepidoteuthis grimaldii*. *Journal of the Marine Biological Association of the United Kingdom* 83:1099–1100
- Jackson GD, Ross A, Howard Choat J (2000a) Can length frequency analysis be used to determine squid growth? – An assessment of ELEFAN. *ICES Journal of Marine Science* 57:948–954
- Jackson GD, Shaw AGP, Lalas C (2000b) Distribution and biomass of two squid species off southern New Zealand: *Nototodarus sloanii* and *Moroteuthis ingens*. *Polar Biology* 23:699–705

- Jamieson JC (1953) Phase equilibrium in the system calcite-aragonite. *The Journal of Chemical Physics* 21:1385
- Jang MK, Kong BG, Jeong YI, Lee CH, Nah JW (2004) Physicochemical characterization of α -chitin, β -chitin, and γ -chitin separated from natural resources. *Journal of Polymer Science, Part A: Polymer Chemistry* 42:3423–3432
- Kristensen TK (1980) Periodical growth rings in cephalopod *Gonatus fabricii* statoliths. *Dana* 1:39–52
- Kurita K, Tomita K, Ishii S, Nishimura SI, Shimoda K (1993a) β -chitin as a convenient starting material for acetolysis for efficient preparation of N-acetylchitooligosaccharides. *Journal of Polymer Science, Part A: Polymer Chemistry* 31:2393–2395
- Kurita K, Tomita K, Tada T, Ishii S, Nishimura SI, Shimoda K (1993b) Squid chitin as a potential alternative chitin source. Deacetylation behavior and characteristic properties. *Journal of Polymer Science, Part A: Polymer Chemistry* 31:485–491
- Landman N, Cochran J, Cerrato R, Mak J, Roper C, Lu C (2004) Habitat and age of the giant squid (*Architeuthis sanctipauli*) inferred from isotopic analyses. *Marine Biology* 144:685–691
- Laptikhovskiy V V., Arkhipkin AI, Hoving HJ (2007) Reproductive biology in two species of deep-sea squids. *Marine Biology* 152:981–990
- Lavall R, Assis O, Campanafilho S (2007) β -Chitin from the pens of *Loligo* sp.: Extraction and characterization. *Bioresource Technology* 98:2465–2472
- Leona M, Stenger J, Ferloni E (2006) Application of surface enhanced Raman scattering techniques to the ultrasensitive identification of natural dyes in works of art. *Journal of Raman Spectroscopy* 37:981–992
- Lipinski M (1986) Methods for the validation of squid age from statoliths. *Journal of the Marine Biological Association of the UK* 66:505–526
- Liu B, Cao J, Truesdell SB, Chen Y, Chen XJ, Tian SQ (2016) Reconstructing cephalopod migration with statolith elemental signatures: a case study using *Dosidicus gigas*. *Fisheries Science*
- Liu B, Chen Y, Chen XJ (2015) Spatial difference in elemental signatures within early ontogenetic statolith for identifying Jumbo flying squid natal origins. *Fisheries Oceanography*: 335–346
- Liu B, Chen XJ, Chen Y, Hu GY (2015a) Determination of squid age using upper beak rostrum sections: technique improvement and comparison with the statolith. *Marine Biology* 162:1685–1693

- Liu B, Chen X, Chen Y, Lu H, Qian W (2011) Trace elements in the statoliths of jumbo flying squid off the Exclusive Economic Zones of Chile and Peru. *Marine Ecology Progress Series* 429:93–101
- Liu B, Chen X, Chen Y, Tian S (2013) Geographic variation in statolith trace elements of the Humboldt squid, *Dosidicus gigas*, in high seas of Eastern Pacific Ocean. *Marine Biology* 160:2853–2862
- Liu B, Chen X, Fang Z, Hu S, Song Q (2015b) A preliminary analysis of trace-elemental signatures in statoliths of different spawning cohorts for *Dosidicus gigas* off EEZ waters of Chile. *Journal of Ocean University of China* 14:1059–1067
- Liu Y, Hu Z, Gao S, Gunther D, Xu J, Gao C, Chen H (2008) In situ analysis of major and trace elements of anhydrous minerals by LA-ICP-MS without applying an internal standard. *Chemical Geology* 257:34–43
- Lorrain A, Argüelles J, Alegre A, Bertrand A, Munaron J-M, Richard P, Cherel Y (2011) Sequential isotopic signature along gladius highlights contrasted individual foraging strategies of jumbo squid (*Dosidicus gigas*). *PLoS ONE* 6:e22194
- Lu CC, Williams R (1994) *Kondakovia longimana* Filippova, 1972 (Cephalopoda: Onychoteuthidae) from the Indian Ocean sector of the Southern Ocean. *Antarctic Science* 6:231–234
- Mattlin, R., Scheibling, R. and Förch E (1985) Distribution, abundance and size structure of arrow squid (*Nototodarus*, sp.) off New Zealand. *NAFO Science Council Studies* 9:39–45
- McKinnon JF (2006) Aspects of the population biology of the southern arrow squid, *Nototodarus sloanii*, in southern New Zealand. Unpublished PhD Thesis, University of Otago :322
- McMullan D (1995) Scanning electron microscopy 1928–1965. *Scanning* 17:175–185
- Meyers MA, Lin AYM, Seki Y, Chen PY, Kad BK, Bodde S (2006) Structural biological composites: An overview. *Biological Materials Mechanics* 58:35–41
- Meynier L, Stockin K a., Bando MKH, Duignan PJ (2008) Stomach contents of common dolphin (*Delphinus* sp.) from New Zealand waters. *New Zealand Journal of Marine and Freshwater Research* 42:257–268
- Milestone Science (2001) Guidelines for microwave acid digestion. :1–9
- Miserez A, Li Y, Waite JH, Zok F (2007) Jumbo squid beaks: inspiration for design of robust organic composites. *Acta Biomaterialia* 3:139–149
- Miserez A, Rubin D, Waite JH (2010) Cross-linking chemistry of squid beak. *Journal of Biological Chemistry* 285:38115–38124

- Miserez A, Schneberk T, Sun C, Zok FW, Waite JH (2008) The transition from stiff to compliant materials in squid beaks. *Science* (New York, NY) 319:1816–1819
- Miserez A, Weaver JC, Pedersen PB, Schneberk T, Hanlon RT, Kisailus D, Birkedal H (2009) Microstructural and biochemical characterization of the nanoporous sucker rings from *Dosidicus gigas*. *Advanced Materials* 21:401–406
- Morris CC, Aldrich FA (1984) Statolith length and increment number for age determination in squid *Illex illecebrosus* (LeSueur, 1821) (Cephalopods: Ommastrephidae). NAFO SCR Doc 901:1–22
- MPI (2013) Fisheries assessment plenary May 2013
- Nakamura Y, Sakurai Y (1991) Validation of daily growth increments in statoliths of Japanese common squid *Todarodes pacificus*. 日本水産学会誌 = Bulletin of the Japanese Society of Scientific Fisheries 57:2007–2011
- Natsukari Y, Komine N (1992) Age and growth estimation of the European squid, *Loligo vulgaris*, based on statolith microstructure. *Journal of the Marine Biological Association of the United Kingdom* 72:271–280
- Nesis K (1987) *Cephalopods of the world: squids, cuttlefishes, and allies* (L Burgess, Ed.). TFH Publications, Neptune City
- Newbury DE, Ritchie NWM (2013) Elemental mapping of microstructures by scanning electron microscopy-energy dispersive X-ray spectrometry (SEM-EDS): extraordinary advances with the silicon drift detector (SDD). *Journal of Analytical Atomic Spectrometry* 28:973
- Nilsson D-E, Warrant EJ, Johnsen S, Hanlon R, Shashar N (2012) A unique advantage for giant eyes in giant squid. *Current Biology* 22:683–688
- O’Dor R (2000) Does geometry limit squid growth? *ICES Journal of Marine Science* 57:8–14
- Onthank K, Lee R (2013) Exploring the life histories of cephalopods using stable isotope analysis of an archival tissue. Unpublished PhD, Washington State University
- Packard A (1972) Cephalopods and fish: the limits of convergence. *Biological Reviews* 47:241–307
- Parry M (2003) The trophic ecology of two Ommastrephid squid species, *Ommastrephes bartramii* and *Sthenotheuthis oualaniensis*, in the North Pacific sub-tropical gyre. Unpublished PhD, University of Hawaii

- Perez J, Aguiar DC De, Santos J a T Dos (2006) Gladius and statolith as tools for age and growth studies of the squid *Loligo plei* (Teuthida: Loliginidae) off southern Brazil. *Brazilian Archives of Biology and Technology* 49:747–755
- Perez J, O’Dor RK (2000) Critical transitions in early life histories of short-finned squid, *Illex illecebrosus* as reconstructed from gladius growth. *Journal of the Marine Biological Association of the UK* 80:509–514
- Phillips KL, Nichols PD, Jackson GD (2003) Size-related dietary changes observed in the squid *Moroteuthis ingens* at the Falkland Islands : stomach contents and fatty-acid analyses. *Polar Biology* 26:474–485
- Pierce GJ, Portela J (2014) Fisheries production and market demand. *Cephalopod culture*. :50–52
- Post D (2002) Using stable isotopes to estimate trophic position: models, methods, and assumptions. *Ecology* 83:703–718
- Princeton Instruments (2012) Raman spectroscopy basics - application note.
- Radtke RL (1983) Chemical and structural characteristics of statoliths from the short-finned squid *Illex illecebrosus*. *Marine Biology* 76:47–54
- Reed WP (1992a) Certificate of analysis, standard reference materials 610 and 611. :3
- Reed WP (1992b) Certificate of analysis, standard reference materials 612 and 613. :3
- Reed S (2010) *Electron microprobe analysis and scanning electron microscopy in geology*, 2nd edn. Cambridge University Press
- Reusch W (2013a) *Infrared spectroscopy. Introduction to Spectroscopy*, Michigan State University
- Reusch W (2013b) *Mass spectrometry. Introduction to Spectroscopy*, Michigan State University
- Rinaudo M (2006) Chitin and chitosan: properties and applications. *Progress in Polymer Science* 31:603–632
- Rodhouse PG, Hatfield EMC (1990) Age determination in squid using statolith growth increments. *Fisheries Research* 8:323–334
- Rodhouse PG, White MG (1995) Cephalopods occupy the ecological niche of the epiipelagic fish in the Antarctic polar frontal zone. *Biological Bulletin* 189:77–80
- Roper CFE, Nigmatullin C, Jereb P (2010) *Cephalopods of the world: an annotated and illustrated catalogue of cephalopod species known to date*.
- Rudall KM (1969) Chitin and its association with other molecules. *Journal of Polymer Science: Part C* 102:83–102

- Ruiz-Cooley RI, Markaida U, Gendron D, Aguíñiga S (2006) Stable isotopes in jumbo squid (*Dosidicus gigas*) beaks to estimate its trophic position: comparison between stomach contents and stable isotopes. *Journal of the Marine Biological Association of the UK* 86:437
- Saibil H (1990) Structure and function of the squid eye. In: Gilbert D, Adelman W, Arnold J (eds) *Squid as Experimental Animals*. Springer US, p 371–397
- Schrader B, Schulz H, Andreev GN, Klump HH, Sawatzki J (2000) Non-destructive NIR-FT-Raman spectroscopy of plant and animal tissues, of food and works of art. *Talanta* 53:35–45
- Sivak JG (1982) Optical properties of a cephalopod eye (the short finned squid, *Illex illecebrosus*). *Journal of Comparative Physiology A* 147:323–327
- Sivak JG, West JA, Campbell MC (1994) Growth and optical development of the ocular lens of the squid (*Sepioteuthis lessoniana*). *Vision Research* 34:2177–2187
- Smith GPS, Gordon KC, Holroyd SE (2013) Raman spectroscopic quantification of calcium carbonate in spiked milk powder samples. *Vibrational Spectroscopy* 67:87–91
- Smith PJ, Mattlin RH, Roeleveld MA, Okutani T (1987) Arrow squids of the genus *Nototodarus* in New Zealand waters: systematics biology and fisheries. *New Zealand Journal of Marine & Freshwater Research* 21:315–326
- Smith PJ, Roberts PE, Hurst RJ (1981) Evidence for two species of arrow squid in the New Zealand fishery. *New Zealand Journal of Marine and Freshwater Research* 15:247–253
- Stephens PR, Young JZ (1978) Semicircular canals in squids. *Nature* 271:444–445
- Stevens D, O'Driscoll R, Dunn M, Ballara S, Horn P (2012) Trawl survey of hoki and middle depth species on the Chatham Rise, January 2011 (TAN1101). *New Zealand Fisheries Assessment Report* 10:98
- Stevens D, O'Driscoll R, Dunn M, Ballara S, Horn P (2015) Trawl survey of hoki and middle-depth species on the Chatham Rise , January 2014.
- Strnad L, Ettler V, Mihaljevic M, Hladil J, Chrastny V (2009) Determination of trace elements in calcite using solution and laser ablation ICP-MS: calibration to NIST SRM glass and USGS MACS carbonate, and application to real landfill calcite. *Geostandards and Geoanalytical Research* 33:347–355
- Swart PK, Elderfield H, Greaves MJ (2002) A high-resolution calibration of Sr/Ca thermometry using the Caribbean coral *Montastraea annularis*. *Geochemistry, Geophysics, Geosystems* 3:1–11

- Tsuchiya K, Okutani T (1991) Growth stages of *Moroteuthis robusta* (Verrill, 1881) with the re-evaluation of the genus. *Bulletin of Marine Science* 49:137-147
- Tung H (1978) On the biology and fishing of the squid *Nototodarus sloanii* (Gray) in the New Zealand waters. Report for the Institute of Fisheries Biology 3:44–64
- University of Colorado (2002) Infrared spectroscopy : theory. In: Online edition for students of organic chemistry lab courses at the University of Colorado, Boulder, Dept of Chem and Biochem.p 155–164
- Uozumi Y (1998) Fishery biology of arrow squids, *Nototodarus gouldi* and *N. sloanii*, in New Zealand waters. *Bulletin of the National Research Institute of Far Seas Fisheries* 0:1–111
- Uozumi Y, Ohara H (1993) Age and growth of *Nototodarus sloanii* (Cephalopoda: Oegopsida) based on daily increment counts in statoliths. *Nippon Suisan Gakkaishi* 59:1469–1477
- Urmos J, Sharma SK, Mackenzie FT (1991) Characterization of some biogenic carbonates with Raman spectroscopy. *American Mineralogist* 76:641–646
- VanHeezik Y, Seddon P (1989) Stomach sampling in the yellow-eyed penguin: erosion of otoliths and squid beaks. *Journal of Field Ornithology* 60:451–458
- Villanueva R (2000a) Differential increment-deposition rate in embryonic statoliths of the loliginid squid *Loligo vulgaris*. *Marine Biology* 137:161–168
- Villanueva R (2000b) Effect of temperature on statolith growth of the European squid *Loligo vulgaris* during early life. *Marine Biology* 136:449–460
- Voight JR (2014) A deep-sea octopus (*Graneledone* cf. *boreopacifica*) as a shell-crushing hydrothermal vent predator. *Journal of Zoology* 252:335–341
- Wang C, Geffen AJ, Nash RDM (2012) Geographical variations in the chemical compositions of veined squid *Loligo forbesi* statoliths. *Zoological Studies* 51:755–761
- Warner RR, Hamilton SL, Sheehy MS, Zeidberg LD, Brady BC, Caselle JE (2009) Geographic variation in natal and early larval trace-elemental signatures in the statoliths of the market squid *Doryteuthis* (formerly *Loligo*) *opalescens*. *Marine Ecology Progress Series* 379:109–121
- Weaver JC, Wang Q, Miserez A, Tantuccio A, Stromberg R, Bozhilov KN, Maxwell P, Nay R, Heier ST, DiMasi E, Kisailus D (2010) Analysis of an ultra hard magnetic biomineral in chiton radular teeth. *Materials Today* 13:42–52
- Welton JE (1984) SEM petrology atlas. American Association of Petroleum Geologists.

- Wolf RE (2013) What is ICP-MS? And more importantly, what can it do? US Geological Survey, Crustal Geophysics and Geochemistry Science Center: 7
- Xavier J, Clarke MR, Magalhaes MC, Stowasser G, Blanco C, Chérel Y (2007) Current status of using beaks to identify cephalopods : III International Workshop and training course on Cephalopod beaks , Faial island , Azores , April 2007. *Life and Marine Sciences* 24:41–48
- Yang F-C, Peters RD, Dies H, Rheinstädter MC (2014) Hierarchical, self-similar structure in native squid pen. *Soft Matter* 10:5541–9
- Zacherl DC (2005) Spatial and temporal variation in statolith and protoconch trace elements as natural tags to track larval dispersal. *Marine Ecology Progress Series* 290:145–163
- Zumholz K (2005) The influence of environmental factors on the micro-chemical composition of cephalopod statoliths. PhD Thesis, University of Kiel :86
- Zumholz K, Hansteen T, Hillion F, Horreard F, Piatkowski U (2007a) Elemental distribution in cephalopod statoliths: NanoSIMS provides new insights into nano-scale structure. *Reviews in Fish Biology and Fisheries* 17:487–491
- Zumholz K, Hansteen TH, Klügel A, Piatkowski U (2006) Food effects on statolith composition of the common cuttlefish (*Sepia officinalis*). *Marine Biology* 150:237–244
- Zumholz K, Klügel A, Hansteen T, Piatkowski U (2007b) Statolith microchemistry traces the environmental history of the boreoatlantic armhook squid *Gonatus fabricii*. *Marine Ecology Progress Series* 333:195–204